9th Panhellenic Conference of the Greek Lipid Forum

Virtual

Current Trends in the Field of Lipids

Book of Abstracts

Hosted by 18th Euro Fed Lipid Congress
17–20 October 2021 · Leipzig · Germany

22 October 2021

In silico and *in vitro* studies for the regio-selective enzymatic lipophilization of flavonoids by lipases

A. Papanikolaou[1], A. V. Chatzikonstantinou[1], A. C. Polydera[1], I. V. Pavlidis[2] and H. Stamatis[1] *

[1] Department of Biological Applications and Technologies, University of Ioannina, 45110 Ioannina, Greece

[2] Department of Chemistry, University of Crete, University Campus-Voutes, 70013 Heraklion, Crete, Greece

* hstamati@uoi.gr

Abstract: Flavonoids are a class of various natural polyphenolic bioactive compounds that are ubiquitously found in plants, such as vegetables, herbs, fruits, grain, etc. These compounds are well known for their beneficial effects, regarding human health, mostly attributed to their high anti-oxidant, anti-inflammatory and anti-carcinogenic properties. However, the numerous hydroxyl groups on their structure grants them moderate hydrophilic properties and can be a limiting factor for their application in the pharma and food industry. One wildly used approach, to tackle this concern, is the structural modification through enzymatic means. This can be achieved by targeting their hydroxyl function and produce ester derivatives, through an acylation reaction, with either aliphatic or aromatic acid derivatives. Among the hydrolytic enzymes, lipases are one the most efficient and well-studied biocatalysts for the acylation of flavonoids. In addition, several studies have reported that the acetylated derivatives of flavonoids demonstrate enhanced biological activities. In the present work, the regio-selectivity of various lipases towards several aglycon flavonoids was investigated, *in silico*, at an atomic level through molecular modeling. Additionally, *in vitro* acylation of the same flavonoids by various lipases was performed in different conditions and the acetyl derivatives were characterized through HPLC and 1D ^{1}H-HMR and 2D ^{1}H-^{13}C HSQC-HMBC NMR analysis. In most cases, the enzymatic modification was carried out successfully achieving high reaction yields and producing various regio-selective derivatives while in silico analysis elucidated some elements regarding the enzymatic regio-selectivity.

Keywords: regioselectivity, flavonoid acylation, biocatalysis, molecular modeling

Acknowledgements: This research has been co-financed by the European Regional Development Fund of the European Union and Greek national funds through the Operational Program Competitiveness, Entrepreneurship, and Innovation, under the call RESEARCH−CREATE□INNOVATE (project code: T2EDK-01410).

IUPAC INTERNATIONAL UNION OF PURE AND APPLIED CHEMISTRY

9th ICGC
IUPAC International Conference on Green Chemistry

9th IUPAC International Conference on Green Chemistry

5-9 September 2022, Athens, Greece

Venue: Zappeion Megaron | www.greeniupac2022.org

Physical and Virtual

CONFERENCE PROCEEDINGS



Organized by:

Association of Greek Chemists

In collaboration with:

IUPAC Interdivisional Committee on Green Chemistry for Sustainable Development

Endorsed by :

IUPAC INTERNATIONAL UNION OF PURE AND APPLIED CHEMISTRY

ACS Chemistry for Life®

EuChemS European Chemical Society

HELLENIC REPUBLIC
National and Kapodistrian University of Athens
EST. 1837
Department of Chemistry

ARISTOTLE UNIVERSITY OF THESSALONIKI
Department of Chemistry

GREEN SCIENCES FOR SUSTAINABLE DEVELOPMENT FOUNDATION

CONTACT INFORMATION
GreenIUPAC 2022 Secretariat

www.greeniupac2022.org

info@greeniupac2022.org

+30 2310 528978

Enotikon 10 Thessaloniki, Greece, GR - 54627

Enzymatic modification of biopolymers with phenolic antioxidants

Archontoula Giannakopoulou[1], Renia Fotiadou[1], Georgia Tsapara[1], Angeliki C. Polydera[1], Alexandra V. Chatzikonstantinou[1], Stamatia Spyrou[1] and Haralambos Stamatis[1*]

[1]*Biotechnology Laboratory, Department of Biological Applications and Technologies, University of Ioannina, 45110 Ioannina, Greece*

**hstamati@uoi.gr*

Abstract

Polymers, such as chitosan (CS) and carboxymethylcellulose (CMC) or hybrids, such as chitosan-gelatin (CS-GEL) are characterized by unique biological properties such as, biocompatibility, biodegradability, nontoxicity, and affinity to proteins [1,2]. Moreover, they contain several reactive amino and hydroxyl groups, susceptible to chemical modifications [3]. The enzymatic targeted modification of polymers has widely attracted the scientific interest for development of innovative biomaterials with enhanced biological properties, such as their antioxidant and antimicrobial activities [4]. The present work describes the application of biocatalytic systems with hydrolytic and redox properties for the targeted crosslinking of various polymers with phenolic bioactive compounds, such as hydroxytyrosol with the ultimate goal of improving their biological and mechanical properties. The successful grafting of the phenolic compounds onto the different polymers was confirmed through various spectroscopic techniques, such as ultraviolet-visible (UV-Vis) spectroscopy. Finally, the modified polymers exhibited strong antimicrobial activity against bacterial populations of *Escherichia coli* BL21DE3 strain as well as an enhancement in their antioxidant activity, suggesting their future potential applications in pharmaceutical and food industry.

Materials

Chitosan from crab shells (low viscosity), carboxymethyl cellulose, sodium salt, low viscosity (CMC) and laccase from *Agaricus bisporus* (>4 U/mg, lyophilized) were purchased from Sigma-Aldrich (St. Louis, MO, USA). Gelatin from porcine skin was purchased from Fluka (Charlotte, North Carolina, US).

Methods

Enzymatic modification of the polymers

The prepared CS, CS-GEL and CMC solutions were enzymatically modified by laccase from *Agaricus bisporus* with phenolic compounds, such as hydroxytyrosol. Specifically, to a final reaction volume of 20 mL, 1.3% w/v CS or 1.3% w/v CS-GEL or 1.3% w/v CMC solution were mixed with 5 mM hydroxytyrosol solution solubilized in MeOH and 0.086 U/mL (60 μg/mL) laccase from *Agaricus bisporus* were added to initiate the reaction. The reactions were plated on petri dishes and incubated at 30 ºC and 80 rpm O/N. At standard time intervals, 1 mL of the reaction was taken in order to monitor the reaction progress through the changes observed in the UV spectra. Finally, the plates were placed open to dry at 45 ºC O/N to form films (as shown in Figure 1).



Figure 1. Enzymatic modification of chitosan with phenolic compounds, such as hydroxytyrosol.

Antimicrobial properties

Initially, 100 μL of bacterial population was inoculated from stock bacterial populations of *Escherichia coli* BL21DE3 strain, stored in glycerol, in 5 mL of fresh Lysogeny Broth (LB). After incubation at 37 °C, O/N under constant stirring at 180 rpm the pre-culture absorbance was measured at 600 nm and diluted with fresh LB so that the new culture reached an optical density (OD) of about 0.08 absorbance. The new culture was incubated at 37 °C, under stirring at 180 rpm, until the bacterial population present an O.D. of 0.2-0.5. The culture was then centrifuged at 4,000 rpm for 5 minutes, the bacterial precipitate was restored and redissolved in saline (0.9% w/v NaCl). After three successive washes the bacterial pellet was redissolved in an equal volume of the culture. Bacterial population samples of 107 CFU/mL were prepared. Approximately 0.5 mg of each sample was added into an Eppendorf tube containing 100 μL of the bacterial population and it was incubated for 12 hours in a cold chamber. 100μL of bacterial in the absence of sample were used as a control. Then, 25 μL of the bacterial population that interacted with the sample, were inoculated into 225 μL of fresh LB medium in an Elisa microplate well. The microplate was then placed in an incubator chamber at 37 °C and measurements of the O.D. at 600 nm were taken after eight hours.

Results and Discussion

The laccase catalyzed oxidation of phenolic compounds, such as hydroxytyrosol (HD) to reactive intermediates and their subsequent reaction with the functional groups of chitosan was examined. Ultraviolet-visible (UV-Vis) spectroscopy was applied to monitor the reaction progress. As shown in Figure 2, the reaction spectrum presents a significant increase in the absorption band in the range 450-550 nm over time, followed by its gradual shift to 520 nm, suggesting the successful modification of chitosan with hydroxytyrosol.

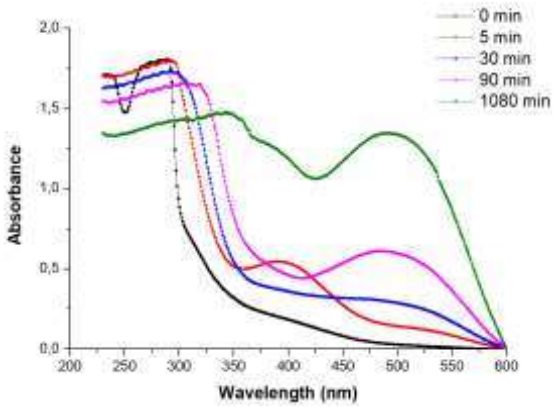


Figure 2. Ultraviolet-visible (UV-Vis) spectrum in the range of 200-600 nm of the reaction progress of the enzymatic functionalization of chitosan (CS) with hydroxytyrosol catalyzed by laccase from *Agaricus bisporus* at standard time intervals.

Also, the antibacterial activity of the enzymatically modified membranes was evaluated and the results are presented on Table 1. Chitosan itself has antimicrobial activity, reducing cell growth to 56% compared to cell growth incubated for 12 hours in the absence of any inhibitory agent. The modified CS almost totally inhibits the bacterial cell growth, as shown in Table 1, suggesting that the enzymatic modification was successful.

Table 1. % Growth of the bacterial cells of strain BL21DE3 after 12 hours in the presence of non-modified and enzymatically modified chitosan membranes with phenolic compounds (the standard deviation was less than 5% in all cases).

Samples	**Growth (%)**
Control	100
Chitosan	56
Enzymatically Modified Chitosan	8

Conclusions

The present work demonstrated that a series of various polymers, including chitosan, cellulose and a hybrid chitosan-gelatin polymer were efficiently functionalized with various phenolic compounds through the action of an oxidoreductase enzyme, namely laccase from *Agaricus bisporus*. The efficient cross-link of the biopolymers with the products derived from the laccase-mediated oxidation of phenolics was confirmed through various spectroscopic methods, such as UV-Vis spectroscopy. Finally, the enzymatically modified derivatives were characterized by strong antimicrobial properties, significantly superior to the biological activities that exhibited the non-modified polymers, implying their future potential application in many areas, from food-packaging to pharmaceuticals and cosmetics.

Acknowledgements

This research has been co-financed by the European Regional Development Fund of the European Union and Greek national funds through the Operational Program Competitiveness, Entrepreneurship, and Innovation, under the call RESEARCH–CREATE-INNOVATE (project code: T2EDK-01410).

References

1. Wang, W., Xue, C., & Mao, X., *International Journal of Biological Macromolecules*, **164** 4532 (2020).
2. Wu, L.-Q., Embree, H. D., Balgley, B. M., Smith, P. J., & Payne, G. F., *Environmental Science & Technology*, **36** 3446 (2002).
3. Karaki, N., Aljawish, A., Humeau, C., Muniglia, L., & Jasniewski, J., *Enzyme and Microbial Technology*, **90** 1 (2016).
4. Yang, J.; Sun, J.; An, X.; Zheng, M.; Lu, Z.; Lu, F.; Zhang, C., *RSC Advances*, **8** 6759 (2018).

IUPAC International Conference on Green Chemistry

UNIVERSITY OF IOANNINA
FACULTY OF HEALTH SCIENCES
DEPARTMENT OF BIOLOGICAL APPLICATIONS AND TECHNOLOGY
BIOTECHNOLOGY LABORATORY

LABORATORY of BIOTECHNOLOGY
University of Ioannina

SCAN ME

Enzymatic modification of biopolymers with phenolic antioxidants

Archontoula Giannakopoulou[1], Renia Fotiadou[1], Georgia Tsapara[1], Angeliki C. Polydera[1], Alexandra V. Chatzikonstantinou[1], Stamatia Spyrou[1] and Haralambos Stamatis[1*]

[1]*Biotechnology Laboratory, Department of Biological Applications and Technologies, University of Ioannina, 45110 Ioannina, Greece*

*hstamati@uoi.gr

Abstract

Polymers, such as chitosan (CS) and carboxymethylcellulose (CMC) or hybrids, such as chitosan-gelatin (CS-GEL) are characterized by unique biological properties such as, biocompatibility, biodegradability, nontoxicity, and affinity to proteins[1]. Moreover, they contain several reactive amino and hydroxyl groups, susceptible to chemical modifications[2]. The enzymatic targeted modification of polymers has widely attracted the scientific interest for the development of innovative biomaterials with enhanced biological properties, such as antioxidant and antimicrobial[3]. The present work describes the application of biocatalytic systems with hydrolytic and redox properties for the targeted crosslinking of various polymers with phenolic bioactive compounds, such as hydroxytyrosol, ferulic acid and luteolin with the ultimate goal of improving their biological and mechanical properties. The successful grafting of the phenolic compounds onto the different polymers was confirmed through various spectroscopic techniques, such as ultraviolet-visible (UV-Vis) spectroscopy. Finally, the modified polymers exhibited strong antimicrobial activity against bacterial populations of *Escherichia coli* BL21DE3 strain as well as an enhancement in their antioxidant activity, suggesting their future potential applications in pharmaceutical and food industry.

Materials & Methods

Chitosan from crab shells (low viscosity), carboxymethyl cellulose, sodium salt, low viscosity (CMC) and laccase from *Agaricus bisporus* (>4 U/mg, lyophilized) were purchased from Sigma-Aldrich (St. Louis, MO, USA). Gelatin from porcine skin was purchased from Fluka (Charlotte, North Carolina, US).

The prepared CS, CS-GEL and CMC solutions were enzymatically modified by laccase from *Agaricus bisporus* with various phenolic compounds. Specifically, to a final reaction volume of 20 mL, 1.3% w/v CS or 1.3% w/v CS-GEL or 1.3% w/v CMC solution were mixed with 5 mM of each phenolic compound solution solubilized in MeOH and 0.086 U/mL (60 μg/mL) laccase from *Agaricus bisporus* were added to initiate the reaction. The reactions were plated on petri dishes and incubated at 30 °C and 80 rpm O/N. Finally, the plates were placed open to dry at 45 °C O/N to form films (as shown in Figure 1). The antimicrobial activity of the prepared films was tested against bacterial populations of *Escherichia coli* BL21DE3 strain while their antioxidant capacity was estimated according to the DPPH protocol and was expressed as SC_{50} values.

Results & Discussion

The laccase catalyzed oxidation of hydroxytyrosol (HD) to reactive intermediates and their subsequent reaction with the functional groups of chitosan was examined. Ultraviolet-visible (UV-Vis) spectroscopy was applied to monitor the reaction progress. As shown in Figure 2, the reaction spectrum presents a significant increase in the absorption band in the range 450-550 nm over time, followed by its gradual shift to 520 nm, suggesting the successful modification of chitosan with hydroxytyrosol.

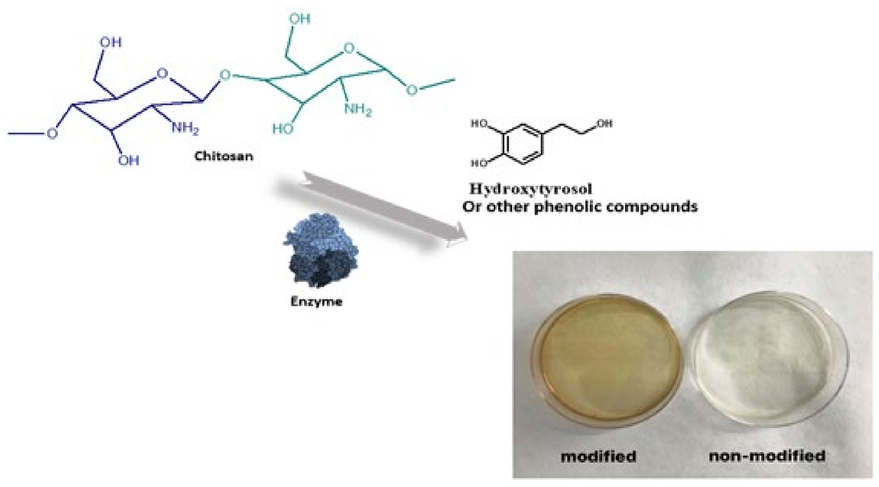


Figure 1. Enzymatic modification of chitosan with phenolic compounds, such as hydroxytyrosol.

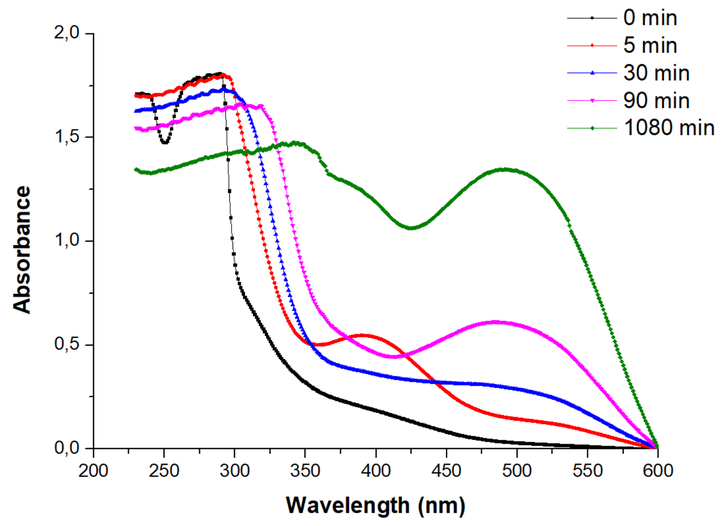


Figure 2. Ultraviolet-visible (UV-Vis) spectrum in the range of 200-600 nm of the reaction progress of the enzymatic functionalization of chitosan (CS) with hydroxytyrosol catalyzed by laccase from *Agaricus bisporus* at standard time intervals.

Also, the antioxidant and antibacterial activity of the enzymatically modified films was evaluated, and the results are presented below, on Tables 1 & 2, respectively. As shown, in all cases the modified membranes exhibit enhanced antimicrobial and antioxidant properties compared to the non-modified films, thus, suggesting that the enzymatic modification was successful.

Table 1. SC50 (mg/mL) values for the individual biopolymers and the enzymatically modified biopolymers with phenolics, according to the DPPH protocol. (The standard deviation was less than 5% in all cases.)

Polymer	Enzymatic Modification	SC_{50} (mg/ml)
CS	Non-Modified Film	70
	Ferulic Acid	11
	Hydroxytyrosol	52
	Luteolin	14
CS/GEL	Non-Modified Film	36
	Ferulic Acid	19
	Hydroxytyrosol	10
	Luteolin	27
CMC	Non-Modified Film	74
	Ferulic Acid	10
	Hydroxytyrosol	21
	Luteolin	29

Table 2. % Growth of the bacterial cells of strain BL21DE3 after 12 hours in the presence of non-modified and enzymatically modified chitosan membranes with phenolic compounds (the standard deviation was less than 5% in all cases).

Samples	Growth (%)
Control	100
CS	56
CS Modified with Ferulic Acid	12
CS Modified with Luteolin	10
CS Modified with Hydroxytyrosol	8

Conclusions

In this work, a series of various polymers, including CS, CMC and a hybrid CS/GEL polymer were efficiently functionalized with various phenolic compounds through the action of laccase from *Agaricus bisporus*. The efficient cross-link of the biopolymers with the products derived from the laccase-mediated oxidation of phenolics was firstly confirmed spectrophotometrically. All the enzymatically modified derivatives were characterized by strong antioxidant antimicrobial properties, significantly superior to the non-modified ones.

References

1. Wang, W., Xue, C., & Mao, X., *International Journal of Biological Macromolecules*, **164** 4532 (2020).
2. Karaki, N., Aljawish, A., Humeau, C., Muniglia, L., & Jasniewski, J., *Enzyme and Microbial Technology*, **90** 1 (2016).
3. Giannakopoulou, A.; Tsapara, G.; Troganis, A.N.; Koralli, P.; Chochos, C.L.; Polydera, A.C.; Katapodis, P.; Barkoula, N.-M.; Stamatis, H., *Biomolecules,* **12** 992 (2022).

Acknowledgements

This research has been co-financed by the European Regional Development Fund of the European Union and Greek national funds through the Operational Program Competitiveness, Entrepreneurship, and Innovation, under the call RESEARCH–CREATE-INNOVATE (project code: T2EDK-01410).

European Union
European Regional Development Fund

HELLENIC REPUBLIC
MINISTRY OF DEVELOPMENT AND INVESTMENTS
SPECIAL SECRETARIAT FOR ERDF & CF PROGRAMMES
MANAGING AUTHORITY OF EPAnEK

EPAnEK 2014-2020
OPERATIONAL PROGRAMME
COMPETITIVENESS
ENTREPRENEURSHIP
INNOVATION

ΕΣΠΑ 2014-2020
ανάπτυξη - εργασία - αλληλεγγύη
Partnership Agreement 2014 - 2020

Co-financed by Greece and the European Union

10th Panhellenic Conference of the Greek Lipid Forum

Current Trends in the Field of Lipids

Hosted by

25 November 2022

Sponsored by

3D printed PLA well-plates for enzyme inhibition studies: The case of Pancreatic Lipase

A. Skonta, E. Gkantzou, S. Spyrou, A. Polydera, H. Stamatis

Department of Biological Applications and Technologies, University of Ioannina, Ioannina, Greece
* hstamati@uoi.gr

Abstract: Obesity is a multifactorial clinical condition that has been associated with the abnormal metabolism of triacylglycerols (TAGs) and has been linked to comorbidities, such as cardiovascular diseases, diabetes, cancer, and causing even mortality. Since the inhibition of pancreatic lipase is considered as an effective treatment for obesity, the detection of inhibitors, e.g. natural products, which could exhibit less side effects than the commercially available inhibitor, orlistat, is on the spotlight. Considering the prerequisites for an efficient screening assay, that is usage of small volumes of reagents, low cost and rapid screening of large numbers of compounds and extracts, assays based on microtiter plates are predominant. Thus, designing and fabricating scaffolds on a similar scale, which could serve as immobilization carriers, and their recruitment in inhibitors screening studies is of great significance, adding both enzyme stability and reuse potentiality of the biocatalytic system in assay merits. Polylactic acid (PLA), a naturally derived polymer, consists one of the most widely used materials regarding 3D printing. Notably, 3D printed PLA has already been demonstrated for several biotechnological applications, including enzymes immobilization. In this work, pancreatic lipase was immobilized on 3D printed PLA microwells that were elaborated for enzyme inhibitors screening. XPS spectroscopy demonstrated the successful modification of PLA scaffolds, while the immobilized enzyme showed high levels of operational, thermal and storage stability in the tested conditions. Moreover, IC_{50} values were calculated for both orlistat, as a model inhibitor compound, and olive leaves extract as a promising natural compound for PPL inhibition. This is the first report regarding the use of 3D printed PLA wells with immobilized enzyme for inhibitors screening assay.
Keywords: 3D printing; lipase; well-plate assay; inhibition; olive leaves extract

Acknowledgements: This research has been co-financed by the European Regional Development Fund of the European Union and Greek national funds through the Operational Program Competitiveness, Entrepreneurship, and Innovation, under the call RESEARCH–CREATE-INNOVATE (project code: T2EDK-01410)

Department of Biological Applications and Technologies,
University of Ioannina, Greece

10ο Πανελλήνιο Συνέδριο
ΣΥΓΧΡΟΝΕΣ ΤΑΣΕΙΣ ΣΤΟΝ ΤΟΜΕΑ ΤΩΝ ΛΙΠΙΔΙΩΝ
Ελληνικό Φόρουμ Επιστήμης και Τεχνολογίας Λιπιδίων
Greek Lipid Forum
Μέλος της Euro Fed Lipid

3D printed PLA well-plates for enzyme inhibition studies: The case of Pancreatic Lipase

A. Skonta, E. Gkantzou, S. Spyrou, A. Polydera, H. Stamatis*
Laboratory of Biotechnology, Department of Biological Applications and Technologies, University of Ioannina, Ioannina, Greece
*Corresponding author: hstamati@uoi.gr

ABSTRACT

Obesity is a multifactorial clinical condition that has been associated with the abnormal metabolism of triacylglycerols (TAGs) and has been linked to comorbidities [1]. Since the inhibition of pancreatic lipase is considered as an effective treatment for obesity, the detection of inhibitors, e.g. natural products, which could exhibit less side effects than the commercially available inhibitor, orlistat, is on the spotlight [1,2]. Considering the prerequisites for an efficient screening assay, that is usage of small volumes of reagents, low cost and rapid screening of large numbers of compounds and extracts, assays based on microtiter plates are predominant [3]. Thus, designing and fabricating scaffolds on a similar scale, which could serve as immobilization carriers, and their recruitment in inhibitor screening studies is of great significance, adding both enzyme stability and reuse potentiality of the biocatalytic system in assay merits. Polylactic acid (PLA), a naturally derived polymer, consists one of the most widely used materials regarding 3D printing [4]. Notably, 3D printed PLA has already been demonstrated for several biotechnological applications, including enzyme immobilization [5]. In this work, pancreatic lipase was immobilized on 3D printed PLA microwells that were elaborated for enzyme inhibitor screening. The immobilized enzyme showed high levels of operational, thermal and storage stability in the tested conditions. Moreover, IC_{50} values were calculated for both orlistat, as a model inhibitor compound, and olive leaf extract as a promising natural compound for PPL inhibition.

RESULTS

1. 3D printed PLA well-plates: from the 3D printing process to the inhibition study

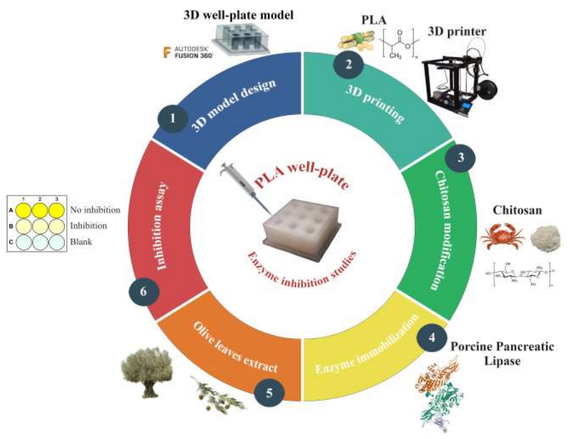


Figure 1. The process for scaffold preparation, enzyme immobilization, and enzyme inhibition studies

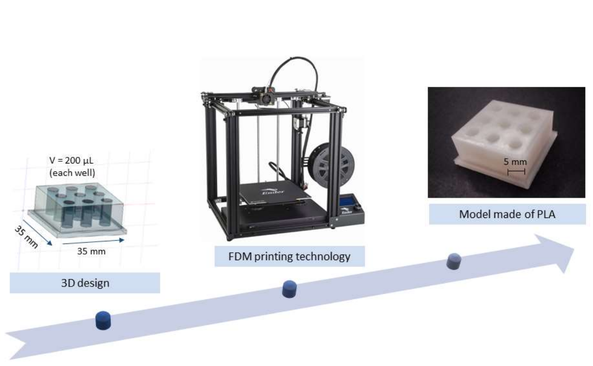
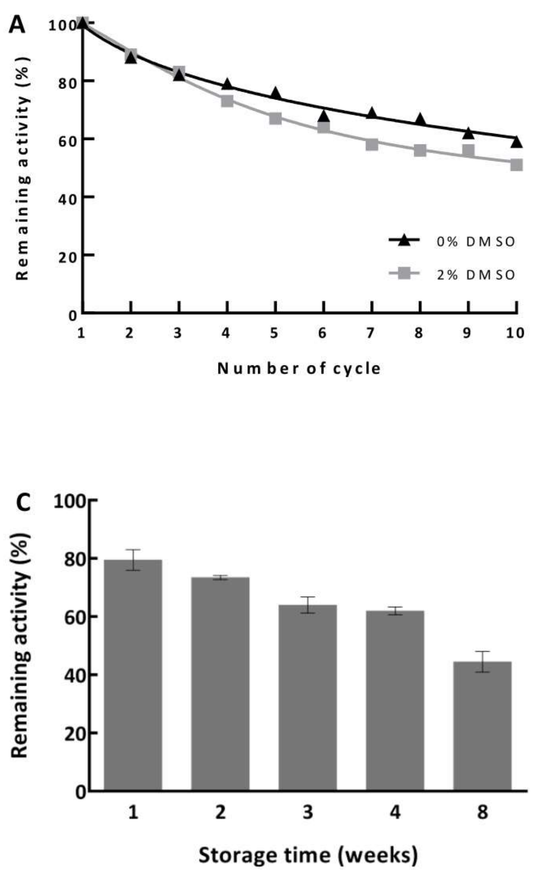


Figure 2. A well plate model was designed using a 3D design software, and an FDM printing technology produced the final model using natural PLA filament.

2. Biocatalytic Characterization of the Immobilized PPL on 3D Printed PLA Scaffolds



PPL form	Km (mM)
Immobilized	0.24±0.06
Free	0.29±0.02

Figure 3: Biocatalytic studies of the immobilized PPL on PLA wells. (A) Operational stability of the immobilized PPL in the presence (2%) and absence (0%) of DMSO for ten cycles of reuse. (B) Thermal stability of the free and the immobilized PPL after incubation at 40°C for 1, 2, 6, and 8 h. (C) Storage stability of the immobilized PPL on PLA wells after incubation at 4°C for 1, 2, 3, 4, and 8 weeks. The reactions were performed at 40 °C for 20 min with 1 mM of the substrate (pNPB) in 0.05 M phosphate buffer (pH 7). (D) Michaelis–Menten plot for the PPL kinetic constant. The reactions were performed at 40°C for 20 min with the substrate (pNPB) concentrations varying from 0.125 to 2 mM.

3. Inhibition Studies

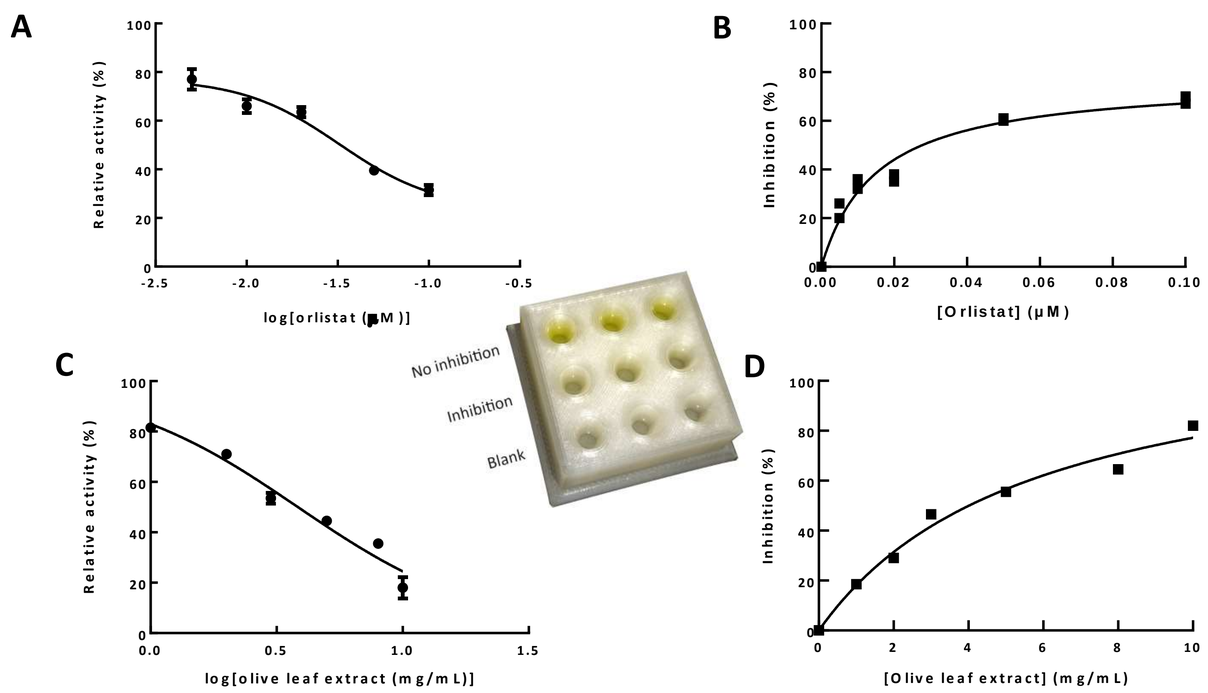


Figure 4: Inhibition studies of the immobilized PPL using Orlistat and olive leaf extract. (A-B) Determining the values of the inhibitory concentration (IC_{50}) of Orlistat for inhibiting immobilized PPL. The orlistat concentrations ranged from 0.005–0.1 μM (2% DMSO) in 0.05 M phosphate buffer (pH 7). (C-D) Determining the values of the inhibitory concentration (IC_{50}) of the olive leaf extract for inhibiting immobilized PPL. The reactions were performed at 40°C for 20 min using 1 mM of the substrate (pNPB). The concentration of the olive leaf extract ranged from 1–10 mg/mL in 0.05 M phosphate buffer (pH 7). There was a 10 min pre-incubation period between the lipase and the inhibitor at 40°C, after which the substrate was added.

Evaluation of the Inhibitor Screening Assay

$$Z' = 1 - \frac{3\delta_s + 3\delta_c}{|q_s - q_c|}$$

q_s and q_c: the average enzyme activity when there is no inhibitor (s, sample) and the inhibition rate is 100% (c, control), respectively
δ_s and δ_c: the average of the respective standard deviations of the data

If 0.5≤Z'≤1➡ the proposed assay for screening inhibitors is accurate and reliable
Herein: Z' factor=0.86

Table 1: Inhibitory potency (IC_{50}) of Orlistat and olive leaf extract on PPL for both its immobilized and free form.

	IC_{50} for the immobilized PPL	IC_{50} for the free PPL
Orlistat	31.73 ± 6.52 nM	8.53 ± 1.68 nM
Olive leaf extract	3.84 ± 0.48 mg/mL	3.46 ± 0.34 mg/mL

CONCLUSIONS

- PPL was successfully immobilized on the interior of the 3D printed PLA well-plates.
- The immobilized enzyme presented high operational, thermal and storage stability thus, demonstrating the potential of the enzyme-immobilized well-plates for a series of biocatalytic studies.
- The proposed inhibitor screening assay is appropriate for the identification of PPL inhibitors.
- Olive leaf extract, with an IC_{50} value of 3.84 mg/mL, presents a promising effect as an inhibitory agent of natural origin

References

1. Birari RB, Bhutani KK. Pancreatic lipase inhibitors from natural sources: Unexplored potential. Drug Discov Today. 2007; 12: 879-889.
2. Bhutani KK, Birari R, Kapat K. Potential anti-obesity and lipid lowering natural products: A review. Nat Prod Commun. 2007; 2: 331-348.
3. Lankatillake C, Luo S, Flavel M, Lenon GB, Gill H, Huynh T, et al. Screening natural product extracts for potential enzyme inhibitors: Protocols, and the standardisation of the usage of blanks in α-amylase, α-glucosidase and lipase assays. Plant Methods. 2021; 17: 3.
4. Baran EH, Erbil HY. Surface modification of 3D printed PLA objects by fused deposition modeling: A review. Colloids Interfaces. 2019; 3: 43.
5. Shao Y, Liao Z, Gao B, He B. Emerging 3D printing strategies for enzyme immobilization: Materials, methods, and applications. ACS Omega. 2022; 7: 11530-11543.

Acknowledgements

This research has been co-financed by the European Regional Development Fund of the European Union and Greek national funds through the Operational Program Competitiveness, Entrepreneurship, and Innovation, under the call RESEARCH−CREATE-INNOVATE (project code: T2EDK-01410)

Co-financed by Greece and the European Union

ΕΛΛΗΝΙΚΗ ΕΤΑΙΡΕΙΑ ΒΙΟΫΛΙΚΩΝ



12ο Πανελλήνιο Συνέδριο Βιοϋλικών

Πρόγραμμα Συνεδρίου

Ενζυμική τροποποίηση βιοπολυμερών με βιοδραστικές ενώσεις για την αναβάθμιση των ιδιοτήτων τους

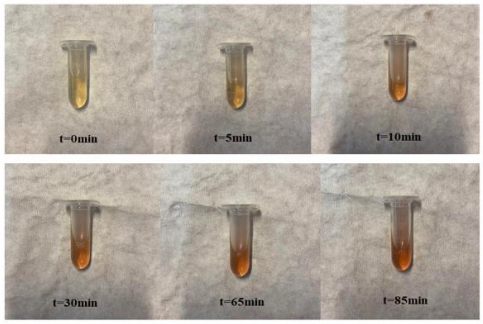
Α. Γιαννακοπούλου[1], Γ. Τσαπάρα[1], Α. Παπανικολάου[1], Α. Τρογκάνης[1], Α. Πολύδερα[1], Ν.Μ. Μπάρκουλα[2], Χ. Σταμάτης[1*]

[1]Εργαστήριο Βιοτεχνολογίας, Τμήμα Βιολογικών Εφαρμογών και Τεχνολογιών, Πανεπιστήμιο Ιωαννίνων,
[2]Εργαστήριο Μηχανικής Συνθέτων & Ευφυών Υλικών, Τμήμα Μηχανικών Επιστήμης Υλικών, Πανεπιστήμιο Ιωαννίνων

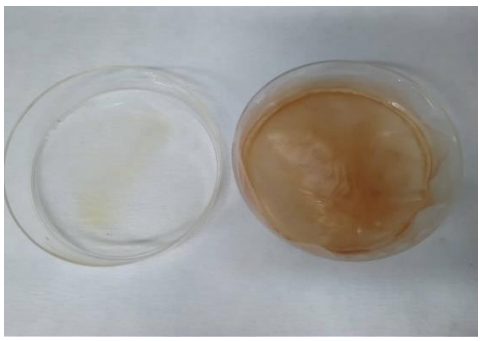
Εισαγωγή: Η τροποποίηση βιοπολυμερών με βιοδραστικές ενώσεις προσελκύει τελευταία αυξημένο ερευνητικό ενδιαφέρον για την παραγωγή καινοτόμων βιοϋλικών με αυξημένες βιολογικές δράσεις[1]. Επιπλέον, λόγω της ανάγκης για την ανάπτυξη φιλικών προς το περιβάλλον διεργασιών, τα ένζυμα αποτελούν σημαντικά εργαλεία για την τροποποίηση των βιοπολυμερών με φυσικά βιοδραστικά προϊόντα και την αξιοποίηση τους σε πληθώρα εφαρμογών[2]. Η παρούσα εργασία περιγράφει την ενζυμικά καταλυόμενη στοχευμένη διασύνδεση βιοπολυμερών, όπως η χιτοζάνη με βιοδραστικά φυσικά προϊόντα, όπως η υδροξυτυροσόλη για την ανάπτυξη υλικών με αυξημένη αντιμικροβιακή και αντιοξειδωτική δράση.

Μεθοδολογία: Για την ενζυμική τροποποίηση της χιτοζάνης με υδροξυτυροσόλη σε τελικό όγκο αντίδρασης 20 mL, προστίθενται το διάλυμα χιτοζάνης (τελικής συγκέντρωσης 1.2% w/v) και 2.5 mg/mL υδροξυτυροσόλης. Για την εκκίνηση της αντίδρασης προστίθενται λακκάση από το μύκητα *Agaricus bisporus* σε τελική συγκέντρωση 0.1 mg/mL. Οι αντιδράσεις επιστρώνονται σε τρυβλία petri και επωάζονται στους 30 ^{o}C για 24 ώρες υπό ανάδευση. Μετά το πέρας των αντιδράσεων, τα τρυβλία τοποθετούνται χωρίς καπάκι για ξήρανση για 24 ώρες ώστε να σχηματιστούν τα φιλμ.

Αποτελέσματα & Συζήτηση: Κατά την ενζυμική τροποποίηση της χιτοζάνης παρατηρήθηκε αλλαγή χρώματος από άχρωμο σε πορτοκαλί αμέσως μετά την προσθήκη του ενζύμου (Εικόνα 1α), ενώ στο αντίστοιχο διάλυμα ελέγχου δεν παρατηρήθηκαν αλλαγές στο χρώμα, υποδεικνύοντας ότι η παρουσία του ενζύμου είναι απαραίτητη για την οξείδωση της υδροξυτυροσόλης και την επακόλουθη σύνδεση των προϊόντων στη χιτοζάνη. Επίσης, η αντίστοιχη αλλαγή χρώματος παρατηρήθηκε και κατά τον σχηματισμό των φιλμ (Εικόνα 1β).



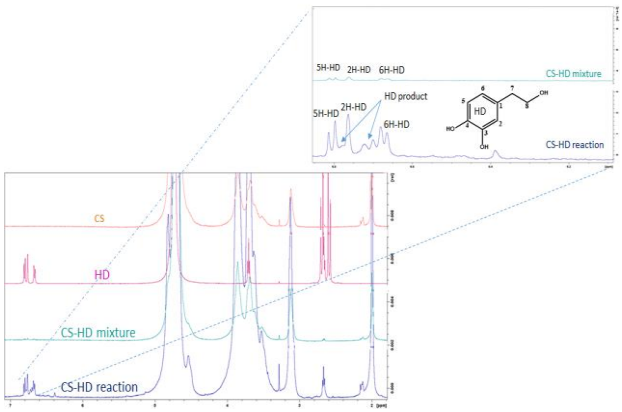
1 (α)



1 (β)

Εικόνα. 1*: Απεικόνιση της χρωματικής αλλαγής του διαλύματος της ενζυμικής αντίδρασης τροποποίησης της χιτοζάνης με υδροξυτυροσόλη (Εικόνα 1α) και του ενζυμικά τροποποιημένου φιλμ χιτοζάνης (Εικόνα 1β) με υδροξυτυροσόλη (αριστερά) και του μη τροποποιημένου φιλμ χιτοζάνης (δεξιά).*

Η επιτυχής τροποποίηση της χιτοζάνης επιβεβαιώθηκε επιπλέον με φασματοσκοπία πυρηνικού μαγνητικού συντονισμού (NMR) και τα αποτελέσματα παρουσιάζονται στο γράφημα που ακολουθεί. Η σύγκριση των φασμάτων υποδηλώνει την επιτυχή βιομετατροπή της χιτοζάνης με τα προϊόντα οξείδωσης της υδροξυτυροσόλης από τη λακκάση.



Διάγραμμα 1*: [1]H-NMR φάσματα της χιτοζάνης (CS), της υδροξυτυροσόλης (HD), του μίγματος CS με HD και της ενζυμικά καταλυόμενης αντίδρασης της CS με HD από τη λακκάση.*

Τέλος, μελετήθηκε και η αντιοξειδωτική δράση του τροποποιημένου βιοπολυμερούς και τα αποτελέσματα παρουσιάζονται στον Πίνακα 1 που ακολουθεί.

Χ. Σταμάτης, email: hstamati@uoi.gr

Πίνακας 1. Τιμές IC_{50} (mg/mL) για το μη τροποποιημένο και τροποποιημένο φιλμ με υδροξυτυροσόλη σύμφωνα με τη μέθοδο DPPH. (Η τυπική απόκλιση ήταν μικρότερη από 5% σε όλες τις περιπτώσεις)

Πολυμερές	Ενζυμική Τροποποίηση	IC_{50} (mg/mL)
Χιτοζάνη	Μη τροποποιημένο φιλμ	70
	Υδροξυτυροσόλη	10

Συμπεράσματα: Στην παρούσα εργασία πραγματοποιήθηκε η ενζυμικά καταλυόμενη στοχευμένη διασύνδεση της χιτοζάνης με φαινολικά βιοδραστικά μόρια, όπως η υδροξυτυροσόλη με σκοπό την ανάπτυξη καινοτόμων βιοϋλικών με βελτιωμένες βιολογικές (αυξημένη αντιμικροβιακή και αντιοξειδωτική δραστικότητα) και μηχανικές ιδιότητες.

Ευχαριστίες: This research has been co-financed by the European Regional Development Fund of the European Union and Greek national funds through the Operational Program Competitiveness, Entrepreneurship, and Innovation, under the call RESEARCH−CREATE-INNOVATE (project code: T2EDK-01410).

Βιβλιογραφία:

[1]M.Patila, A.Kouloumpis, D. Gournis, P. Rudolf, H.Stamatis, Sensors, 2 (2016), 287.

[2]Giannakopoulou, A.; Tsapara, G.; Troganis, A.N.; Koralli,P.; Chochos, C.L.; Polydera, A.C.; Katapodis, P.; Barkoula, N.-M.; Stamatis, H., Biomolecules, 12 (2022) 992.

Χ. Σταμάτης, email: hstamati@uoi.gr

Open Access

Catalysis Research

LIDSEN Publishing Inc.

Original Research

3D Printed Polylactic Acid (PLA) Well Plates for Enzyme Inhibition Studies: The Case of Pancreatic Lipase

Anastasia Skonta [1], Elena Gkantzou [1,*], Konstantinos Spyrou [2], Stamatia Spyrou [1], Angeliki Polydera [1], Dimitrios Gournis [2], Haralambos Stamatis [1,*]

1. Laboratory of Biotechnology, Department of Biological Applications and Technologies, University of Ioannina, Ioannina, Greece; E-Mails: anastasiasko@yahoo.gr; e.gkantzou@uoi.gr; stamatiaspyrou@yahoo.gr; apolyder@uoi.gr; hstamati@uoi.gr
2. Department of Materials Science and Engineering, University of Ioannina, Ioannina, Greece; E-Mails: konstantinos.spyrou1@gmail.com; dgourni@uoi.gr

* **Correspondences:** Elena Gkantzou and Haralambos Stamatis; E-Mails: e.gkantzou@uoi.gr; hstamati@uoi.gr

Academic Editor: Agnieszka Kolodziejczak Radzimska

Special Issue: Enzyme Immobilization

Catalysis Research
2022, volume 2, issue 4
doi:10.21926/cr.2204032

Received: July 31, 2022
Accepted: September 19, 2022
Published: October 08, 2022

Abstract

3D printed PLA has already been demonstrated for several biotechnological applications, including enzymes immobilization. The prerequisites for an efficient screening assay include using small volumes of reagents, low cost, and rapid screening of large numbers of compounds and extracts. Hence, assays based on microtiter plates are predominant. Thus, designing and fabricating scaffolds on a similar scale, which could serve as immobilization carriers, and their recruitment in inhibitors screening studies is of great significance, adding both enzyme stability and reuse potentiality of the biocatalytic system in assay merits. In this work, pancreatic lipase was immobilized on 3D-printed PLA microwells for enzyme inhibitor screening. XPS analysis demonstrated the successful modification of the PLA scaffolds. The immobilized enzyme displayed high levels of operational, thermal, and storage stability under the tested conditions. The IC_{50} values for PPL inhibition were calculated for Orlistat, a model

© 2022 by the author. This is an open access article distributed under the conditions of the Creative Commons by Attribution License, which permits unrestricted use, distribution, and reproduction in any medium or format, provided the original work is correctly cited.

lipase inhibitor, and olive leaf extract, a promising natural compound. This is the first study reporting the use of 3D-printed PLA wells with an immobilized enzyme for inhibitor screening assay.

Keywords
3D printing; lipase; well-plate assay; inhibition; olive leaf extract

1. Introduction

Obesity is a multifactorial, clinical condition associated with abnormal metabolism of triacylglycerols (TAGs) resulting from homeostatic imbalance [1]. It is characterized by excess accumulation of body fat and is linked to cardiovascular diseases, diabetes, cancer, and even mortality [2]. Hence, new treatment approaches are vital to expand the toolbox of the currently available therapeutic choices and provide improved alternatives. One of the most effective treatments for obesity involves lipase inhibitors [3]. Lipases, particularly pancreatic lipases, are prominently involved in catalyzing TAG hydrolysis and metabolism. This enzyme hydrolyzes 50% to 70% of the total dietary fats in the small intestine [1]. The porcine pancreatic lipase (PPL) is a monomeric small globular protein often used as the model enzyme for inhibition studies because of its higher amino acid sequence homology (86%) with the human pancreatic lipase [4-6].

Orlistat is the only pancreatic lipase inhibitor in use to date, approved by the Food and Drug Administration (FDA) and European Medicines Agency (EMA), while its weight loss properties along with cardioprotective, anti-diabetic and others have been discussed thoroughly [3, 7, 8]. Although orlistat is a highly selective inhibitor, several side effects have been reported, mostly gastrointestinal [9]. Therefore, nowadays natural products are in the spotlight for the identification of inhibitory agents of pancreatic lipase, which are anticipated to have fewer side effects than chemically synthesized compounds due to their natural origin [1, 10].

Biocatalysis requires enzymes in an immobilized form for long-term operational stability and cost-effectiveness [11]. Immobilization of enzymes exhibits several advantages, such as the feasibility of enzyme recovery and reuse, rapid termination of the enzymatic assay, enhanced storage, and thermal and operational stability [11, 12]. Three-dimensional (3D) printing or additive manufacturing produces immobilization carriers that are easily isolated from the reaction media and have large specific surface areas, thereby improving the mass transfer effect [13]. Polylactic acid (PLA) is a naturally-derived polymer. It is biodegradable, biocompatible, non-toxic, non-carcinogenic, and has good optical, mechanical, and rheological properties [13-15]. Moreover, its printing process is simple and consumes less energy than that required for other polymers. Hence, PLA is one of the most popular choices for biotechnological applications [13, 15]. So far, 3D printed scaffolds using PLA, carbon fiber-reinforced PLA (C-PLA), and nylon have been investigated extensively for optimizing enzyme immobilization [16-18]. Other examples of enzymes used in their free or immobilized form include the fabrication of 3D printed platforms for optical colorimetric enzymatic assays [19, 20]. Additionally, the construction of 3D-printed bioanalytical devices suitable for genetic tests has been reported in diagnostics [21-23].

In the scope of enzyme inhibition studies, microtiter plates and cuvettes are widely used [24]. Nevertheless, considering the prerequisites for an efficient screening assay, that is usage of small volumes of reagents, low cost and rapid screening of large numbers of compounds and extracts, assays based on microtiter plates are predominant. Thus, designing and fabricating scaffolds on a similar scale to function as immobilized enzyme carriers is essential. Such biocatalytic scaffolds can be applied in inhibitor screening studies because they render enzyme stability and reusability to the sustainable bioprocess.

PLA often undergoes modifications to alter specific characteristics, for instance, hydrophilicity, surface free energy, reactive functionalities, and roughness [15]. In previous studies, different methodologies, like the utilization of polyethylene glycol, polydopamine, and chitosan, were adopted [25-28]. Our research team proposed a novel protocol based on chitosan to functionalize 3D-printed PLA scaffolds. The method facilitated subsequent enzyme immobilization. Thus, biocatalytic systems with high stability, product yields, and turnover number were produced [29]. The present study proposed innovative, inexpensive, and environment-friendly 3D-printed PLA wells as sustainable matrices for enzyme inhibition studies. The well plates were designed and 3D-printed. The lipase from the porcine pancreas was immobilized in the interior of each well after appropriately modifying the scaffold surfaces. After that, spectroscopic and biocatalytic characterization of the immobilized 3D printed scaffolds was performed. Finally, the developed biocatalytic systems were successfully applied in the inhibition study of PPL. Inhibition was initially evaluated with the model inhibitor of PPL, Orlistat, and then with a promising natural compound, the extract of olive leaf . The half-maximal inhibitory concentration (IC_{50}) was determined for both reactions. The innovation of the present work stems from the fabrication of a well-plate through the utilization of the 3D printing technology, which enables the customization of the number and the volume of the wells. Moreover, the enzyme was directly immobilized on the surface of the well, adopting an eco-friendly, simple, time- and cost-efficient protocol. Interestingly, the average cost of one test (one PLA well fabrication, modification, PPL immobilization, and activity measurement) was calculated to be as low as 0.04€. Since the prepared scaffolds could be reused and stored without significant activity losses, they constitute a valuable tool in inhibition studies. To our knowledge, this is the first report involving 3D-printed PLA wells with immobilized enzymes for inhibitor screening assays.

2. Materials and Methods

2.1 Materials

PLA filament for FDM 3D printers (PrimaValue™) in a natural form was obtained from Prima Creator (Sweden). The 3D printer used was Ender 5 from Creality 3D (China). Sodium hydroxide (NaOH) with >98% purity was obtained from PanReac Applichem (USA). The following reagents were obtained from Merck (Sigma-Aldrich, USA): chitosan from crab shells (85% deacetylated), acetic acid (>99.8%), lipase Type II from porcine pancreas (100–500 U/mg protein in lyophilized form), and p-nitrophenyl butyrate (pNPB, >98%). Orlistat (98%) was obtained from Alfa Aesar (USA). HPLC-grade acetonitrile (ACN) and dimethylsulfoxide (DMSO) were obtained from Fisher Scientific (USA). All solutions used in the present work were prepared in double-distilled (dd) water.

2.2 Methods

2.2.1 3D Design and Printing of PLA Scaffolds

PLA scaffolds were designed according to our previous reports using the Fusion 360 CAD program from Autodesk (USA) [29, 30]. Briefly, well plates were designed with a 200 µL volume capacity for each well. The number of wells on each plate depended on the number of samples for each experiment. An example of a 9-well plate is demonstrated in Figure 1. The final design was sent to the slicing software Ultimaker Cura (Netherlands). Appropriate settings were selected depending on the filament and the 3D printer model. Print settings included a 0.16 mm layer height (resolution), 100% infill density, and 80 mm/s print speed. The printing temperature was set at 200 °C, and the build plate temperature was set at 50 °C. Natural PLA filament was used as the feeding material, with a diameter of 0.75 mm, extruded from a nozzle of 0.4 mm. Printing parameters are summarized in Table 1. A copy of the .STL file is provided as supplementary material. The model printed (Figure 1) was leak free, with a rigid structure, and ready-to-use for further experimentation (no post-printing processing needed).

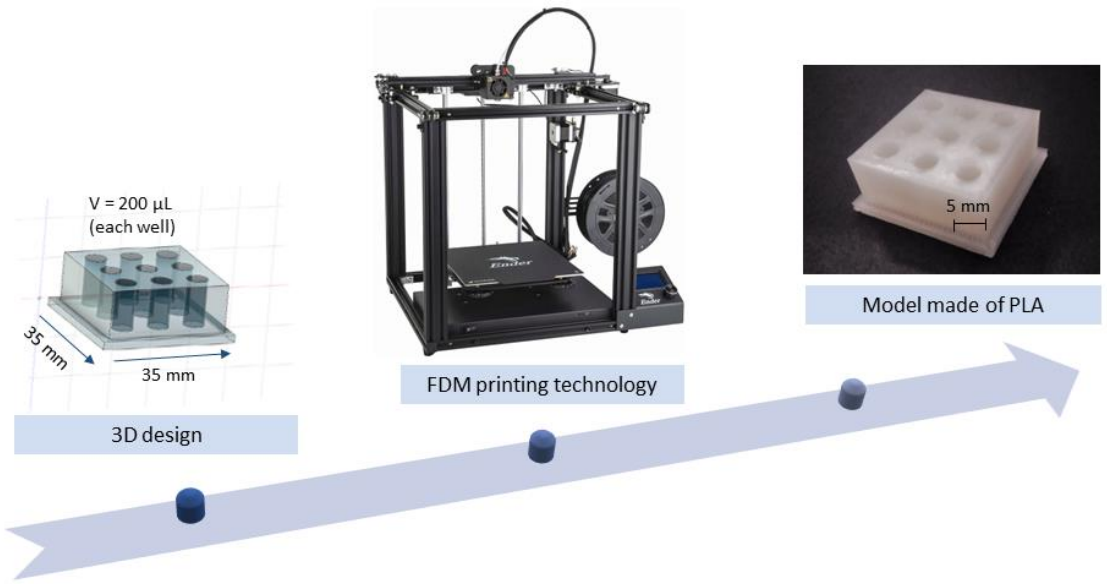


Figure 1 Demonstration of the 3D printing process. A well plate model was designed using a 3D design software, and an FDM printing technology produced the final model using natural PLA filament.

Table 1 Printing settings at the slicing software

Layer Height	0.16 mm
Infill Density	100%
Printing Temperature	200 °C
Build Plate Temperature	50 °C
Print Speed	80 mm/s
Nozzle Size	0.4 mm
Filament Diameter	1.75 mm

2.2.2 Surface Modification of the 3D Printed PLA Scaffolds

The surface of the PLA wells was modified as described in Gkantzou et al. 2022. Firstly, the 3D printed wells were incubated with a 1 M NaOH solution at room temperature for 2 h. The solution was then removed; the wells were washed twice with dd H_2O and dried under a vacuum for 30 min. After that, the wells were incubated with a 0.2% (w/v) chitosan solution for 1 min. After removing the solution, the wells were incubated with 1 M NaOH solution for 1 min. The solution was removed, and the wells were dried under a vacuum for 30 min. Porcine pancreatic lipase (PPL) was immobilized on PLA wells through non-covalent interactions. Briefly, PPL was dissolved in 50 mM phosphate buffer (pH 7) to a final concentration of 1 mg/mL and then subjected to vigorous shaking, followed by centrifugation at 10,000 rpm for 10 min. The supernatant was used afresh as the enzyme solution. The enzymatic solution (200 µL) was added to each well, and the plate was incubated at 30 °C for 1 h. Subsequently, the enzyme solution was removed, and the wells were washed thrice with the phosphate buffer solution. The well plate was dried under a vacuum for 30 min and stored at 4 °C until further use.

2.2.3 Enzymatic Activity Measurement in the PLA Well Plates

The activity of immobilized PPL was determined with a photometric assay using p-nitrophenyl butyrate (pNPB) as the substrate. A stock solution of 50 mM pNPB was prepared in acetonitrile (ACN) so that each reaction solution contained a fixed percentage (2% v/v of ACN). Each well was filled with 200 µL of 1 mM pNPB solution in 50 mM sodium phosphate buffer (pH 7). The enzymatic activity was determined at 40 °C at regular intervals for up to 20 min, that was proved to be sufficient time for the yield of the reaction product p-nitrophenol (pNP). The reaction solution was then transferred to a microplate and the absorbance of the produced pNP was measured using an ELISA plate reader (Multiskan SkyHigh Microplate Spectrophotometer, Thermo Fisher Scientific, USA) at 405 nm.

2.2.4 Estimation of the Immobilization Yield

To determine the amount of enzyme that was loaded during immobilization process, an activity test was conducted for the enzymatic solution before and after immobilization. A sample from the enzymatic solution before its loading on a well was measured with the pNPB protocol described above, and a sample of the enzymatic solution after incubation in the corresponding scaffold was also measured with the same process. Equation 1 was used for the calculation of the active enzyme amount loaded during immobilization in each scaffold.

$$\text{Immobilization yield } \% = 100 - \frac{\text{activity after immobilization} \times 100}{\text{activity before immobilization}} \quad (1)$$

2.2.5 Stability Studies of the Immobilized PPL

Biocatalytic characterization is critical to investigate the possible use of the developed enzyme system in further studies. Therefore, the immobilized PLA wells were studied initially in terms of operational, thermal, and storage stability. All experiments were performed in triplicates (one well-one experiment).

Operational stability The operational stability of the immobilized PPL on PLA wells was examined for ten successive cycles of use. The hydrolysis reaction of pNPB was monitored (as described in Section 2.2.3) in two different reaction media – the one containing 2% v/v DMSO and the other without added DMSO. After completion of each cycle (20 min), the reaction solution was removed, and the corresponding well was washed thrice with the reaction buffer. Fresh substrate solution was then filled in each well, and the process was repeated. The remaining activity was determined using equation 2 compared to the first cycle.

$$\text{Remaining activity } \% = \frac{\text{activity in each cycle} \times 100}{\text{activity in the first cycle}} \quad (2)$$

Thermal stability The thermal stability of the immobilized system was evaluated after 1, 2, 6, and 8 h of incubation at 40 °C. The activity of PPL in each well was measured at zero time (as described in Section 2.2.3). For every interval tested, two wells were filled with buffer solution and placed in an incubator at 40 °C. After each incubation, the remaining activity of PPL in each well was calculated with the same procedure. Finally, the percentage of thermal stability was estimated using equation 3. The same experiment was conducted for the free lipase using the same method but with some differences: the remaining activity was determined after 5 min of incubation and under stirring at 750 rpm.

$$\text{Remaining activity } \% = \frac{\text{activity before incubation } \times 100}{\text{activity after incubation}} \quad (3)$$

Storage Stability The storage stability of the immobilized system was studied after incubating for 1, 2, 3, 4, and 8 weeks at 4 °C under dry conditions. The activity of PPL in each well was measured before incubation (as described in Section 2.2.3). Subsequently, the remaining activity of the lipase in each well was calculated after each time interval, as mentioned previously. Equation 3 was used for extracting the percentage of storage stability.

2.2.6 Kinetics Study of the Immobilized PPL

The Michaelis-Menten constant (K_m) represents an essential parameter of the enzyme kinetic reaction. It indicates the affinity between the enzyme and the substrate. The value of K_m was calculated by the Michaelis-Menten equation (4):

$$V = \frac{Vmax \times [S]}{Km + [S]} \quad (4)$$

where V and V_{max} are the initial and maximal velocities of the enzymatic reaction, respectively, and [S] is the concentration of the substrate.

For determining the K_m value of the free or the immobilized PPL, 0.125, 0.25, 0.5, and 1 mM concentrations of the pNPB solution were incubated with the biocatalyst for up to 20 min at 40 °C as described before. The K_m was obtained by the nonlinear regression of the Michaelis–Menten diagrams using Prism® 9.0 (GraphPad Software, USA).

2.2.7 X-ray Photoelectron Spectroscopy (XPS)

X-ray photoelectron spectroscopy (XPS) measurements were performed under an ultrahigh vacuum at a base pressure of 7×10^{-9} mbar using a FlexPS spectrometer (SPECS GmbH, Germany). The instrument was equipped with a monochromatic MgKα source (hv = 1253.6 eV) and a PHOIBOS 100 hemispherical analyzer (SPECS GmbH, Germany). The spectra were collected in normal emission, and the energy resolution was set to 1.16 eV to minimize the measuring time. The spectral analysis included a Shirley background subtraction and a peak deconvolution employing mixed Gaussian-Lorentzian functions in a least-squares curve-fitting program (WinSpec) developed at the Laboratoire Interdisciplinaire de Spectroscopie Electronique, University of Namur, Belgium.

2.2.8 Inhibition Assays

Inhibition by OrlistatOrlistat, a commercially available pancreatic lipase inhibitor, was chosen as the model compound for the inhibition studies. The stock solution of Orlistat was prepared by dissolution in DMSO, and concentrations of 0.005, 0.01, 0.02, 0.05, and 0.1 μM were used to determine the half-maximal inhibitory concentration (IC_{50}) at the fixed substrate concentration of 1 mM. In particular, the assay for evaluating the inhibition consisted of the following steps: (1) measuring the initial activity of the immobilized PPL (as described in Section 2.2.3), (2) pre-incubating the enzyme with the inhibitor solution for 10 min at 40 °C, and (3) adding the substrate and determining the remaining enzyme activity as described before. Wells with immobilized PPL were treated similarly but without any inhibitor as the controls. The percentage of DMSO in each reaction solution was fixed to 2% v/v. The inhibition rate was calculated by equation 5:

$$I(\%) = \frac{A_0 - A_i}{A_0} \times 100\% \quad (5)$$

where I (%) represents the inhibition rate, A_i and A_0 represent the enzymatic activity with or without inhibitors, respectively. The value of IC_{50} was obtained by the dose-response nonlinear regression equation using the PRISM® 9.0 software.

Evaluation of the Inhibitor Screening Assay The accuracy and reliability of the inhibition rate were evaluated by the Z' factor [31], which was calculated by equation 6:

$$Z' = 1 - \frac{3\delta_s + 3\delta_c}{|q_s - q_c|} \quad (6)$$

where q_s and q_c represent the average enzyme activity when there is no inhibitor (s, sample) and the inhibition rate is 100% (c, control), respectively. δ_s and δ_C refer to the average of the respective standard deviations of the data. q_c and δ_C are equal to 0 when the inhibition rate is 100%. Therefore, equation 6 is simplified to equation 7:

$$Z' = 1 - \frac{3\delta_s}{q_s} \quad (7)$$

A Z' value within the range of 0.5 to 1 indicates the accuracy and reliability of the proposed assay for screening inhibitors. The higher values suggest more accurate and reliable assays [31].

Inhibition by Olive Leaf Extract

(i) Preparation of the Olive leaf Extract The plant material, olive (*Olea europaea* L.) leaf (*Chondrolia Chalkidikis* cultivar), were collected from an olive orchard (Serres, Greece). The leaf were rinsed multiple times with tap water and then with dd H_2O and air-dried before use. The extraction method was according to Chatzikontantinou et al. [32]. In a standard procedure, 50 g of dry olive leaf were macerated in 250 mL dd H_2O and boiled for 60 min. The extract was filtered, and the water was removed through freeze-drying to obtain 3 g of dried material of aqueous olive leaf extract.

(ii) Inhibition Study The constructed PPL wells were used to screen the inhibitory activity of the olive leaf extract. A stock solution of the extract was prepared in 50 mM phosphate buffer (pH 7). The concentrations of 1, 2, 3, 5, 8, and 10 mg/mL of the extract were tested. The inhibition was evaluated using the method mentioned in Section 2.2.8. The value of IC_{50} was calculated in accordance with section 2.2.8.

3. Results

3.1 3D Printed Scaffolds for PPL Inhibition Studies

The present study elaborated on 3D printing technology for producing ready-to-use well plates for enzymatic assays. Previous reports have demonstrated the importance of developing multi-plate bioassay methods for enzyme inhibition studies and immobilized enzymes [24, 33]. The advantages include reduced reagent volumes, rapid testing of multiple compounds, and cost-efficiency. The study immobilized PPL inside 3D printed PLA wells to screen enzyme inhibitors, providing an efficient and low-cost (approximately 0.04€ per test) analytical tool. A synopsis of this process is presented in Figure 2. After designing and printing the desired model, the surfaces of the 3D scaffolds were modified according to our previous work [30]. The lipase from the porcine pancreas was immobilized inside the modified PLA wells with non-covalent interactions. An immobilization yield of 50% ± 6% was obtained for all samples using a fixed initial enzyme concentration. The prepared well plates were used for biocatalytic studies, as described in the following sections.

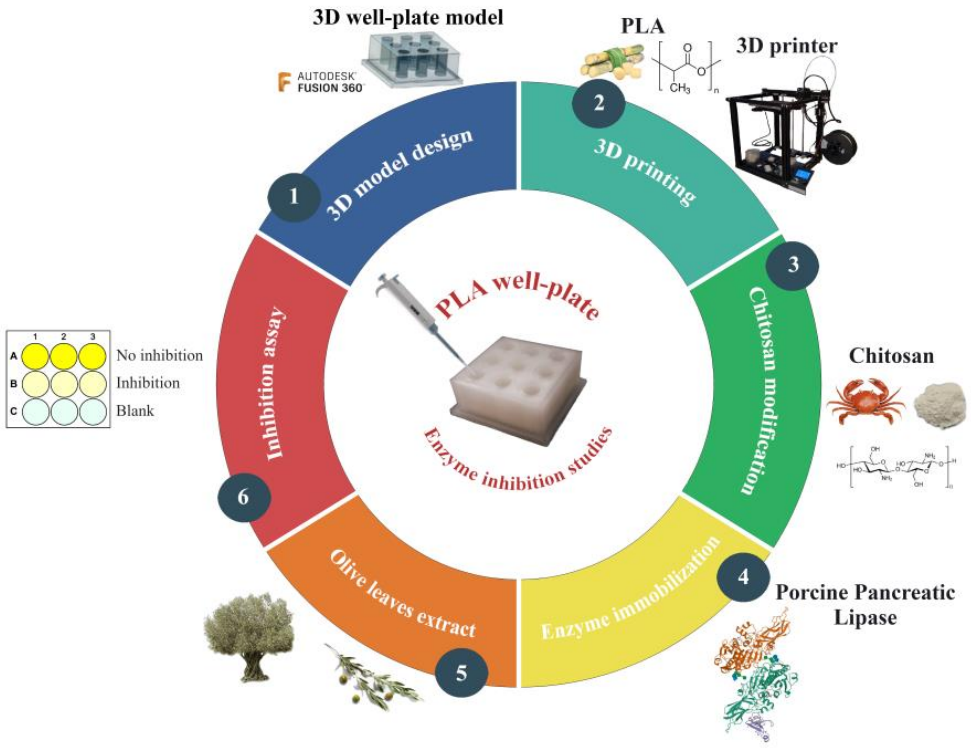


Figure 2 The process for scaffold preparation, enzyme immobilization, and enzyme inhibition studies

3.2 Spectroscopic Characterization of the Modified 3D Printed PLA Scaffolds

X-ray photoelectron spectroscopy (XPS) was performed after the NaOH-CS (0.2%) treatment for more profound information on the printed PLA scaffolds. The characteristic C-C/C-H, C-OH, C =O, and C(O)O peaks represented 65.0%, 11.6%, 13.5%, and 9.9% of the C1s photoelectron spectra, respectively (Figure 3A). These XPS analysis results are in accordance with our previous results for the same treatment [29]. The N1s peak demonstrated the existence of chitosan on the surface of the 3D-printed PLA scaffold. The atomic percentages are displayed in Table 1.

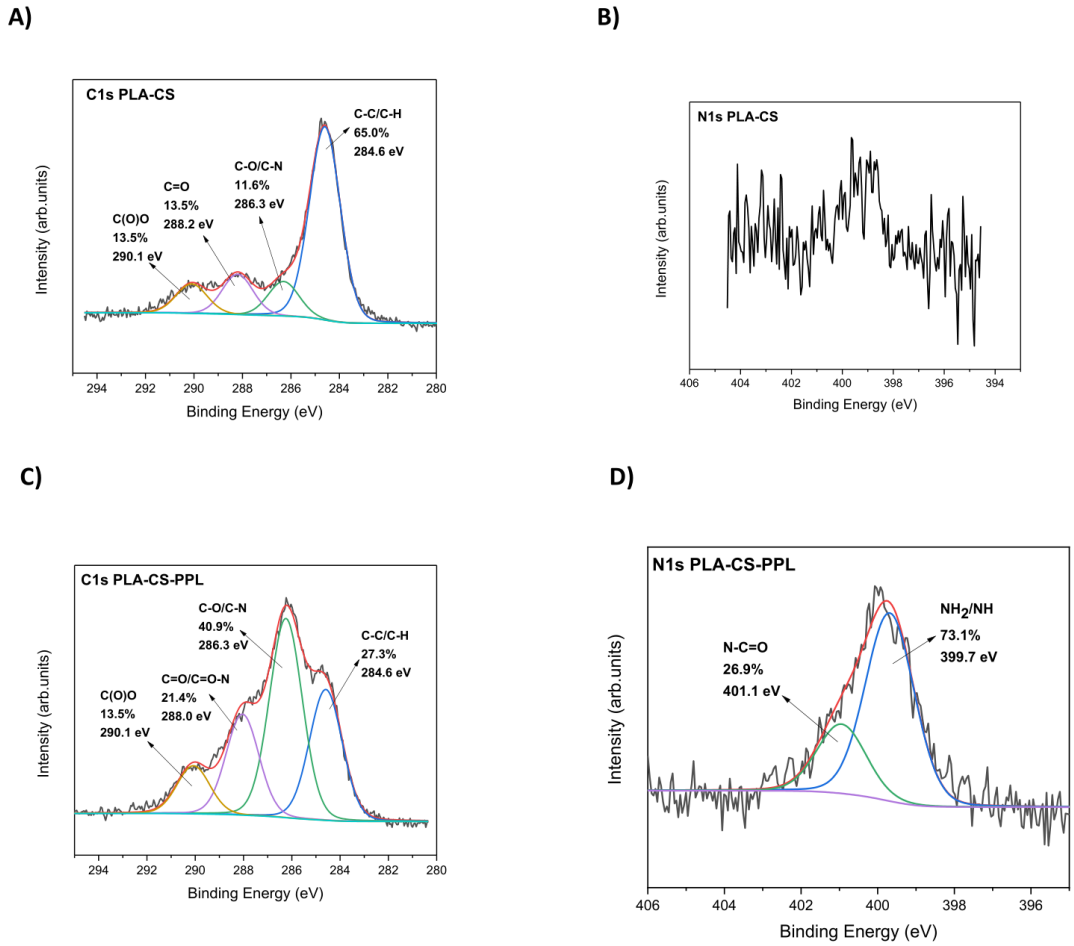


Figure 3 The C1s photoelectron spectra of (A) PLA-CS and (C) PLA-CS-PPL. The N1s photoelectron spectra of (B) PLA-CS and (D) PLA-CS-PPL.

After immobilizing PPL on the surface of PLA-NaOH-CS (0.2%), the C1s photoelectron peak changed significantly, indicating the successful incorporation of the enzyme (Figure 3C). The percentage of the major C-C peak reduced to 27.3%, while the C-OH peak at 286.3 eV dramatically increased to 40.9%. The C-N bonds from PPL also contributed to the same peak. The following peak at 288.0 eV is attributed to the C =O bonds and amide bonds of the PPL representing 21.4% of the whole carbon amount. Finally, the last peak at 290.1 eV may be due to the carboxylated groups. The N1s photoelectron peak is deconvoluted into two peaks, one main peak centered at 399.7 eV (73.1%) due to the NH_2/NH groups and one at 401.1 eV due to the amide formation of PPL (27.9%) (Figure 3B, Figure 3D). The atomic percentages are displayed in Table 2 and describe the increase of the Oxygen and the Nitrogen atoms compared to PLA-NaOH-CS 0.2%.

Table 2 Atomic percentages (%) of PLA modified with chitosan (PLA-CS), and PLA modified with chitosan and immobilized with PPL (PLA-CS-PPL).

Atom	PLA-CS	PLA-CS-PPL
C	72.9%	64.0%
O	25.9%	31.8%
N	1.2%	4.2%

3.3 Biocatalytic Characterization of the Immobilized PPL on 3D Printed PLA Scaffolds

3.3.1 Operational Stability

Enzyme immobilization plays a major partis important in catalyst stabilization, allowing for the repeated use of the active biocatalytic system. In fact, enzyme reuse is a prerequisite when establishing sustainable bioprocesses. Since organic solvents are frequently used for solubilization, their effects on enzymes have been studied for many years [34-36]. DMSO (dimethyl sulfoxide) is a well-known protein denaturant. Hence, it is essential to understand its effect on the enzyme activity in advance, especially when subjecting the enzyme to consecutive reactions. Literature reports on PPL suggest using less than 5% (v/v) of DMSO in enzymatic reactions because higher concentrations affect enzyme performance [37-40].

The reusability of the non-covalently immobilized PPL on the PLA wells was explored in terms of PPL activity in the presence of two reaction media − one without DMSO, while the other contained 2% (v/v) of DMSO. The substrate concentration was fixed at 1 mM, and ten consecutive reaction cycles were performed. After determining the activity of each cycle, the wells were washed, dried, and re-incubated with the corresponding reaction solution. The remaining (residual) activity of the immobilized PPL after each cycle is depicted in Figure 4A. Notably, at 0% DMSO concentration, the system maintained 59% of its initial activity in the 10^{th} cycle. At 2% DMSO concentration, the residual activity was reduced slightly (51%). The gradual activity loss at each cycle could be attributed to desorption, denaturation, or conformational changes in the enzyme molecules [41, 42]. Comparatively, the operational activity of the PPL immobilized non-covalently on different carriers was lower than that reported in the present work. For example, PPL adsorption on mesoporous chitosan beads retained 38% of the activity after ten cycles of reuse while hydrolyzing p-nitrophenyl palmitate (pNPP) [42]. However, its immobilization onto TiO_2/chitosan composite beads by adsorption and cross-linking exhibited nearly 50% of the activity after seven cycles of reuse while hydrolyzing p-nitrophenyl palmitate (pNPP [41]. Thus, the current study demonstrated the application of the immobilized PPL in successive reactions in both reaction media (0% or 2% DMSO for water-soluble or water-insoluble screened compounds, respectively). The lipase maintained more than half of its initial activity after ten cycles of reuse.

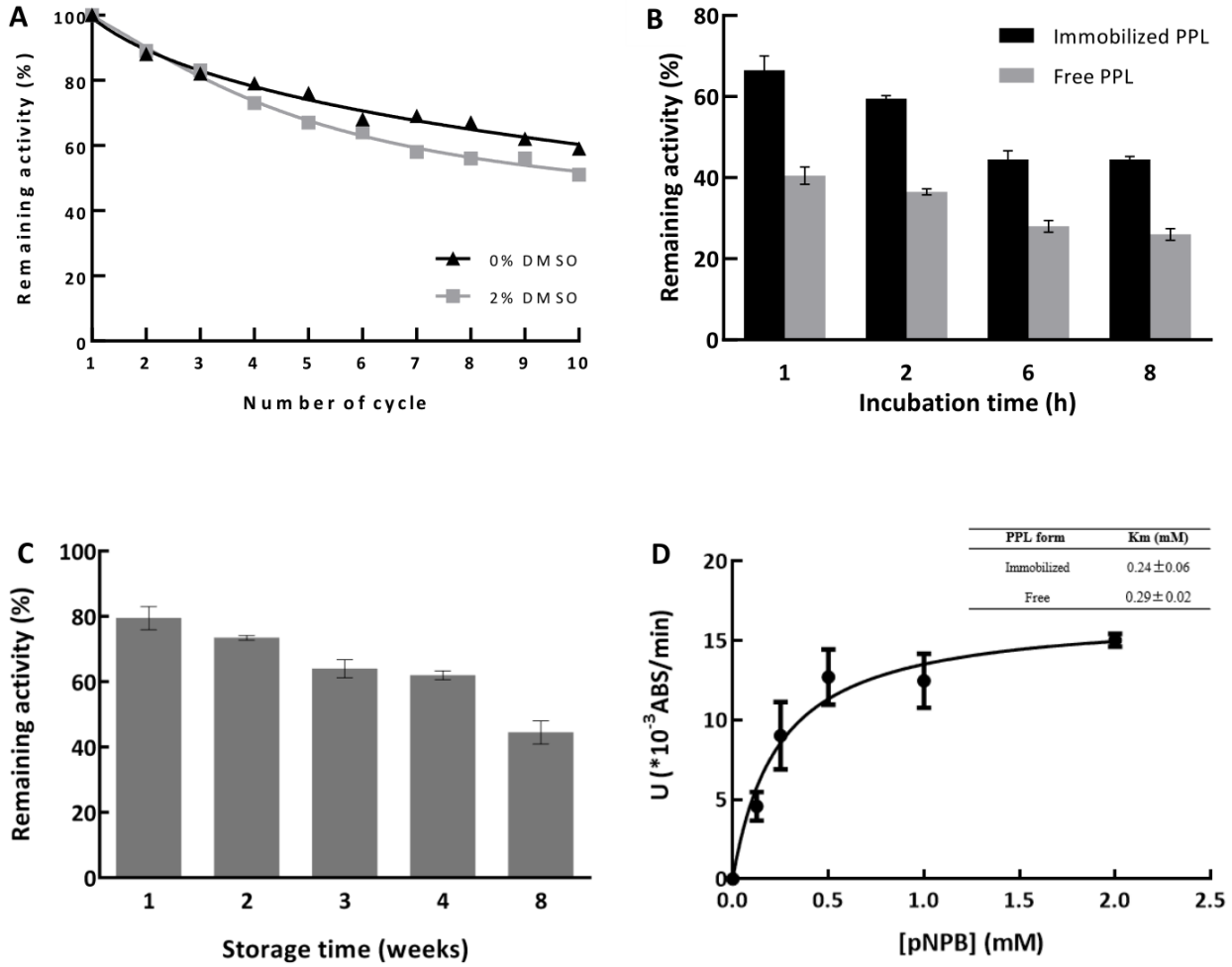


Figure 4 Biocataytic studies of the immobilized PPL on PLA wells. **(A)** Operational stability of the non-covalently immobilized PPL on PLA wells in the presence (2%) and absence (0%) of DMSO for ten cycles of reuse. The activity measured after the first use is considered 100%. (**B)** Thermal stability of the free and non-covalently immobilized PPL on PLA wells after incubation at 40 °C for 1, 2, 6, and 8 h. The activity exhibited before incubation is considered 100%. (**C)** Storage stability of the non-covalently immobilized PPL on PLA wells after incubation at 4 °C for 1, 2, 3, 4, and 8 weeks. The activity exhibited before storage is considered 100%. The reactions were performed at 40 °C for 20 min with 1 mM of the substrate (pNPB) in 0.05 M phosphate buffer (pH 7). (**D)** Michaelis–Menten plot for the PPL kinetic constant. The reactions were performed at 40 °C for 20 min with the substrate (pNPB) concentrations varying from 0.125 to 2 mM.

3.3.2 Thermal Stability

The thermal stability of a biocatalyst is its ability to withstand thermal denaturation without any substrate at high temperatures. Such a study is significant because the function of an enzyme is inseparable from its structure [43, 44]. Herein, the thermal stability of the immobilized and the free PPL was assessed for up to 8 h of incubation at 40 °C, the reaction temperature. The residual activity of the immobilized PPL indicates the activity of the free enzyme during each time interval tested. The immobilization of PPL was advantageous to lipase stability (Figure 4B). The immobilized PPL

retained 45% of its initial activity after 8 h of incubation at 40 °C, while the free PPL retained 26% under similar conditions. Indeed, other chitosan-based scaffolds support the above results [45-47]. The carefully designed immobilization carriers stabilize the biocatalytic system and offer a microenvironment that protects the enzyme from denaturation and, hence, activity loss.

3.3.3 Storage Stability

Storage stability is another aspect that should be tested when evaluating the efficiency of a biocatalytic system. Immobilization facilitates enzymatic stability, ensuring longer shelf life. The storage stability of the immobilized PPL was assessed after 1, 2, 3, 4, and 8 weeks of storage at 4 °C (Figure 4C). A sharp decline of about 20% was observed in the residual activity after the 1st week, possibly due to enzyme desorption. A comparable decrease in the activity of the immobilized form of PPL was also noted by Kilinç et al. (2002) in the first ten days of storage [48]. After eight weeks of storage, the residual activity of the PLA-immobilized PPL was 45%. Interestingly, the free enzyme lost more than half of its initial activity in the first week of storage. Thus, the biocatalytic system developed in the present study was stable and could be helpful in various applications.

3.3.4 Kinetic Study of the Immobilized PPL on PLA Wells

The effect of immobilization on the catalytic behavior of PLL was determined from the Michaelis-Menten plot. Several substrate concentrations (0.125–2 mM) were used to derive the Michaelis-Menten constants (K_m) of the free and immobilized enzymes (Figure 4D). The K_m value of the immobilized PPL was 0.24 ± 0.06 mM, which was similar to the K_m value of the free PPL (0.29 ± 0.02 mM). Thus, lipase adsorption on chitosan-modified PLA wells did not initiate steric hindrance of the active site. Hence, substrate accessibility and binding occurred without significant limitations.

3.4 Inhibition Studies

3.4.1 Inhibition by Orlistat

Evaluating PPL inhibition is clinically significant in obesity and related diseases. Also, establishing more efficient inhibition assays is critical. Hence, the prepared immobilized PPL wells were further applied in inhibitor screening assays. Orlistat, a commercially available pancreatic lipase inhibitor, was employed as the positive control to verify the proposed method. Varying concentrations (0.005–0.1 μM) of Orlistat were tested at a fixed substrate concentration (1 mM) to determine the half-maximal inhibitory concentration (IC_{50}) according to the dose-response nonlinear regression equation (Figure 5A, Figure 5B). The IC_{50} value for the immobilized PPL was 31.73 ± 6.52 nM, whereas that of the free lipase was 8.53 ± 1.68 nM. Therefore, the immobilized system detected the inhibitory effect exerted by the model compound, but 50% inhibition of PPL required a higher concentration. The observed difference between the two values could be attributed to the immobilization of the lipase on chitosan-modified PLA wells. Similarly, different inhibition rates between the free and immobilized form of cathepsin D were realized in some cases when the same extract or compound was incubated with both forms of the enzyme [49]. Notably, the IC_{50} values of Orlistat reported for PPL in the literature often are not comparable. They deviate largely among a variety of studies, ranging from (0.38 ± 0.05) × 10^{-3} μM to 60.48 ± 0.02 μM [39, 50]. These fluctuations may be due to the variations between the distinct assays. Hence, a more reliable

criterion was required to assess the inhibitory capacity of the immobilized enzyme. The Z' factor is a parameter that extensively reinforces the accurate detection and reliability of enzyme inhibitors in an assay procedure (Section 2.2.8.2). The present study identified 0.86 (n = 8) as the value of the Z' factor, indicating that the proposed method was ideal for recognizing PPL inhibitors [31]. The results mentioned above summarize that the immobilized PLA wells could be successfully incorporated in inhibition studies of various possible inhibitors of natural origin.

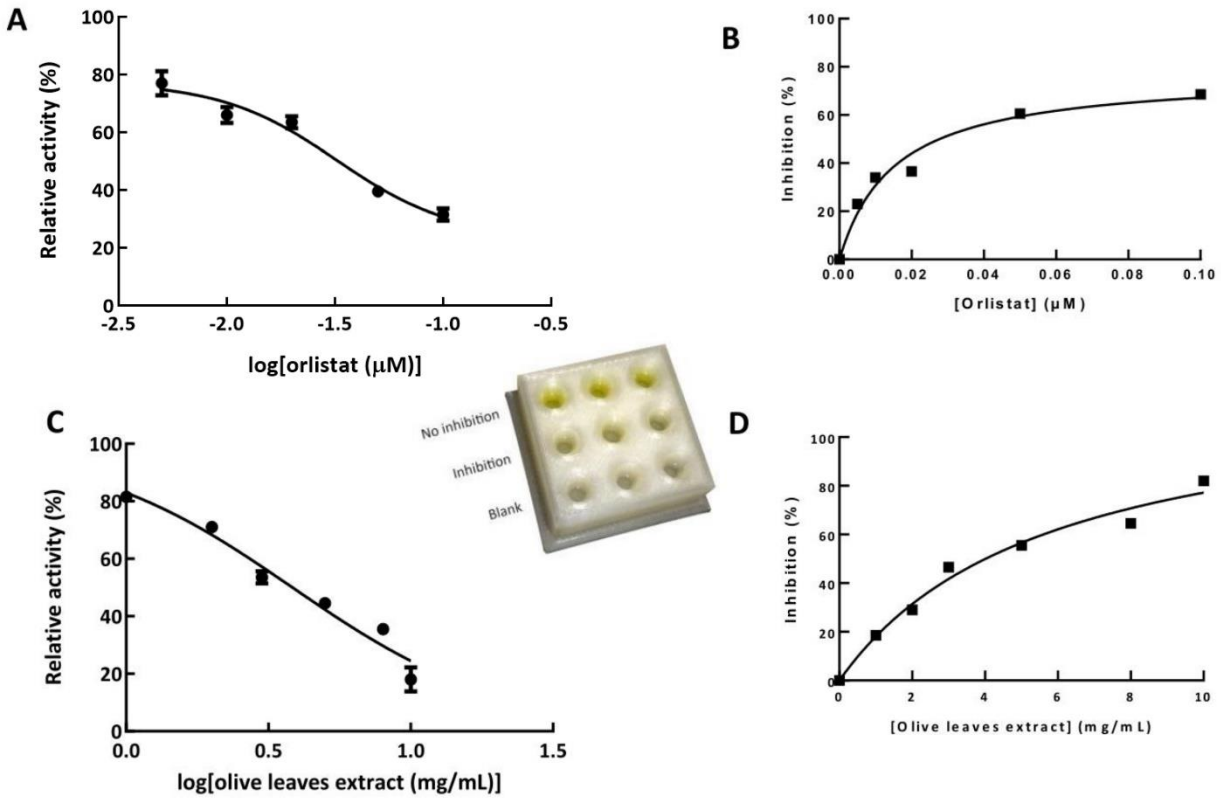


Figure 5 Inhibition studies of the immobilized PPL using Orlistat and olive leaf extract. **(A-B)** Determining the values of the inhibitory concentration (IC_{50}) of Orlistat for inhibiting immobilized PPL. The reactions were performed at 40 °C for 20 min using 1 mM of the substrate (pNPB). The orlistat concentrations ranged from 0.005–0.1 μM (2% DMSO) in 0.05 M phosphate buffer (pH 7). (**C-D)** Determining the values of the inhibitory concentraton (IC_{50}) of the olive leaf extract for inhibiting immobilized PPL. The reactions were performed at 40 °C for 20 min using 1 mM of the substrate (pNPB). The concentration of the olive leaf extract ranged from 1–10 mg/mL in 0.05 M phosphate buffer (pH 7). There was a 10 min pre-incubation period between the lipase and the inhibitor at 40 °C, after which the substrate was added.

3.4.2 Inhibition by Olive Leaf Extract

In a further study, a natural product, olive leaf extract, was also assessed for its inhibitory effect on PPL. When the assay was first performed with free PPL, the enzyme activity was reduced. Subsequently, the extract was used to determine the IC_{50} values of both forms. Varying concentrations (1–10 mg/mL) of the extract were investigated at a fixed substrate concentration (1 mM). The IC_{50} value of the olive leaf extract was 3.84 ± 0.48 mg/mL for the immobilized PPL (Figure

5C, Figure 5D, Table 3). This value was similar to that obtained for the free form (3.46 ± 0.34 mg/mL). Thus, the potentiality of the present assay for screening inhibitors was validated.

The inhibitory effect of extracts derived from *Olea europaea* L. on PPL has been also previously demonstrated. Buchholz and Melzig (2016) studied the PPL inhibitory activity of two olive leaf extracts. They obtained 0.186 ± 0.012 mg/mL and 6.772 ± 0.479 mg/mL as the respective IC_{50} values for the methanol and the aqueous extracts [50]. Consequently, the extraction solvent causes differences in the active components, thereby causing differences in the inhibitory potency of each extract. The differences in the content of the olive leaf extract used in the present study due to environmental and climatic conditions and the extraction method applied could be responsible for the different IC_{50} values of the aqueous extract.

Table 3 Inhibitory potency (IC_{50}) of Orlistat and olive leaf extract on PPL for both its immobilized and free form.

	IC_{50} for the immobilized PPL	**IC_{50} for the free PPL**
Orlistat	31.73 ± 6.52 nM	8.53 ± 1.68 nM
Olive leaf extract	3.84 ± 0.48 mg/mL	3.46 ± 0.34 mg/mL

Summing up, this study established a method for the development of a screening assay elaborating immobilized enzymes. The requirements for the development of a drug screening assay have been discussed thoroughly elsewhere [51]. Briefly, an inhibition assay must be able to detect inhibitors accurately and reliably; thus, which contributes to the assurance of assay quality as is denoted by Z' factor. In addition, the developed assay must be reproducible and of low cost. Another aspect that should be investigated is the influence of the presence of organic solvents, such as DMSO, to the assay performance, because this class of solvents are commonly used for chemical compounds preservation. Herein, the effect of the DMSO solvent on the enzymatic activity was evaluated and the value of Z' factor was determined as 0.86 (n = 8), which clarifies that the proposed method is accurate and reliable; therefore, appropriate for the identification of PPL inhibitors. Regarding the reproducibility and cost of the proposed method, a key feature of this study lies on the fabrication of the PLA well-plates through 3D printing, which allows for the adjustment of the number and volume of the wells, with a naturally-derived and low-cost feeding material. The surface modification of PLA with an eco-friendly, simple, time- and cost-efficient protocol based on chitosan, and the immobilization of PPL, which was found to be highly stable, allow for a highly reproducible method to develop biocatalytic systems.

4. Conclusions

The present work describes a method for enzyme immobilization and elaboration for inhibitors screening. 3D printed well-plates, served as immobilization scaffolds allowing for fast production of identical models of high quality and functionality to facilitate parameter testing. PLA was utilized as the immobilization matrix, being a material of agricultural origin, biocompatible and biodegradable, while pancreatic lipase was studied for being an important enzyme related to metabolic diseases. The study showed that the immobilized enzyme retains its catalytic characteristics presenting high

operational, thermal and storage stability; thus, demonstrating the potential of the enzyme-immobilized well-plates for a series of biocatalytic studies.

The prepared biocatalytic system was evaluated as an analytical tool for inhibitors screening, both for a model inhibitor-orlistat, and for a novel potential inhibitor-olive leaf extract. For the inhibition study, the value of Z' factor was determined as 0.86 (n = 8), which clarifies that the proposed method is appropriate for the identification of PPL inhibitors. The IC_{50} factor calculated for the olive leaf extract was 3.84 mg/mL, presenting a promising effect as an inhibitory agent of natural origin.

Thus, designing and fabricating scaffolds in a similar scale, which could serve as immobilization carriers, and their recruitment in inhibitors screening studies could be a promising bioanalytical tool, adding enzyme stability and reuse potentiality of the biocatalytic system, as essential prerequisites for sustainable bioprocess design.

Author Contributions

Anastasia Skonta: Conceptualization, Methodology, Investigation, Writing-Original draft, Elena Gkantzou: Conceptualization, Methodology, Investigation, Writing-Original draft-Review and Editing, Konstantinos Spyrou: Investigation, Data curation, Stamatia Spyrou: Investigation, Data curation, Angeliki Polydera: Writing-Review and Editing, Dimitrios Gournis: Writing-Review and Editing, Haralambos Stamatis: Conceptualization, Fund raising, Writing-Review and Editing, Supervision.

Funding

This research has been co-financed by the European Regional Development Fund of the European Union and Greek national funds through the Operational Program Competitiveness, Entrepreneurship, and Innovation, under the call RESEARCH–CREATE-INNOVATE (project code: T2EDK-01410).

Competing Interests

The authors have declared that no competing interests exist.

Additional Materials

The following additional material is uploaded at the page of this paper.

.STL file of well-plate model

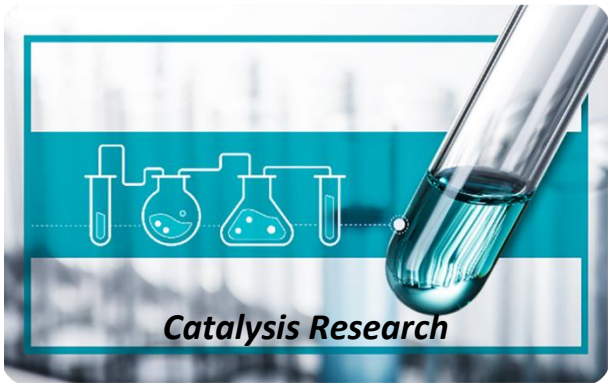
References

1. Birari RB, Bhutani KK. Pancreatic lipase inhibitors from natural sources: Unexplored potential. Drug Discov Today. 2007; 12: 879-889.
2. Hruby A, Hu FB. The epidemiology of obesity: A big picture. Pharmacoeconomics. 2015; 33: 673-689.

3. Liu TT, Liu XT, Chen QX, Shi Y. Lipase inhibitors for obesity: A review. Biomed Pharmacother. 2020; 128: 110314.
4. Zhu YT, Ren XY, Liu YM, Wei Y, Qing LS, Liao X. Covalent immobilization of porcine pancreatic lipase on carboxyl-activated magnetic nanoparticles: Characterization and application for enzymatic inhibition assays. Mater Sci Eng C Mater Biol Appl. 2014; 38: 278-285.
5. Winkler FK, D'Arcy A, Hunziker W. Structure of human pancreatic lipase. Nature. 1990; 343: 771-774.
6. de Caro J, Boudouard M, Bonicel J, Guidoni A, Desnuelle P, Rovery M. Porcine pancreatic lipase. Completion of the primary structure. Biochim Biophys Acta. 1981; 671: 129-138.
7. Heck AM, Yanovski JA, Calis KA. Orlistat, a new lipase inhibitor for the management of obesity. Pharmacotherapy. 2000; 20: 270-279.
8. Qi X. Review of the clinical effect of orlistat. IOP Conf Ser Mater Sci Eng. 2018; 301: 012063.
9. Rucker D, Padwal R, Li SK, Curioni C, Lau DC. Long term pharmacotherapy for obesity and overweight: Updated meta-analysis. BMJ. 2007; 335: 1194-1199.
10. Bhutani KK, Birari R, Kapat K. Potential anti-obesity and lipid lowering natural products: A review. Nat Prod Commun. 2007; 2: 331-348.
11. Sheldon RA. Enzyme immobilization: The quest for optimum performance. Adv Synth Catal. 2007; 349: 1289-1307.
12. Liu DM, Chen J, Shi YP. Advances on methods and easy separated support materials for enzymes immobilization. Trends Analyt Chem. 2018; 102: 332-342.
13. Shao Y, Liao Z, Gao B, He B. Emerging 3D printing strategies for enzyme immobilization: Materials, methods, and applications. ACS Omega. 2022; 7: 11530-11543.
14. Farah S, Anderson DG, Langer R. Physical and mechanical properties of PLA, and their functions in widespread applications — A comprehensive review. Adv Drug Deliv Rev. 2016; 107: 367-392.
15. Baran EH, Erbil HY. Surface modification of 3D printed PLA objects by fused deposition modeling: A review. Colloids Interfaces. 2019; 3: 43.
16. Spano MB, Tran BH, Majumdar S, Weiss GA. 3D-printed labware for high-throughput immobilization of enzymes. J Org Chem. 2020; 85: 8480-8488.
17. Ye J, Chu T, Chu J, Gao B, He B. A versatile approach for enzyme immobilization using chemically modified 3D-printed scaffolds. ACS Sustain Chem Eng. 2019; 7: 18048-18054.
18. Peris E, Okafor O, Kulcinskaja E, Goodridge R, Luis SV, Garcia-Verdugo E, et al. Tuneable 3D printed bioreactors for transaminations under continuous-flow. Green Chem. 2017; 19: 5345-5349.
19. Sirjani E, Migas M, Cragg PJ, Dymond MK. 3D printed UV/VIS detection systems constructed from transparent filaments and immobilised enzymes. Addit Manuf. 2020; 33: 101094.
20. Tothill AM, Partridge M, James SW, Tatam RP. Fabrication and optimisation of a fused filament 3D-printed microfluidic platform. J Micromech Microeng. 2017; 27: 035018.
21. Mulberry G, White KA, Vaidya M, Sugaya K, Kim BN. 3D printing and milling a real-time PCR device for infectious disease diagnostics. PLoS One. 2017; 12: e0179133.
22. Pantazis AK, Papadakis G, Parasyris K, Stavrinidis A, Gizeli E. 3D-printed bioreactors for DNA amplification: Application to companion diagnostics. Sens Actuators B Chem. 2020; 319: 128161.

23. Chudobova D, Cihalova K, Skalickova S, Zitka J, Rodrigo MA, Milosavljevic V, et al. 3D-printed chip for detection of methicillin-resistant staphylococcus aureus labeled with gold nanoparticles. Electrophoresis. 2015; 36: 457-466.
24. Lankatillake C, Luo S, Flavel M, Lenon GB, Gill H, Huynh T, et al. Screening natural product extracts for potential enzyme inhibitors: Protocols, and the standardisation of the usage of blanks in α-amylase, α-glucosidase and lipase assays. Plant Methods. 2021; 17: 3.
25. Kao CT, Lin CC, Chen YW, Yeh CH, Fang HY, Shie MY. Poly(dopamine) coating of 3D printed poly(lactic acid) scaffolds for bone tissue engineering. Mater Sci Eng C Mater Biol Appl. 2015; 56: 165-173.
26. Li S, Zhao S, Hou Y, Chen G, Chen Y, Zhang Z. Polylactic acid (PLA) modified by polyethylene glycol (PEG) for the immobilization of lipase. Appl Biochem Biotechnol. 2020; 190: 982-996.
27. Wang J, Nor Hidayah Z, Razak SIA, Kadir MRA, Nayan NHM, Li Y, et al. Surface entrapment of chitosan on 3D printed polylactic acid scaffold and its biomimetic growth of hydroxyapatite. Compos Interfaces. 2019; 26: 465-478.
28. Yeh CH, Chen YW, Shie MY, Fang HY. Poly(dopamine)-assisted immobilization of Xu Duan on 3D printed poly(lactic acid) scaffolds to up-regulate osteogenic and angiogenic markers of bone marrow stem cells. Materials. 2015; 8: 4299-4315.
29. Gkantzou E, Skonta A, Tsakni A, Polydera A, Moschovas D, Spyrou K, et al. 3D printed PLA enzyme microreactors: Characterization and application for the modification of bioactive compounds. J Biotechnol. 2022; 350: 75-85.
30. Gkantzou E, Skonta A, Vasios AG, Stamatis H. 3D printed polylactic acid well-plate for multi-enzyme immobilization. In: Multienzymatic assemblies: Methods and protocols. New York: Springer; 2022. pp. 163-175.
31. Zhang JH, Chung TD, Oldenburg KR. A simple statistical parameter for use in evaluation and validation of high throughput screening assays. J Biomol Screen. 1999; 4: 67-73.
32. Chatzikonstantinou AV, Giannakopoulou A, Spyrou S, Simos YV, Kontogianni VG, Peschos D, et al. Production of hydroxytyrosol rich extract from Olea europaea leaf with enhanced biological activity using immobilized enzyme reactors. Environ Sci Pollut Res Int. 2022; 29: 29624-29637.
33. Cacciotti I, Pallotto F, Scognamiglio V, Moscone D, Arduini F. Reusable optical multi-plate sensing system for pesticide detection by using electrospun membranes as smart support for acetylcholinesterase immobilisation. Mater Sci Eng C Mater Biol Appl. 2020; 111: 110744.
34. Lindsay RJ, Johnson QR, Evangelista W, Nellas RB, Shen T. DMSO enhanced conformational switch of an interfacial enzyme. Biopolymers. 2016; 105: 864-872.
35. Mangiagalli M, Carvalho H, Natalello A, Ferrario V, Pennati ML, Barbiroli A, et al. Diverse effects of aqueous polar co-solvents on Candida antarctica lipase B. Int J Biol Macromol. 2020; 150: 930-940.
36. Tsuzuki W, Ue A, Kitamura Y. Effect of dimethylsulfoxide on hydrolysis of lipase. Biosci Biotechnol Biochem. 2001; 65: 2078-2082.
37. George G, S˙N˙C˙ S, Paul AT. Investigation of synergistic potential of green tea polyphenols and orlistat combinations using pancreatic lipase assay-based synergy directed fractionation strategy. S Afr J Bot. 2020; 135: 50-57.
38. Itoh K, Matsukawa T, Murata K, Nishitani R, Yamagami M, Tomohiro N, et al. Pancreatic lipase inhibitory activity of Citrus unshiu leaf extract. Nat Prod Commun. 2019; 14: 1934578X19873439.

39. Li S, Pan J, Hu X, Zhang Y, Gong D, Zhang G. Kaempferol inhibits the activity of pancreatic lipase and its synergistic effect with orlistat. J Funct Foods. 2020; 72: 104041.
40. Ong SL, Mah SH, Lai HY. Porcine pancreatic lipase inhibitory agent isolated from medicinal herb and inhibition kinetics of extracts from Eleusine indica (L.) Gaertner. J Pharm (Cairo). 2016; 2016: 8764274.
41. Deveci I, Doğaç YI, Teke M, Mercimek B. Synthesis and characterization of chitosan/TiO_2 composite beads for improving stability of porcine pancreatic lipase. Appl Biochem Biotechnol. 2015; 175: 1052-1068.
42. Gilani SL, Najafpour GD, Moghadamnia A, Kamaruddin AH. Stability of immobilized porcine pancreas lipase on mesoporous chitosan beads: A comparative study. J Mol Catal B Enzym. 2016; 133: 144-153.
43. Zeiske T, Stafford KA, Palmer AG. Thermostability of enzymes from molecular dynamics simulations. J Chem Theory Comput. 2016; 12: 2489-2492.
44. Georis J, de Lemos Esteves F, Lamotte-Brasseur J, Bougnet V, Devreese B, Giannotta F, et al. An additional aromatic interaction improves the thermostability and thermophilicity of a mesophilic family 11 xylanase: Structural basis and molecular study. Protein Sci. 2000; 9: 466-475.
45. Bayramoğlu G. Methacrylated chitosan based UV curable support for enzyme immobilization. Mater Res. 2017; 20: 452-459.
46. Desai PD, Dave AM, Devi S. Alcoholysis of Salicornia oil using free and covalently bound lipase onto chitosan beads. Food Chem. 2006; 95: 193-199.
47. Ji S, Liu W, Su S, Gan C, Jia C. Chitosan derivative functionalized carbon nanotubes as carriers for enzyme immobilization to improve synthetic efficiency of ethyl caproate. LWT. 2021; 149: 111897.
48. Kilinç A, Önal S, Telefoncu A. Chemical attachment of porcine pancreatic lipase to crosslinked poly(vinyl alcohol) by means of adipoyldichloride. Process Biochem. 2002; 38: 641-647.
49. Cornelio VE, de Moraes MC, de Cassia Domingues V, Fernandes JB, das Gracas Fernandes da Silva MF, Cass QB, et al. Cathepsin D immobilized capillary reactors for on-flow screening assays. J Pharm Biomed Anal. 2018; 151: 252-259.
50. Buchholz T, Melzig MF. Medicinal plants traditionally used for treatment of obesity and diabetes mellitus - Screening for pancreatic lipase and α-amylase inhibition. Phytother Res. 2016; 30: 260-266.
51. Hughes JP, Rees S, Kalindjian SB, Philpott KL. Principles of early drug discovery. Br J Pharmacol. 2011; 162: 1239-1249.



Enjoy *Catalysis Research* by:

1. Submitting a manuscript
2. Joining in volunteer reviewer bank
3. Joining Editorial Board
4. Guest editing a special issue

For more details, please visit:
http://www.lidsen.com/journals/cr

micromachines

Article

Development of 3D Printed Enzymatic Microreactors for Lipase-Catalyzed Reactions in Deep Eutectic Solvent-Based Media

Myrto G. Bellou [1], Elena Gkantzou [1,*], Anastasia Skonta [1], Dimitrios Moschovas [2], Konstantinos Spyrou [2], Apostolos Avgeropoulos [2], Dimitrios Gournis [2] and Haralambos Stamatis [1,*]

[1] Laboratory of Biotechnology, Department of Biological Applications and Technologies, University of Ioannina, 45110 Ioannina, Greece
[2] Department of Materials Science and Engineering, University of Ioannina, 45110 Ioannina, Greece
* Correspondence: e.gkantzou@uoi.gr (E.G.); hstamati@uoi.gr (H.S.)

Abstract: In this study, 3D printing technology was exploited for the development of immobilized enzyme microreactors that could be used for biocatalytic processes in Deep Eutectic Solvent (DES)-based media. 3D-printed polylactic acid (PLA) microwell plates or tubular microfluidic reactors were modified with polyethylenimine (PEI) and lipase from *Candida antarctica* (CALB) was covalently immobilized in the interior of each structure. DESs were found to have a negligible effect on the activity and stability of CALB, and the system proved highly stable and reusable in the presence of DESs for the hydrolysis of p-nitrophenyl butyrate (p-NPB). A kinetic study under flow conditions revealed an enhancement of substrate accessibility in the presence of Betaine: Glycerol (Bet:Gly) DES, while the system was not severely affected by diffusion limitations. Incubation of microreactors in 100% Bet:Gly preserved the enzyme activity by 53% for 30 days of storage at 60 °C, while the buffer-stored sample had already been deactivated. The microfluidic enzyme reactor was efficiently used for the trans-esterification of ethyl ferulate (EF) with glycerol towards the production of glyceryl ferulate (GF), known for its antioxidant potential. The biocatalytic process under continuous flow conditions exhibited 23 times higher productivity than the batch reaction system. This study featured an effective and robust biocatalytic system with immobilized lipase that can be used both in hydrolytic and synthetic applications, while further optimization is expected to upgrade the microreactor system performance.

Keywords: 3D printing; immobilization; enzyme microreactor; deep eutectic solvents; lipase

check for updates

Citation: Bellou, M.G.; Gkantzou, E.; Skonta, A.; Moschovas, D.; Spyrou, K.; Avgeropoulos, A.; Gournis, D.; Stamatis, H. Development of 3D Printed Enzymatic Microreactors for Lipase-Catalyzed Reactions in Deep Eutectic Solvent-Based Media. *Micromachines* **2022**, *13*, 1954. https://doi.org/10.3390/mi13111954

Academic Editor: Andrea Ehrmann

Received: 23 October 2022
Accepted: 9 November 2022
Published: 11 November 2022

Publisher's Note: MDPI stays neutral with regard to jurisdictional claims in published maps and institutional affiliations.

Copyright: © 2022 by the authors. Licensee MDPI, Basel, Switzerland. This article is an open access article distributed under the terms and conditions of the Creative Commons Attribution (CC BY) license (https://creativecommons.org/licenses/by/4.0/).

1. Introduction

The narrative about miniaturized analytical systems (MAS) has been rapidly established in recent years, and, currently, 3D printing technology is gaining more and more space in this field of study. It is commonly accepted that microfluidic networks have greatly impacted the way experimentation and data analysis is performed on several levels, from complexity to robustness and testing speed. Incorporating additive manufacturing into this kind of microsystem allows the creation of integrated devices by end-users and at the point of use while providing freedom to create and change without prior knowledge [1]. Three-dimensional printed microfluidic channels have already been demonstrated for bio-based applications like protein detection, cell deposition and simulation, bacterial communities, tissue constructs, organ-on-a-chip, and microfluidic reactionware [2,3].

Enzymes are a class of macromolecule consisting of one or more folded amino chains forming a three-dimensional structure. They have the ability to bind molecules in the substrate binding pocket and perform catalysis in the adjacent active site, and they are especially known for their ability to surpass other catalysts with respect to chemical specificity, and regio- and enantio-selectivity. Biocatalysis, as a research field, employs one or

more enzymes (biocatalysts) to convert substrates into higher-value compounds, and biocatalytic systems have been realized in different industrial processes, from food products, pharmaceuticals, cosmetics, and textiles, to biofuels and water purification [4]. However, the water solubility of biocatalysts hinders their recovery and recyclability, essential prerequisites for a circular economy. The development of enzyme immobilization has proved a revolutionary technology in this respect, changing radically enzyme performance, since biocatalytic systems that are highly reusable and stable under different reaction conditions are now a fact. Different types of biocatalytic systems with immobilized enzymes have been explored, utilizing nanomaterials or micro-scale materials as immobilization scaffolds [5,6]. Three-dimensional printing technology has come to offer such immobilization scaffolds, which can be designed with programmable structures in a scalable and cost-effective form. The advantages of merging these technologies include strong operability since complex structures are printed with pores and channels at low cost, while the enzyme-immobilized scaffold will not suffer material loss or make use of undesirable chemical reagents [7]. In addition, 3D printing materials are (bio)degradable and recyclable, leaving no environmental footprint. In view of these advantages, researchers have explored 3D printing for enzyme immobilization for industrial and healthcare applications [8].

Deep Eutectic Solvents (DESs) and their natural counterparts (NaDESs) have lately been employed in the biocatalysis field, where a plethora of different enzymes (mainly hydrolases and oxidoreductases), such as β-glucosidases [9,10], cytochrome P450 [11], laccases [12,13], and lipases [14], have been studied in the presence of DESs that act as co-solvents in DES-buffer solutions. This is because they are nontoxic, nonvolatile, nonflammable, and even biodegradable, rendering them a cost-efficient and enzyme-compatible reaction media [15]. DESs have a eutectic nature and are prepared by mixing a hydrogen bond donor (HBD) and a hydrogen bond acceptor (HBA) while being stirred and heated until a liquid is formed. The DES retains its liquid form at ambient temperature due to the formation of intramolecular hydrogen bonds, thus leading to a decreased freezing point. DESs are usually produced by using inexpensive quaternary ammonium salts such as choline chloride, millions of tons of which are produced every year, combined with HBDs from renewable sources such as sugars, amino acids, alcohols, and process wastes such as glycerol, depending on the desired application [16]. In addition to the concept of reaction media, research is moving toward the 2-in-1 concept in which the DES simultaneously acts as the reaction medium and the substrate pool, one (or both) of its components being the substrate of the biotransformation reaction, thus promoting the sustainability of the system [16–20].

Combining the above knowledge, this study proposes the use of 3D printing technology to develop microdevices for biocatalytic applications exploiting the effect of DESs on immobilized enzyme performance. The material of choice was polylactic acid (PLA), a widely used thermoplastic polymer known for its excellent biocompatibility and biodegradability, exploited in several bio-related applications as a common 3D printable material [21]. Our group has already demonstrated the potential of PLA for immobilized enzyme microreactor development [22]. However, biocatalytic processes in 3D-printed scaffolds are currently being performed merely in aqueous solution [23], since organic solvents that have been exploited for synthetic reactions with other support materials [24] have been proved improper for 3D-printed PLA structures, as was indicated in a recent study [25]. For this reason, herein, DESs were explored as alternative solvents for biocatalytic processes both in aqueous and non-aqueous reaction systems. As a biocatalyst, lipase from *Candida antarctica* B was used, one of the first enzymes exploited in DES-based processes and widely studied for its diverse biotechnological applications [26]. The incorporation of DESs into continuous biocatalytic processes in microreactor systems has been recently exerted by experts in the field of the application of DESs in biocatalysis [18,27]. More specifically, it has been proposed that the employment of DESs as alternative solvents in microfluidic bioprocesses renders these systems sustainable and highly efficient [27].

This study describes the use of 3D-printed well plates as screening platforms for immobilized lipase performance in the presence of different DESs. The most promising DES in terms of enzyme activity and stability was tested for its performance as a reaction medium component for continuous flow biocatalysis in 3D-printed microreactors. Biocatalytic characteristics for immobilized lipase were investigated in terms of enzyme concentration, flow rate (kinetic characteristics), operational stability, and stability after storage in 100% DES solution. The potential for a lipase-catalyzed transesterification reaction in a 100% DES medium was also demonstrated in a continuous flow system.

2. Materials and Methods

Choline chloride > 98%, betaine 98%, D(+)-glucose 99.5%, D(-)-fructose, polyethyleneimine, branched (PEI), ethyl-4-hydroxy-3-methoxycinnamate (ethyl ferulate) 4-nitrophenyl butyrate (pNPB) > 98%, and p-nitrophenol (pNP) were obtained from Sigma-Aldrich, St. Louis, MI, USA. Choline dihydrogen phosphate >98% was bought from IOLITEC, (Heilbronn, Germany), ethylammonium chloride from Merck (Sigma-Aldrich, USA), urea > 99% from Fluka (Sigma-Aldrich, USA), glycerol 0.5% max water, and Glutaraldehyde 25% solution from Fisher Scientific (Hampton, NH, USA), ethylene glycol from AppliChem (Darmstadt, Germany), 1,2-butanediol > 98% from TCI (Japan), 1,2-propanediol 99% from Acros Organics (Waltham, MA, USA), and sodium hydroxide > 98% from Panreac (Barcelona, Spain). The HPLC solvents acetonitrile, methanol, and water were of HPLC grade and the water used was double distilled. The lipases from *Candida antarctica* Lipozyme CALB L (liquid) and Novozym 435 (immobilized) were kindly offered by Novozymes (Bagsværd, Denmark). PLA filament designed for use with FDM 3D printers (PrimaValue™) was purchased from Prima Creator (Malmö, Sweden). The 3D printer used was an Ender 5 from Creality 3D (Shenzhen, China).

2.1. Three-Dimensional Design and Printing of PLA Models

PLA models were designed using the Fusion 360 CAD program from Autodesk (California, USA), as described in our previous works [22,28]. Briefly, well plates with a customized number of wells were designed with a 150 µL volume capacity for each well. Accordingly, microreactors with a serpentine-like internal structure were designed with a 150 µL working volume. Examples of a nine-well plate and a microreactor model are presented in Figure 1. The final designs were forwarded to the slicing software Cura (Ultimaker, Utrecht, The Netherlands), where appropriate slicing settings were applied, depending on the filament type and the 3D printer used. The printing parameters set by the slicing software are summarized in Table 1. The final printed models were leak-free and ready to use for further experimentation. This was confirmed by filling the printed models with buffer solution and leaving them for 24 h at room temperature. At the end of this period, the total volume collected was the same as the total volume loaded, so no leakage was observed. Additionally, when different flow rates were applied in the microreactor, the total volumes measured at the input and output of the microreactor were identical.

Table 1. Printing parameters set by the slicing software.

Parameter	Value
Layer Height	0.16 mm
Infill Density	100%
Printing Temperature	200 °C
Build Plate Temperature	50 °C
Print Speed	80 mm/s
Nozzle Size	0.4 mm
Filament Diameter	1.75 mm

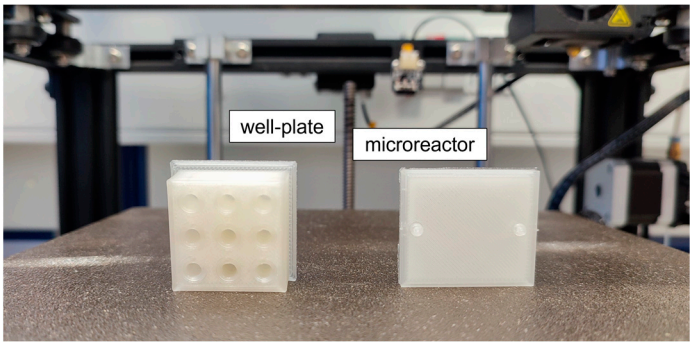


Figure 1. 3D-printed models made of natural polylactic acid (PLA). The well plate can be designed with a customized number of wells depending on the experimental needs, while the microreactor bares a serpentine-like internal shape in order to hold more volume in a smaller space. The models are ready-to-use after printing (no post-printing treatment needed).

2.2. Surface Modification and Enzyme Immobilization on PLA Models

The modification of the PLA scaffolds and the immobilization of lipase were based on previously reported 3D-printed PLA modification protocol [29]. Sodium hydroxide (NaOH) was used for surface etching in order to promote hydrophilicity of the PLA surface, and polyethylenimine (PEI) was used as the main modification agent. Previous studies have shown that NaOH treatment significantly enhances PLA surface roughness [30], making interactions with modification agents more feasible [31,32]. Covalent and non-covalent immobilization methods were investigated. Lipase was either linked on the PEI surface by a glutaraldehyde cross-linking method or absorbed on the PEI-modified PLA, and the corresponding enzyme activity was determined. The results are presented in Supplementary Figure S2, and the covalent linkage was chosen for the subsequent studies.

Firstly, the PLA surface was modified with sodium hydroxide (NaOH). A 150 μL sample of 1 M aqueous solution was added to each well followed by incubation at 25 °C for 2 h. Afterward, the NaOH solution was removed, and the wells were washed twice using 150 μL of double distilled water. Then, the well plate was dried under vacuum for 30 min. Next, 150 μL of 2 mg/mL PEI aqueous solution were added to each well and incubated at 25 °C for 1h. After the incubation, the PEI solution was removed, and the wells were washed twice using 150 μL of double-distilled water. Then, the plate was dried under a N_2 stream for 30 s. In the next step, glutaraldehyde (GA) was used as the cross-linking agent between PEI and Candida antarctica lipase B (CALB) for the covalent immobilization of the enzyme on the support. A 150 μL sample of 2.5% *v*/*v* GA solution in 50 mM pH 7 phosphate buffer was added to each well and incubation at 30 °C for 1 h followed. After, the GA solution was removed, the wells were washed thrice using 150 μL of 50 mM pH 7 phosphate buffer. The well plate was dried under a N_2 stream for 30 s. For the enzyme immobilization, a solution of 0.175 mg/mL CALB was prepared in 50 mM phosphate buffer pH 7.5. Each well was filled with 150 μL of the CALB solution and incubation at 30 °C for 1 h followed. Next, the CALB solution was removed and the well was washed thrice using 150 μL of 50 mM phosphate buffer pH 7.5. The well plate was dried under vacuum for 30 min and stored at 4 °C until further use.

The same protocol was used for the modification of the PLA microreactors, with the exception that each microreactor was filled with 150 μL of each solution using disposable 1 mL syringes. The concentrations of the solutions were the same, except for the enzyme solution whose concentration was 0.044 mg/mL and was prepared in 50 mM phosphate buffer pH 7.5 (unless stated otherwise). Additionally, drying was performed under a N_2 stream for 30 s in every case. The estimation of the concentration of the protein contained in the commercial liquid enzyme preparation was conducted using the Bradford assay [33].

2.3. Activity of Immobilized CALB on PLA Well plates

The activity measurement of the immobilized lipase was achieved by photometrically observing the hydrolysis of the model substrate p-nitrophenyl butyrate (pNPB). For this purpose, a stock solution of 12.5 mM pNPB was prepared in acetonitrile. A 150 μL sample of 0.25 mM pNPB solution in 50 mM phosphate buffer pH 7.5 (2% acetonitrile) was added to each well and the well plate was incubated at 40 °C for 5 min in order for the reaction to progress. The absorbance of the p-nitrophenol (pNP) that was produced from the hydrolysis of pNPB was measured in an ELISA plate reader at 405 nm. Measurements were conducted in triplicate. A standard curve of pNP was prepared and used for the calculation of the units of lipase activity.

2.4. Preparation of Deep Eutectic Solvents (DESs)

Certain quantities of a series of HBAs and HBDs were weighted and mixed in a glass vial in order to form the DESs of the required molar ratio (Table 2). The prepared mixtures were then incubated at 80 °C at 180 rpm until a clear solution was formed (~1 h). The prepared DESs were stored at 30 °C until further use.

Table 2. The prepared DESs used in this study.

DES [HBA: HBD (: HBD)]	Molar Ratio	Name Code
Choline Chloride: Glycerol	1:2	ChCl:Gly
Choline Chloride: Butylene Glycol	1:4	ChCl:BG
Choline Chloride: Propylene Glycol	1:2	ChCl:PG
Choline Chloride: Ethylene Glycol	1:2	ChCl:EG
Betaine: Glycerol	1:3	Bet:Gly
Betaine: Ethylene Glycol	1:3	Bet:EG
Choline Chloride: Glycerol: Ethylene Glycol	1:1:1	ChCl:Gly:EG
Choline Chloride: Urea: Ethylene Glycol	1:1:1	ChCl:U:EG
Choline Chloride: U: Glycerol	1:1:1	ChCl:U:Gly
Choline Chloride: Urea	1:2	ChCl:U
Ethylammonium Chloride: Urea	1:1.5	EAC:U
Ethylammonium Chloride: Ethylene Glycol	1:1.5	EAC:EG
Ethylammonium Chloride: Glycerol	1:1.5	EAC:Gly
Choline Dihydrogen Phosphate: Glycerol	1:3	Chol DHP:Gly
Choline Dihydrogen Phosphate: Ethylene Glycol	1:3	Chol DHP:EG
Choline Chloride: Fructose: H_2O	5:2:5	ChCl:Fru:H_2O
Choline Chloride: Glucose: H_2O	5:2:5	ChCl:Glc:H_2O

2.5. Effect of DESs on the Activity of Immobilized CALB

The activity of the immobilized lipase on PLA wells was screened in a series of DES-buffer solutions of varied DES concentrations. The enzyme activity was measured as described in Section 2.3, with the alteration that the 150 μL of 0.25 mM pNPB solution in 50 mM phosphate buffer pH 7.5 that were added to the wells contained 10% *v*/*v*, 20% or 50% *v*/*v* of each DES. Measurements were conducted in triplicate.

2.6. Effect of DESs on the Stability of Immobilized CALB

The stability of the immobilized lipase on PLA well plates was assessed for a 1 h incubation at 40 °C, in the presence of several DESs at different concentrations. First, the enzyme activity was measured as described in Section 2.3. Then, wells were washed thrice with phosphate buffer and dried under a N_2 stream for 30 s. Then, 150 μL of different concentrations of DESs in 50 mM phosphate buffer pH 7.5 (0, 10, 20, 50, and 100% *v*/*v* DES) were added to the wells, and these were incubated at 40 °C for 1 h. After the incubation, the solutions were removed, and the well plates were washed thrice with phosphate buffer and dried under a N_2 stream for 30 s. Then, the enzyme activity was measured again. All measurements were conducted in triplicate. For each well, the remaining activity of the lipase is expressed as follows:

$$\text{Remaining activity (\%)} = \text{Activity after incubation} \times 100/\text{Activity before incubation (\%)} \quad (1)$$

2.7. Storage Stability of Immobilized CALB on PLA Well plates

The storage stability of the immobilized system was evaluated for up to 2 months of storage at 4 °C. The enzyme activity was determined as described in Section 2.3 and wells were washed thrice with phosphate buffer and dried under a N_2 stream for 30 s. Subsequently, the enzymatic activity of the immobilized CALB was measured after 1, 3, 4, 5, and 8 weeks of storage, and the remaining activity was estimated. Measurements were conducted in triplicate.

2.8. Spectroscopic and Morphological Characterization

X-ray photoelectron spectroscopy (XPS) measurements were performed in an ultrahigh vacuum at a base pressure of 7×10^{-9} mbar with a SPECS GmbH spectrometer equipped with a monochromatic MgKa source (hv = 1253.6 eV) and a Phoibos-100 hemispherical analyzer (Berlin, Germany). The spectra were collected in normal emission and the energy resolution was set to 1.16 eV to minimize measuring time. The spectral analysis, including a Shirley background subtraction and a peak deconvolution employing mixed Gaussian-Lorentzian functions, was performed in a least squares curve-fitting program (WinSpec) developed at the Laboratoire Interdisciplinaire de Spectroscopie Electronique, University of Namur, Namur, Belgium.

Scanning electron microscopy (SEM) images were obtained using a JEOL JSM-6510 LV SEM Microscope (JEOL Ltd., Tokyo, Japan) equipped with an X–Act EDS-detector by Oxford Instruments, Abingdon, Oxfordshire, UK (an acceleration voltage of 20 kV was applied). Prior to SEM analysis, the samples were coated with an Au/Pd thin film (4–8 nm) in a sputtering machine (SC7620, Quorum Technologies, Lewes, UK).

2.9. Assays in PLA Microreactors

2.9.1. Activity Measurement of Immobilized CALB in PLA Microreactors

The activity of the immobilized lipase in the PLA microreactor was determined as described in Section 2.3 with the exception that the substrate solution was loaded in the microreactor by using a syringe pump system with a flow rate of 300 μL/min and residence time (t_R) 30 s (unless stated otherwise). The effluent (150 μL) of the microreactor was collected and the absorbance of the produced pNP was measured in an ELISA plate reader at 405 nm. Measurements were conducted in triplicate.

2.9.2. Effect of Enzyme Concentration

In order to examine the effect of different enzyme concentrations on the activity of the biocatalytic microreactor system, seven enzyme concentrations from 0.01 mg/mL to 3.5 mg/mL were tested. The enzyme immobilization process was performed as described in Section 2.2, except for the varying concentrations of the enzymatic solutions that were used. After the lipase immobilization, the determination of the enzymatic activity of the microreactor followed, as referred at Section 2.9.1. All measurements were conducted in triplicate.

2.9.3. Determination of the Immobilization Yield

The estimation of the immobilization yield was performed as described by the following equation:

$$\text{Immobilization yield (\%)} = 100 - (\text{activity after immobilization} \times 100)/(\text{activity before immobilization}) \text{ (\%)} \quad (2)$$

Measurements were conducted in triplicate.

2.9.4. Effect of Flow Rate in the Presence or Absence of DES

For the evaluation of the effect of the flow rate on the system performance, different substrate concentrations in combination with different flow rates were applied. Substrate solutions containing different concentrations of pNPB (0.125, 0.25, 0.5, 1, 2, and 4 mM) and 10% v/v DES (in the case of the presence of DES) in 50 mM phosphate buffer pH 7.5 were introduced into the microreactor at four different flow rates (75, 150, 300, and 600 μL/min), respectively. Then, the effluent (150 μL) was collected and the absorbance of the produced pNP was measured in an ELISA plate reader at 405 nm. The Lilly–Hornby model, as an adaptation of the classical Michaelis–Menten kinetic model, is used for investigating the flow kinetics of enzymes immobilized in microreactors and is described by the following equation:

$$f \times [A]_0 = K_{m(app)} \times \ln(1 - f) + \frac{C}{Q} \quad (3)$$

where f is the fraction of the substrate converted to the final product during the reaction, Q is the flow rate of the substrate, $[A]_0$ is the initial substrate concentration, C is the reaction capacity of the microreactor, and $K_{m(app)}$ is the apparent Michaelis constant.

For the estimation of the lipase kinetics in a batch system, a 5 μL/mL (87.5 μg/mL) stock of free CALB was prepared in 50 mM phosphate buffer pH 7.5. A 3 μL sample of the enzyme stock (1.3 μg/mL) was added to solutions containing different concentrations of pNPB (0.125, 0.25, 0.5, 1, 2, and 4 mM,) and 10% v/v DES (in the case of the presence of DES) at a final volume of 200 μL in a 96-well plate. The reaction progress was determined spectrophotometrically using an ELISA plate reader at 405 nm, at 40 °C for 5 min, to determine the initial reaction rate. In order to calculate the kinetic constants, nonlinear regression fitting of the initial reaction data depended on the pNPB concentrations was performed, by applying the Michaelis–Menten model (EnzFitter, Biosoft, UK). All measurements were conducted in triplicate.

2.9.5. Operational Stability in the Presence or Absence of DES

The operational stability of the immobilized CALB in PLA microreactors was evaluated for 100 subsequent cycles of use (55 min of continuous use) in the presence or absence of DES. One cycle was defined as the transition of 150 μL of the substrate solution through the microreactor. A syringe pump was used which was loaded with the corresponding volume of 0.25 mM pNPB solution in 50 mM phosphate buffer pH 7.5. After every 10 cycles of use (cycles of 30 s, flow rate 300 μL/min) the tenth effluent (150 μL) was collected, and the absorbance of the produced pNP was measured in an ELISA plate reader at 405 nm. The same procedure was followed for the determination of the operational stability of immobilized lipase in 10% v/v DES. All measurements were conducted in triplicate.

2.9.6. Thermal Stability of Immobilized CALB in 100% DES

The stability of the immobilized lipase in PLA microreactors was tested in the presence of 100% DES and 100% buffer solution at 60 °C for a total period of one month. Initially, the activity of the lipase was measured as mentioned in Section 2.9.1. Then, the microreactors were washed thrice with 200 μL 50 mM phosphate buffer pH 7.5 and dried under a N_2 stream for 30 s. Next, the microreactors were filled with 100% DES or 100% phosphate buffer, and the edges were tightly covered with parafilm, in order for the buffer not to evaporate. The microreactors were incubated at 60 °C and at regular time intervals (1, 2, 3, 6, 9, 20, and 30 days), the DES or the buffer was removed, the microreactors were washed and dried, and the remaining enzyme activity was determined as described above. All measurements were conducted in triplicate.

2.9.7. Transesterification Reactions in Microreactor and Batch Systems

The microreactor was used for the transesterification of ethyl ferulate with glycerol. A solution of 2 mM of ethyl ferulate (0.44 mg/mL) in 100% v/v DES Bet:Gly was prepared and incubated at 60 °C, 800 rpm until ethyl ferulate was fully dissolved in the DES. A

peristaltic pump was used for the transition of 150 μL of the substrate solution through the microreactor. The continuous flow transesterification was performed for a total residence time (t_R) of 4 h under a peristaltic flow pattern (24 runs × 10 min) with a flow rate of 15 μL/min. The temperature was kept constant at 60 °C. At the end of the experiment, the effluent was collected in an Eppendorf tube. In addition, 450 μL of methanol were pumped through the microreactor with a flow rate of 150 μL/min in order to collect any amount of substrate or product that might have not been collected. The reaction product was determined as described in Section 2.9.8.

The transesterification reaction was also performed in batch systems, catalyzed by free CALB and its commercial immobilized form (Novozyme 435). The enzyme concentration used for free CALB was 0.03 mg/mL (1.7 μL/mL) and for Novozyme 435 was 0.3 mg/mL (comparable with the amount of protein immobilized in the microreactor system). The lipases were added in 1 mL of 2 mM ethyl ferulate dissolved in 100% v/v Bet:Gly and incubated for 4 h at 60 °C and 800 rpm. At the end of the experiment, the reaction product was analyzed through HPLC, as described in Section 2.9.8. All measurements were conducted in triplicate.

2.9.8. HPLC Analysis

The transesterification reaction of ethyl ferulate with glycerol was analyzed through high-performance liquid chromatography (HPLC) in an HPLC system equipped with a μBondapak C18 reversed-phase column (particle size 10 μm, length 300 mm, diameter 3.9 mm) and a diode array UV detector. The mobile phase consisted of 40% Acetonitrile (A) and 60% water with 0.1% acetic acid (B) and the elution was isocratic with a flow rate of 1 mL min^{-1}. The temperature of the column was set to 35 °C and the injection volume was 20 μL. The substrate ethyl ferulate and the transesterification product glyceryl ferulate were detected at 320 nm. A 100 μL sample of the reaction mixture was obtained at the beginning (0 h) and again at the end of the reaction time (4 h), respectively, and was added to 300 μL of HPLC Water, 20 μL from which were injected into the system for the analysis. No dilution was performed for the methanol effluent. Blank samples were also prepared and analyzed. Calibration curves were constructed by different concentrations of ethyl ferulate. The total conversion yield was determined by the decrease in the amount of ethyl ferulate.

3. Results

In the first part of this study, the effect of various DESs on the biocatalytic performance of the immobilized CALB on 3D-printed PLA structures was investigated. Biocatalytic studies were conducted in 3D-printed PLA well plates where the enzyme was immobilized in the interior walls, according to the methodology presented in our previous works [28,34]. The surface of the 3D-printed PLA structures was modified with PEI, which has been previously demonstrated as an effective modification agent for 3D-printed PLA structures [29], while it has also been exploited in enzymatic studies for its protective role against biomolecules and its stabilization effect on immobilized lipases [35–37].

3.1. Characterization Studies of Modified 3D-Printed PLA Scaffolds

3.1.1. X-ray Photoelectron Spectroscopy (XPS)

In order to investigate the surface modification of the 3D-printed PLA structures before and after enzyme grafting, XPS analysis was performed. Figure 2 shows the high-resolution C1s photoelectron spectra of (a) NaOH-PEI, and (b) NaOH-PEI-CALB. The fitted peaks reveal the characteristic bonds on the surface of the modified 3D-printed structures before and after the enzyme immobilization. In Figure 2a the four fitted peaks are attributed to C-C/C=C/C-H bonds at 284.6 eV, C-O and C-N bonds at 285.9 eV, C-O-C at 287.1 eV, and carboxylic bonds centered at 288.6 eV. All these functionalities are ascribed to the surface of the reduced surface of PLA after treatment with NaOH, as stated in our previous work [22], and the PEI moieties that have been deposited on the surface. The carbon spectrum after the enzyme immobilization changes significantly, and this is compelling evidence of the

successful interaction of the enzyme and the surface. The C-N peak centered at 285.6 eV (Figure 2b) increases due to the amine-rich environment of the enzyme on the surface. A new peak revealed at 288.1 eV provides proof of the covalent immobilization by which the enzyme interacts with the amine groups of the PEI [38]. It is noteworthy that the newly fitted peaks revealed at high energy levels (291.3 eV) may derive from some p-p* electrostatic interactions between adjacent enzymes.

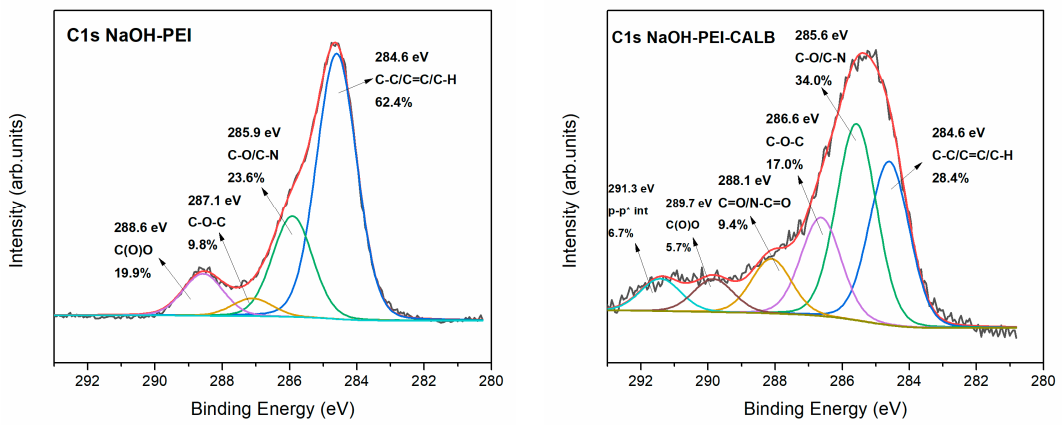


Figure 2. C1s photoelectron spectra for the modified 3D-printed PLA structures (**a**) before enzyme immobilization, (**b**) after enzyme immobilization.

3.1.2. Scanning Electron Microscopy (SEM)

SEM analysis was conducted in order to investigate the effect of a DES on the surface morphology of modified 3D-printed PLA structures. Representative micrographs of the SEM study are presented in Figure 3. Modified PLA structures were incubated at 60 °C in a 100% v/v Bet:Gly solution for 2 h and for 24 h, which were the most extreme conditions for the intended experimentation in the next stages of this work. The SEM study revealed a slight distortion of the surface of the modified PLA after interaction with the DES solution. The effect was already obvious from 2 h incubation, while after 24 h incubation the distortion was more profound. Micrographs with higher magnification can be found in the supplementary material (Figure S3) where it is determined that the surface quality before and after DES incubation does not change significantly. As a result, the PLA structures maintained their macroscopic rigidity, so they were exploited for further biocatalytic studies to reassure immobilized enzyme performance on these structures.

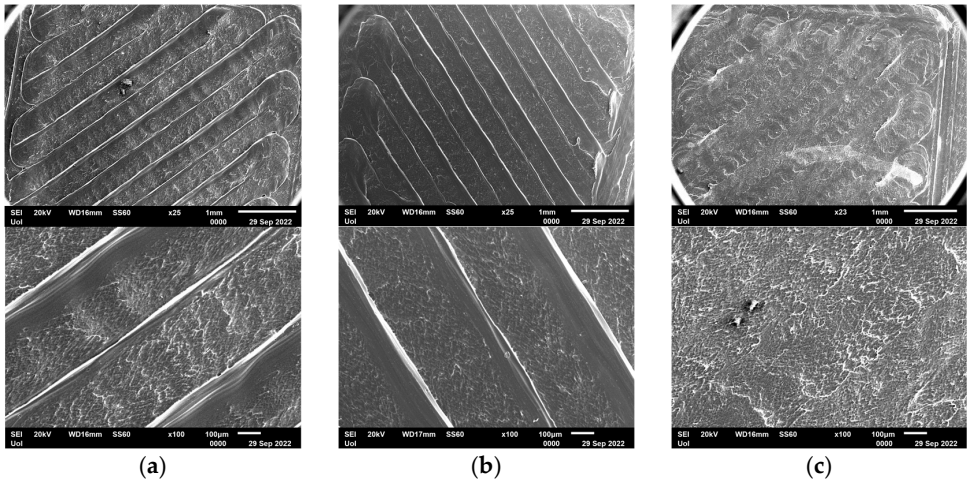


Figure 3. SEM micrographs of modified PLA structures. (**a**) modified PLA, (**b**) modified PLA incubated in 100% DES for 2 h, (**c**) modified PLA incubated in 100% DES for 24 h.

Previous studies have demonstrated that organic solvents, which are also commonly used in biocatalysis research, cause severe distortion of PLA structures and cannot be used for long exposures times [39,40], so this study shows that DESs can be proposed as alternative solvents for biocatalytic applications without causing severe deformation of the 3D-printed structure.

3.2. Enzyme Catalytic Performance in Well plates

3.2.1. Effect of DESs on the Activity of Immobilized CALB

The activity of the immobilized CALB on PLA multi-well plates was initially screened at various DES-buffer solutions in which the concentration of each DES was 10% v/v. As can be seen in Figure 4a, the activity of the enzyme depended on the DES used. Specifically, among the DESs whose HBA is ChCl, the best activity was observed in the case of the DESs ChCl:Fru:H_2O (92%) and ChCl:Glc:H_2O (94%), and among the DESs that contain Urea as HBD, ChCl:U (87%), ChCl:U:EG (89%), and ChCl:U:Gly (82%). The activity of the immobilized lipase in the aqueous solutions that contain DESs whose HBDs are alcohols was lower (56–77%). Concerning the DESs Bet:Gly and Bet:EG, the enzyme activity was found to be the highest in the presence of Bet: Gly (95%) and was similar to the activity that was observed in the case of the ChCl-based DESs that contain sugars (92% and 94%). Furthermore, the enzyme activity was even lower in the presence of 10% v/v EAC-based DESs (35–43%) and even more decreased in the presence of Chol DHP-based DESs (3–7%).

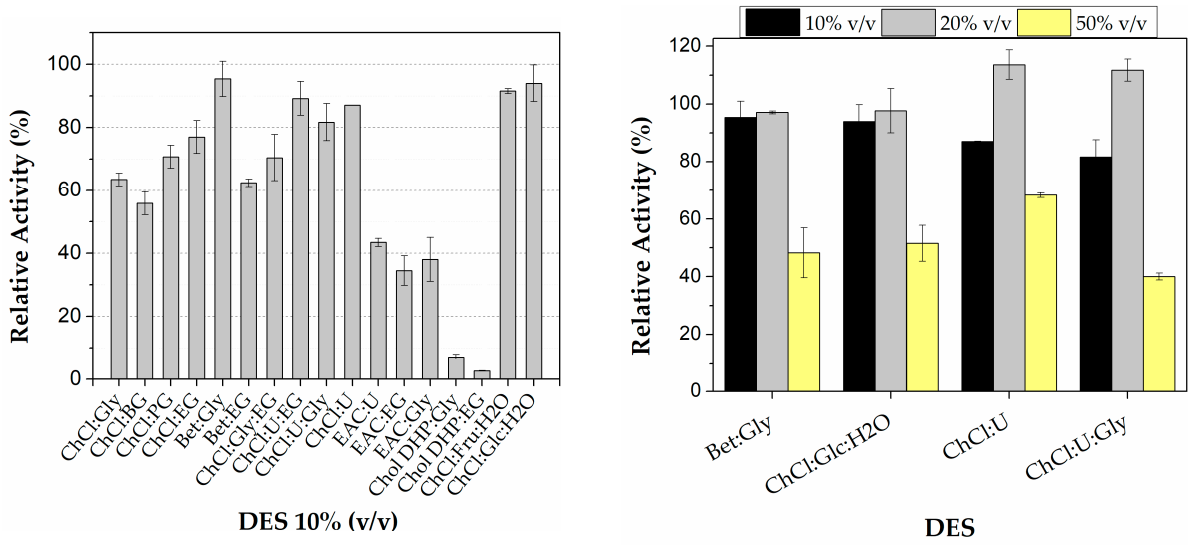


Figure 4. Relative activity of immobilized CALB on PLA well plates (**a**) in various 10% v/v DES:buffer solutions and (**b**) in increased concentrations of certain ones. 100% is defined as the activity of the immobilized enzyme in buffer (0% v/v DES). Reaction conditions: 0.25 mM pNPB in 50 mM phosphate buffer pH 7.5, 10, 20, or 50% v/v DESs, 40 °C, reaction time 5 min.

Elgharbawy et al., who studied the role of sugar-based NaDESs on the hydrolytic activity of various lipases including CALB (recombinant) immobilized on Immobead 150, also reported that the activity of the lipases in the hydrolysis of pNPP depended on both the nature of NaDESs and the type of lipase used. Specifically, when they tested the aqueous NaDES ChCl:Fru:H_2O (5:2:5), while it showed a stabilizing effect in most of the lipases, the activity of CALB dropped to 40% compared to the activity in the buffer, whereas in the case of ChCl:Glc:H_2O (5:2:5), an activation up to 140% was observed [41]. Kim et al., who also studied the effect of several DESs (10% v/v) on the *Candida rugosa* lipase activity on the pNPP hydrolysis, reported an activation of the lipase in the ChCl-based DESs [42]. Concerning Bet-based DESs, Nian et al. observed an activation of CALB in the hydrolysis of

pNPP in Bet:Gly [43], while Ribeiro et al., who used up to 20% m/m of various ChCl- and Betaine hydrochloride-based DES, demonstrated that a stabilization, or even an activation, took place [14]. In the present study, the presence of 10% v/v EAC-based DESs resulted in diminished hydrolytic activity compared to the results of another work [44]. In the case of the Chol DHP-based DESs, Álvarez et al. studied the activity of CALB in the hydrolysis of p-nitrophenyl laurate in such DESs and found it to be >60% at the concentration of 10% v/v [45].

From all the above it can be deduced that a certain DES may have a different impact on the enzymatic activity of a lipase depending on the type of the lipase and its form (free or immobilized), as well as on the nature (combination of HBD/HBA) and concentration of the DES used, as the physicochemical properties of the medium varies in terms of polarity, viscosity, density, and pH, which are factors that affect the enzyme structure or/and the enzyme-substrate interaction, and. thus, the catalytic activity, leading to enhanced or lowered yields [46]. However, in the current study, sugar-based, Urea-based, and Betaine-based DESs seem to have the best impact on the activity of immobilized CALB on PLA wells.

In order to further investigate the influence of the concentration of the DESs on the enzymatic activity of the immobilized CALB on the PLA-wells, the DESs Bet:Gly, ChCl:Glc:H_2O, ChCl:U, and ChCl:U:Gly in which the enzyme demonstrated high activity (in 10% v/v) were selected and tested in increasing concentrations (20 and 50% v/v). The results are presented in Figure 4b. For all the DESs examined, it can be deduced that a slight rise in their concentration (20% v/v) led to enhanced activity (97% for Bet:Gly and 98% for ChCl:Glc:H_2O) and even to an observed activation of the lipase in the case of the U-based DESs (about 110%), whereas a greater rise in the concentration (50% v/v) resulted in lower activity (up to 68%). The activation of CALB in these media has also been reported for *Candida rugosa* lipase [42]. The decrease in the enzyme activity noted in higher concentrations of DESs was also observed elsewhere [14,41] and may be associated with the formation of more viscous solutions in which mass transfer phenomena take place and hinder the enzyme-substrate interaction [41].

3.2.2. Effect of DESs on the Stability of Immobilized CALB

The stability of the immobilized CALB was examined in buffer (0% v/v DES) and different concentrations (10, 20, 50, and 100% v/v) of the four selected DESs. The remaining enzymatic activities after 1h incubation at 40 °C are shown in Figure 5. In general, the remaining activity of the immobilized enzyme was $\geq$90% in all concentrations of DESs tested, indicating that these selected solvents did not destabilize the immobilized lipase. More specifically, in the low-to-medium concentrations of the U-based DESs (10–50% v/v), the remaining activity was up to 105%, showing a slight enzyme activation. It is interesting to note that even at 100% v/v concentration of U-based DESs the immobilized enzyme retained 90% of its initial activity. A significant stabilizing effect was also observed in the case of a high concentration of Bet:Gly, and especially in ChCl:Glc:H_2O, where no significant loss of activity was observed at any concentration, demonstrating the protective role of these sugar-based DESs. This stabilizing effect of these DES is similar to that observed for other lipase preparations [41,43,47].

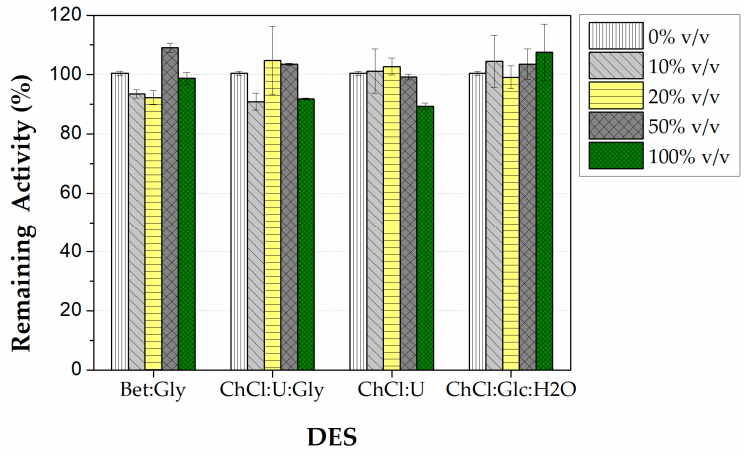


Figure 5. Stability of immobilized CALB on PLA wells after 1h of incubation at different concentrations (0–100% *v*/*v*) of particular DESs at 40 °C. One hundred percent is defined as the initial activity (before the incubation) in buffer (0% *v*/*v* DES). Reaction conditions: 0.25 mM pNPB in 50 mM phosphate buffer pH 7.5, 40 °C, reaction time 5 min.

3.2.3. Storage Stability of Immobilized CALB on PLA Well plates

The storage stability of the immobilized lipase on PLA wells was also investigated. The PLA wells with immobilized CALB were stored at 4 °C and the remaining activity of the immobilized enzyme was measured over a period of two months. As can be seen in Figure 6, the biocatalyst retained 90% of its initial activity after a storage time of two months, which is similar to that observed for immobilized CALB on lysine-modified magnetic nanoparticles [48] and remarkably higher than that observed for the immobilized CALB on functionalized mesoporous material MCM-41, where a remaining activity of 50% after incubation for 5.7 weeks at 4 °C was observed [49].

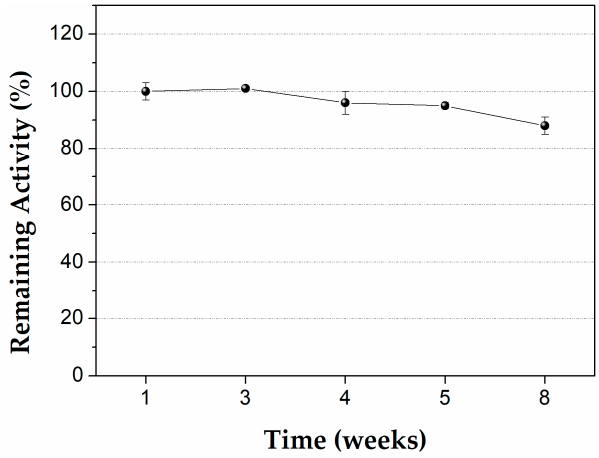


Figure 6. Storage stability of immobilized CALB on PLA wells, at 4 °C. One hundred percent is defined as the initial activity (activity before the storage). Reaction conditions: 0.25 mM pNPB in 50 mM phosphate buffer pH 7.5, 40 °C, reaction time 5 min.

3.3. Enzyme Performance in PLA Microreactors

In the present work, 3D-printed PLA continuous-flow microreactors were developed and used for biocatalytic transformations in DES-based media. In this case, the DES Bet:Gly was selected for two reasons; firstly, the lipase activity and stability were among the highest that were presented according to the screening test in PLA wells, and, secondly, this DES can fulfill the 2-in-1 concept for DES elaboration in biocatalysis, acting both as a solvent and a substrate in the transesterification of ethyl ferulate with glycerol.

The developed microreactor operated under a laminar flow regime (Reynolds number < 2100) and the assays were performed using an automated syringe pump, an incubator for reaction temperature control, and Tygon tubing for the intermediate conjunctions, as demonstrated in Figure S1.

3.3.1. Effect of Enzyme Concentration

The preparation of a viable biocatalytic system lies in the determination of the proper amount of enzyme that will be used in the immobilization process, as the cost of such systems strongly depends on this. In order to determine the optimal concentration of CALB for its immobilization in the microreactor, several concentrations were used and associated with the amount of pNP produced by each biocatalytic system. In addition, the immobilization yield was estimated, by measuring the activity of the enzyme solution before and after the microreactor loading. As shown in Figure 7, the increase in enzyme concentration was followed by an increment in the product formation until a critical point (0.04 mg/mL), beyond which the productivity of the biocatalytic system decreased gradually. In terms of the immobilization yield, almost all the CALB seemed to have been immobilized up to a concentration of 0.02 mg/mL. At higher enzyme amounts, the immobilization yield sharply declined, indicating that the immobilization capacity of the reactor was limited. At the concentration where maximum enzyme productivity was observed (0.04 mg/mL), the immobilization yield was 70%. The decline in enzyme productivity possibly occurred due to an oversaturation of enzyme molecules in the microreactor that led to inactivation or hindrance. Similar assumptions have been made in previous studies for enzymatic microreactors either with immobilized or free enzyme forms in the interior of microreactors, using different enzymes [22,50,51]. Hence, the optimum enzyme concentration of 0.04 mg/mL was selected for further studies.

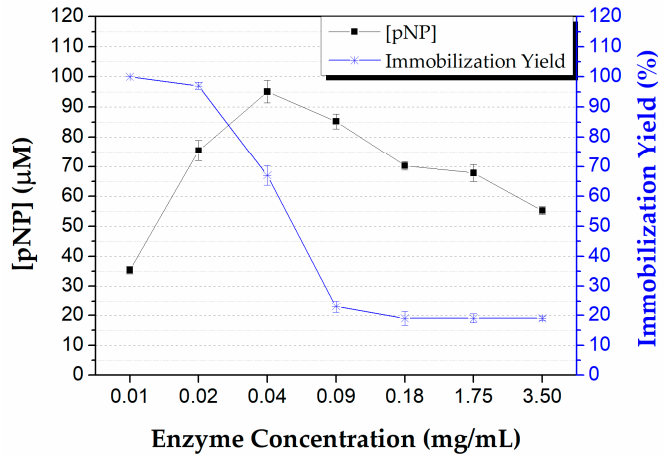


Figure 7. Effect of enzyme concentration on the microreactor's biocatalytic performance and immobilization yield. Reaction conditions: 0.25 mM pNPB in 50 mM phosphate buffer pH 7.5, 40 °C, flow rate 300 μL/min (t_R = 30 s).

3.3.2. Operational Stability in the Presence or Absence of DES

The biocatalytic microreactor system was evaluated in terms of its operational stability by performing 100 successive cycles of use, in the absence or the presence of 10% v/v Bet:Gly. The hydrolysis of pNPB was used as the model reaction and each cycle was deemed when the whole microreactor volume (150 μL) passed through the microreactor. As presented in Figure 8, the immobilized CALB in PLA microreactor retained its initial activity at 100% after 55 min of continuous use in both 0% and 10% v/v Bet:Gly. This suggests that the presence of DES did not affect the operational stability of the biocatalyst, thus rendering its use feasible in long-lasting hydrolysis reactions. The remarkable operational stability of immobilized enzymes in microreactor systems has been previously reported both for

hydrolytic and synthetic bioprocesses, suggesting the potential of microfluidic systems in terms of process efficiency and sustainability [22,50,52].

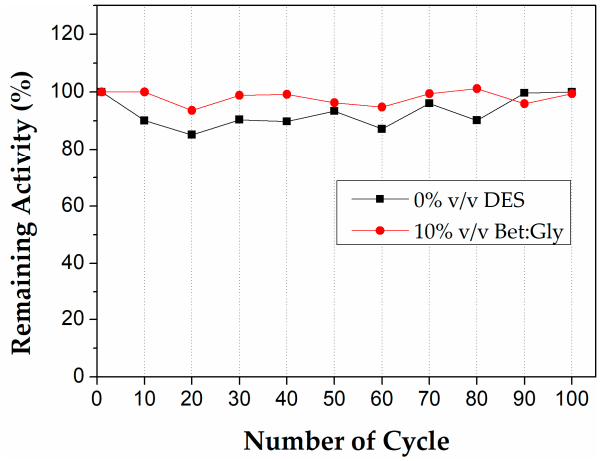


Figure 8. Operational stability of immobilized CALB in PLA microreactors in the absence and the presence of 10% v/v Bet:Gly for 100 cycles of use. Reaction conditions: 0.25 mM pNPB in 50 mM phosphate buffer pH 7.5, 0 or 10% v/v Bet:Gly, 40 °C, flow rate 300 μL/min (t_R = 30 s).

3.3.3. Thermal Stability of Immobilized CALB in Microreactor

The robustness of the enzymatically modified PLA microreactor was also tested by filling the microreactor with 100% Bet:Gly and incubating at 60 °C. In this manner, the stability of the immobilized lipase would be evaluated, and insight would be gained into the capability of the microbioreactor to be used in synthetic reactions that include this DES. So, at specific points in time, the DES was removed, the microbioreactor was washed and dried and the activity of the lipase was measured. The results regarding the stability of the immobilized CALB in the PLA microreactor for a period of one month are presented in Figure 9. In the case of the incubation in DES, the lipase demonstrated great stability, as it retained more than 50% of its initial activity after one month compared to the control, where the microreactor was fulfilled with buffer and the activity of CALB was diminished. These results give prominence to the stabilizing effect that betaine-based DES has on the protein molecules. The stabilizing effect of Bet:Gly on free CALB has also been reported elsewhere [43]. A possible explanation for the enzyme stabilization that some DESs offer at elevated temperatures could be that the hydrogen bonding of the DES's ingredients helps to maintain the enzymatic structure by absorbing the heat of the medium and thus, the enzyme molecules do not get dehydrated [41].

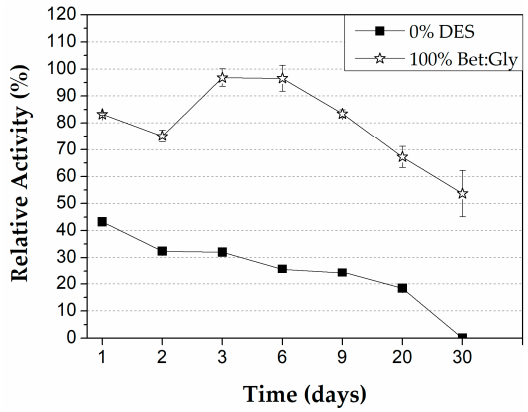


Figure 9. Thermal stability of immobilized CALB in PLA microreactor, at 60 °C, after incubation in 100% DES Bet:Gly and 100% buffer. Reaction conditions: 0.25 mM pNPB in 50 mM phosphate buffer pH 7.5, 40 °C, flow rate 300 μL/min (t_R = 30 s).

3.3.4. Continuous Flow Kinetics of Immobilized Lipase in the Presence or Absence of DES

To give better insight into the biocatalytic behavior of the immobilized lipase, the effect of the flow rate on the hydrolysis of the model substrate pNPB in the presence or absence of 10% v/v of the selected DES Bet:Gly was evaluated. According to previous works, mass transfer phenomena are expected to affect the kinetic behavior of enzymes confined in the interior of microreactor systems [53,54]. The flow kinetics and the presence of any diffusion or mass transfer effects that may conceal the true kinetics (Q = 0) were estimated by applying the Lilly–Hornby model, as an adaptation of the classical Michaelis–Menten kinetic model, used for investigating flow kinetics of enzymes immobilized in microreactor systems [55].

From the kinetic data collected at an initial substrate concentration of from 0.25 mM to 4 mM, at varying flow rates of from 75 µL/min to 600 µL/min, linear plots of $f[A]_0$ versus $-\ln(1-f)$ were obtained (Figure 10a,b). The slopes of the lines, that correspond to the $K_{m(app)}$ values (Table 3), seem to decrease with increasing flow rate, indicating a better performance of the immobilized enzyme in faster residence times. Moreover, the system does not seem to get significantly affected by mass transfer phenomena since the zero flow rate value (0.638 mM) (y-intercept, Figure 10a) does not match the Michaelis constant for the free enzyme form (0.348 mM) [55]. It seems that the accessibility of the substrate to the enzyme molecules may have decreased due to the immobilization process (higher $K_{m(app)}$ values than the free enzyme) but is not affected by diffusion limitations [53].

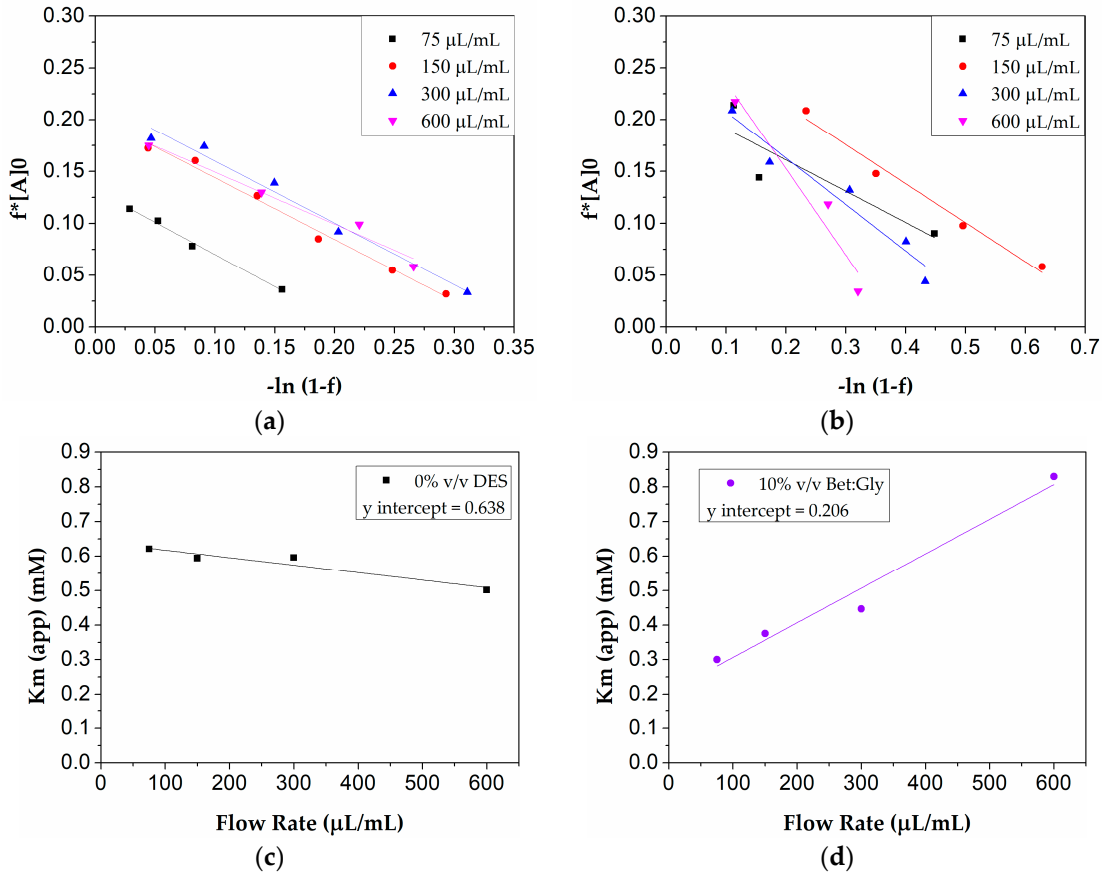


Figure 10. Effect of flow rate on the hydrolysis of p-NPB in CALB immobilized microreactors under continuous flow conditions (enzyme concentration 43 µg/mL, T = 40 °C, pH = 7.5). (**a**) Application of the Lilly–Hornby model on the data collected for different enzyme concentrations and flow rates in a buffer system (0% v/v DES), and (**b**) in 10% Bet:Gly system. (**c**) Linear fitting of the $K_{m(app)}$ values against flow rate in a buffer system, and (**d**) in 10% Bet:Gly system.

Table 3. Apparent Michaelis constant ($K_{m(app)}$) calculated from the Lilly−Hornby model for the microreactor system and Michaelis constant for the free enzyme calculated from the Michaelis−Menten model, under the same reaction conditions.

	Flow Rate (μL min^{-1})	$K_{m(app)}$ (mM)	
		0% *v*/*v* DES (R^2)	10% *v*/*v* Bet:Gly (R^2)
Free CALB	-	0.35 (0.88)	0.39 (0.93)
Microreactor immobilized CALB	75	0.62 (0.99)	0.30 (0.78)
	150	0.59 (0.98)	0.38 (0.98)
	300	0.60 (0.99)	0.45 (0.95)
	600	0.50 (0.98)	0.83 (0.94)

However, when 10% *v*/*v* Bet:Gly is added to the system, its kinetic behavior alters significantly. In this case, an increase in the slopes of the lines (Figure 10b,d) is observed with increasing flow rate indicating mass transfer effects. However, moving from the lowest to the highest flow rates tested, only a 2.6-fold increase in the $K_{m(app)}$ values are observed, proving that the mass transfer effects are not considered strong [53,55]. The $K_{m(app)}$ for zero flow rate in this case (0.206 mM) is lower than that observed for the free enzyme form (0.392 mM), indicating more effective substrate accessibility in the immobilized enzyme acting in a DES-based system. Such an observation has been previously reported for immobilized enzyme microreactors and is indicative of the increased stabilization of the biocatalyst along with the more effective substrate diffusion within the system [50,55].

Inferring from the above, the designed microreactor system is not remarkably affected by mass transfer phenomena, while the addition of Bet:Gly solvent in the system greatly improves the substrate diffusion within the immobilized enzyme molecules.

3.4. Implementation of the Enzyme Microreactor in a Transesterification Reaction

Glyceryl ferulate (GF) is a natural compound widely distributed among the plant kingdom that is especially known for its antioxidant and UV light-absorbing properties [56]. However, its isolation from natural sources is limited, so the de novo synthesis methods through esterification and transesterification reactions have been proposed [57,58]. Herein, the transesterification reaction of ethyl ferulate with glycerol towards the synthesis of GF (Figure 11) is demonstrated for the first time in a continuous flow microreactor system, elaborating Bet:Gly as a novel, green reaction solvent, that could play a double role as a solvent component and a reaction substrate at the same time (the 2-in-1 concept). The transesterification reaction was also performed in batch reaction systems. Free CALB and commercially immobilized CALB (Novozym 435) were used under the same reaction conditions and the productivity of the different systems is presented in Table 4.

Table 4. Comparative data for the transesterification of ethyl ferulate with glycerol in microreactor and batch systems.

Biocatalytic System	Amount of Enzyme (μg)	Reaction Volume (mL)	Amount of Product (μg)	Reaction Time (h)	Productivity (μg Product min^{-1} μg enzyme^{-1})
Microbioreactor	4.5	0.15	18.6	24 runs × 10 min	17.20×10^{-3}
Immobilized CALB (Novozyme 435)	30	1	5.4	4	0.75×10^{-3}
Free CALB	30	1	97.9	4	13.60×10^{-3}

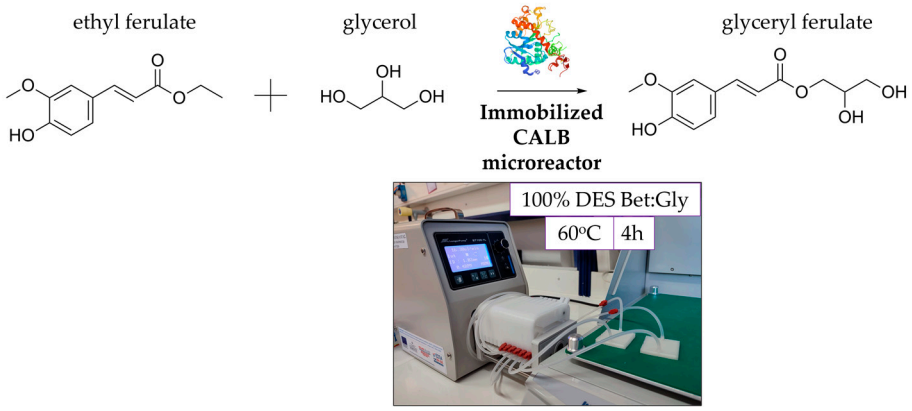


Figure 11. Reaction scheme for the transesterification of ethyl ferulate with glycerol in 100% Bet:Gly DES acting both as solvent and substrate, towards the production of glyceryl ferulate. The reaction was performed in a microreactor system with immobilized CALB, at 60 °C for a total retention time of 4 h (24 runs × 10 min).

The HPLC analysis revealed only one reaction product, with a retention time of 3.3 min, which presumably is GF, according to previously published works [57]. Further studies, which are beyond the scope of the present work, would shed light on the identity of this product. Interestingly, the microreactor system presented the highest productivity, which was 23 times higher than that of the commercial immobilized lipase and 1.2 times higher than the productivity of free CALB. Previously published works have showcased similar results [18,50,52,59], confirming the superiority of enzyme microreactors as an alternative to batch reactor systems when productivity is of critical importance.

4. Conclusions

The incorporation of novel technologies and solvent systems into biocatalysis is urgent for new reactions to be feasible and enzymes to be more resistant and productive. Herein, 3D printing technology was exploited for the development of carriers for lipase immobilization, in the form of microwell plates and in the form of microfluidic reactors. The 3D-printed PLA structures were properly modified in order to host covalently immobilized lipase, and several biocatalytic assays were performed regarding the effect of DESs on the enzyme performance. Different DESs were shown to have a stabilizing effect on enzymatic activity, even at 100% v/v DES concentration. The residual activity of the immobilized enzyme at 4 °C was 90% after two months of storage, indicating good storage stability. In 3D-printed microfluidic reactors, a kinetic study showed that the presence of the DES Bet:Gly in the reaction system improved greatly the apparent kinetic constant of the enzyme, while the system was not severely affected by diffusion limitations. It is also noteworthy that the enzyme microreactor system showed exceptional thermal stability after incubation in 100% v/v DES at 60 °C, retaining 53% of its activity after 30 days of storage, while the microreactor stored in buffer solution had been completely deactivated. These experiments confirmed that the slight surface distortion after DES incubation observed in the SEM study, does not affect the biocatalytic performance of the system; thus making these solvents ideal alternatives for non-aqueous biocatalytic processes. A continuous flow transesterification reaction was also demonstrated in this study, showing the potential of the system to reach productivities significantly higher than batch reaction systems under the same conditions.

This study featured an effective and robust biocatalytic system with immobilized lipase that can be used both in hydrolytic and synthetic processes with the incorporation of environmentally friendly solvents such as DESs. Further optimization, either with different solvents or with different microreactor systems, could upgrade its performance. This microreactor system is based on natural and recyclable starting materials and it is readily reusable, providing a sustainable option for biocatalysts design.

Supplementary Materials: The following supporting information can be downloaded at: https://www.mdpi.com/article/10.3390/mi13111954/s1, Figure S1: Microfluidic apparatus used in this study; Figure S2: Activity of immobilized CALB on PLA well plates modified with PEI.

Author Contributions: M.G.B.: Methodology, Investigation, Visualization, Writing-Original draft preparation, E.G.: Conceptualization, Methodology, Investigation, Visualization, Writing-Original draft preparation; A.S.: Investigation; D.M.: Investigation, Formal analysis; K.S.: Investigation, Formal analysis; A.A.: Resources, Formal analysis; D.G.: Resources, Formal analysis; H.S.: Conceptualization, Funding acquisition, Writing-Review and Editing, Supervision. All authors have read and agreed to the published version of the manuscript.

Funding: Part of this research has been co-financed by the European Regional Development Fund of the European Union and Greek national funds through the Operational Program Competitiveness, Entrepreneurship, and Innovation, under the call RESEARCH CREATE-INNOVATE (project code: T2EDK-01410). Financial support from the Empirikion Foundation (Greece) is gratefully acknowledged.

Data Availability Statement: Not applicable.

Conflicts of Interest: The authors declare no conflict of interest.

References

1. Dixit, C.K.; Kadimisetty, K.; Rusling, J. 3D-Printed Miniaturized Fluidic Tools in Chemistry and Biology. *TrAC Trends Anal. Chem.* **2018**, *106*, 37–52. [CrossRef] [PubMed]
2. Kong, Y.L.; Gupta, M.K.; Johnson, B.N.; McAlpine, M.C. 3D Printed Bionic Nanodevices. *Nano Today* **2016**, *11*, 330–350. [CrossRef] [PubMed]
3. Zhou, Y. The Recent Development and Applications of Fluidic Channels by 3D Printing. *J. Biomed. Sci.* **2017**, *24*, 80. [CrossRef] [PubMed]
4. Basso, A.; Serban, S. Industrial Applications of Immobilized Enzymes—A Review. *Mol. Catal.* **2019**, *479*, 110607. [CrossRef]
5. Gkantzou, E.; Chatzikonstantinou, A.V.; Fotiadou, R.; Giannakopoulou, A.; Patila, M.; Stamatis, H. Trends in the Development of Innovative Nanobiocatalysts and Their Application in Biocatalytic Transformations. *Biotechnol. Adv.* **2021**, *51*, 107738. [CrossRef]
6. Lyu, X.; Gonzalez, R.; Horton, A.; Li, T. Immobilization of Enzymes by Polymeric Materials. *Catalysts* **2021**, *11*, 1211. [CrossRef]
7. Pose-Boirazian, T.; Martínez-Costas, J.; Eibes, G. 3D Printing: An Emerging Technology for Biocatalyst Immobilization. *Macromol. Biosci.* **2022**, *22*, 2200110. [CrossRef]
8. Shao, Y.; Liao, Z.; Gao, B.; He, B. Emerging 3D Printing Strategies for Enzyme Immobilization: Materials, Methods, and Applications. *ACS Omega* **2022**, *7*, 11530–11543. [CrossRef]
9. Ma, Z.; Mi, Y.; Han, X.; Li, H.; Tian, M.; Duan, Z.; Fan, D.; Ma, P. Transformation of Ginsenoside via Deep Eutectic Solvents Based on Choline Chloride as an Enzymatic Reaction Medium. *Bioprocess. Biosyst. Eng.* **2020**, *43*, 1195–1208. [CrossRef]
10. Fotiadou, R.; Bellou, M.G.; Spyrou, K.; Yan, F.; Rudolf, P.; Gournis, D.; Stamatis, H. Effect of Deep Eutectic Solvents on the Biocatalytic Properties of β-Glucosidase@ZnOFe Nano-Biocatalyst. *Sustain Chem. Pharm.* **2022**, *30*, 100886. [CrossRef]
11. Sun, H.; Xin, R.; Qu, D.; Yao, F. Mechanism of Deep Eutectic Solvents Enhancing Catalytic Function of Cytochrome P450 Enzymes in Biosynthesis and Organic Synthesis. *J. Biotechnol.* **2020**, *323*, 264–273. [CrossRef] [PubMed]
12. Chan, J.C.; Zhang, B.; Martinez, M.; Kuruba, B.; Brozik, J.; Kang, C.; Zhang, X. Structural Studies of Myceliophthora Thermophila Laccase in the Presence of Deep Eutectic Solvents. *Enzyme Microb. Technol.* **2021**, *150*, 109890. [CrossRef] [PubMed]
13. Toledo, M.L.; Pereira, M.M.; Freire, M.G.; Silva, J.P.A.; Coutinho, J.A.P.; Tavares, A.P.M. Laccase Activation in Deep Eutectic Solvents. *ACS Sustain. Chem. Eng.* **2019**, *7*, 11806–11814. [CrossRef]
14. Ribeiro, B.D.; de Carvalho Iff, L.; Coelho, M.A.Z.; Marrucho, I.M. Influence of Betaine- and Choline-Based Eutectic Solvents on Lipase Activity. *Curr. Biochem. Eng.* **2019**, *5*, 57–68. [CrossRef]
15. Domínguez de María, P.; Guajardo, N.; Kara, S. Enzyme Catalysis: In DES, with DES, and in the Presence of DES. In *Deep Eutectic Solvents: Synthesis, Properties, and Applications*; Wiley: New York, NY, USA, 2019; pp. 257–271. ISBN 9783527818471.
16. Pätzold, M.; Siebenhaller, S.; Kara, S.; Liese, A.; Syldatk, C.; Holtmann, D. Deep Eutectic Solvents as Efficient Solvents in Biocatalysis. *Trends Biotechnol.* **2019**, *37*, 943–959. [CrossRef]
17. Guajardo, N.; Schrebler, R.A.; Domínguez de María, P. From Batch to Fed-Batch and to Continuous Packed-Bed Reactors: Lipase-Catalyzed Esterifications in Low Viscous Deep-Eutectic-Solvents with Buffer as Cosolvent. *Bioresour. Technol.* **2019**, *273*, 320–325. [CrossRef]
18. Guajardo, N.; Domínguez de María, P.; Canales, R. Integrating Biocatalysis with Viscous Deep Eutectic Solvents in Lab-On-A-Chip Microreactors. *ChemSusChem* **2022**, *15*, 1–8. [CrossRef]
19. Zeng, C.-X.; Qi, S.-J.; Xin, R.-P.; Yang, B.; Wang, Y.-H. Enzymatic Selective Synthesis of 1,3-DAG Based on Deep Eutectic Solvent Acting as Substrate and Solvent. *Bioprocess. Biosyst. Eng.* **2015**, *38*, 2053–2061. [CrossRef]

20. Hümmer, M.; Kara, S.; Liese, A.; Huth, I.; Schrader, J.; Holtmann, D. Synthesis of (-)-Menthol Fatty Acid Esters in and from (-)-Menthol and Fatty Acids—Novel Concept for Lipase Catalyzed Esterification Based on Eutectic Solvents. *Mol. Catal.* **2018**, *458*, 67–72. [CrossRef]
21. Ilyas, R.A.; Sapuan, S.M.; Harussani, M.M.; Hakimi, M.Y.A.Y.; Haziq, M.Z.M.; Atikah, M.S.N.; Asyraf, M.R.M.; Ishak, M.R.; Razman, M.R.; Nurazzi, N.M.; et al. Polylactic Acid (PLA) Biocomposite: Processing, Additive Manufacturing and Advanced Applications. *Polymers* **2021**, *13*, 1326. [CrossRef]
22. Gkantzou, E.; Skonta, A.; Tsakni, A.; Polydera, A.; Moschovas, D.; Spyrou, K.; Avgeropoulos, A.; Gournis, D.; Houhoula, D.; Stamatis, H. 3D Printed PLA Enzyme Microreactors: Characterization and Application for the Modification of Bioactive Compounds. *J. Biotechnol.* **2022**, *350*, 75–85. [CrossRef] [PubMed]
23. Ye, J.; Chu, T.; Chu, J.; Gao, B.; He, B. A Versatile Approach for Enzyme Immobilization Using Chemically Modified 3D-Printed Scaffolds. *ACS Sustain. Chem. Eng.* **2019**, *7*, 18048–18054. [CrossRef]
24. Kumar, A.; Dhar, K.; Kanwar, S.S.; Arora, P.K. Lipase Catalysis in Organic Solvents: Advantages and Applications. *Biol. Proced. Online* **2016**, *18*, 2. [CrossRef] [PubMed]
25. Erokhin, K.S.; Gordeev, E.G.; Ananikov, V.P. Revealing Interactions of Layered Polymeric Materials at Solid-Liquid Interface for Building Solvent Compatibility Charts for 3D Printing Applications. *Sci. Rep.* **2019**, *9*, 20177. [CrossRef] [PubMed]
26. Dudu, A.I.; Bencze, L.C.; Paizs, C.; Toşa, M.I. Deep Eutectic Solvents—a New Additive in the Encapsulation of Lipase B from *Candida Antarctica*: Biocatalytic Applications. *React. Chem. Eng.* **2022**, *7*, 442–449. [CrossRef]
27. Guajardo, N.; Domínguez de María, P. Continuous Biocatalysis in Environmentally-Friendly Media: A Triple Synergy for Future Sustainable Processes. *ChemCatChem* **2019**, *11*, 3128–3137. [CrossRef]
28. Gkantzou, E.; Skonta, A.; Vasios, A.-G.; Stamatis, H. 3D Printed Polylactic Acid Well-Plate for Multi-Enzyme Immobilization. In *Methods in Molecular Biology*; Stamatis, H., Ed.; Springer US: New York, NY, USA, 2022; Volume 2487, pp. 163–175.
29. Baran, E.; Erbil, H. Surface Modification of 3D Printed PLA Objects by Fused Deposition Modeling: A Review. *Colloids Interfaces* **2019**, *3*, 43. [CrossRef]
30. Jaidev, L.R.; Chatterjee, K. Surface Functionalization of 3D Printed Polymer Scaffolds to Augment Stem Cell Response. *Mater. Des.* **2019**, *161*, 44–54. [CrossRef]
31. Hildebrand, H.F.; Blanchemain, N.; Mayer, G.; Chai, F.; Lefebvre, M.; Boschin, F. Surface Coatings for Biological Activation and Functionalization of Medical Devices. *Surf. Coat. Technol.* **2006**, *200*, 6318–6324. [CrossRef]
32. Douglas, J.F. How Does Surface Roughness Affect Polymer-Surface Interactions? *Macromolecules* **1989**, *22*, 3707–3716. [CrossRef]
33. Bradford, M.M. A Rapid and Sensitive Method for the Quantitation of Microgram Quantities of Protein Utilizing the Principle of Protein-Dye Binding. *Anal. Biochem.* **1976**, *72*, 248–254. [CrossRef]
34. Skonta, A.; Gkantzou, E.; Spyrou, K.; Spyrou, S.; Polydera, A.; Gournis, D.; Stamatis, H. 3D Printed Polylactic Acid (PLA) Well Plates for Enzyme Inhibition Studies: The Case of Pancreatic Lipase. *Catal. Res.* **2022**, *2*, 1–19. [CrossRef]
35. Zaak, H.; Fernandez-Lopez, L.; Otero, C.; Sassi, M.; Fernandez-Lafuente, R. Improved Stability of Immobilized Lipases via Modification with Polyethylenimine and Glutaraldehyde. *Enzyme Microb. Technol.* **2017**, *106*, 67–74. [CrossRef] [PubMed]
36. Rios, N.S.; Arana-Peña, S.; Mendez-Sanchez, C.; Lokha, Y.; Cortes-Corberan, V.; Gonçalves, L.R.B.; Fernandez-Lafuente, R. Increasing the Enzyme Loading Capacity of Porous Supports by a Layer-by-Layer Immobilization Strategy Using PEI as Glue. *Catalysts* **2019**, *9*, 576. [CrossRef]
37. Patel, V.; Shah, C.; Deshpande, M.; Madamwar, D. Zinc Oxide Nanoparticles Supported Lipase Immobilization for Biotransformation in Organic Solvents: A Facile Synthesis of Geranyl Acetate, Effect of Operative Variables and Kinetic Study. *Appl. Biochem. Biotechnol.* **2016**, *178*, 1630–1651. [CrossRef]
38. Chalmpes, N.; Patila, M.; Kouloumpis, A.; Alatzoglou, C.; Spyrou, K.; Subrati, M.; Polydera, A.C.; Bourlinos, A.B.; Stamatis, H.; Gournis, D. Graphene Oxide–Cytochrome c Multilayered Structures for Biocatalytic Applications: Decrypting the Role of Surfactant in Langmuir–Schaefer Layer Deposition. *ACS Appl. Mater. Interfaces* **2022**, *14*, 26204–26215. [CrossRef]
39. Valerga, A.; Batista, M.; Fernandez-Vidal, S.; Gamez, A. Impact of Chemical Post-Processing in Fused Deposition Modelling (FDM) on Polylactic Acid (PLA) Surface Quality and Structure. *Polymers* **2019**, *11*, 566. [CrossRef] [PubMed]
40. Valerga, A.P.; Fernandez-Vidal, S.R.; Girot, F.; Gamez, A.J. On the Relationship between Mechanical Properties and Crystallisation of Chemically Post-Processed Additive Manufactured Polylactic Acid Pieces. *Polymers* **2020**, *12*, 941. [CrossRef]
41. Elgharbawy, A.A. Shedding Light on Lipase Stability in Natural Deep Eutectic Solvents. *Chem. Biochem. Eng. Q.* **2018**, *32*, 359–370. [CrossRef]
42. Kim, S.H.; Park, S.; Yu, H.; Kim, J.H.; Kim, H.J.; Yang, Y.-H.; Kim, Y.H.; Kim, K.J.; Kan, E.; Lee, S.H. Effect of Deep Eutectic Solvent Mixtures on Lipase Activity and Stability. *J. Mol. Catal. B Enzym.* **2016**, *128*, 65–72. [CrossRef]
43. Nian, B.; Cao, C.; Liu, Y. How Candida Antarctica Lipase B Can Be Activated in Natural Deep Eutectic Solvents: Experimental and Molecular Dynamics Studies. *J. Chem. Technol. Biotechnol.* **2020**, *95*, 86–93. [CrossRef]
44. Papadopoulou, A.A.; Tzani, A.; Polydera, A.C.; Katapodis, P.; Voutsas, E.; Detsi, A.; Stamatis, H. Green Biotransformations Catalysed by Enzyme-Inorganic Hybrid Nanoflowers in Environmentally Friendly Ionic Solvents. *Environ. Sci. Pollut. Res.* **2018**, *25*, 26707–26714. [CrossRef] [PubMed]
45. Álvarez, M.S.; Longo, M.A.; Deive, F.J.; Rodríguez, A. Synthesis and Characterization of a Lipase-Friendly DES Based on Cholinium Dihydrogen Phosphate. *J. Mol. Liq.* **2021**, *340*, 117230. [CrossRef]

46. Xu, P.; Zheng, G.-W.; Zong, M.-H.; Li, N.; Lou, W.-Y. Recent Progress on Deep Eutectic Solvents in Biocatalysis. *Bioresour. Bioprocess.* **2017**, *4*, 34. [CrossRef] [PubMed]
47. Fredes, Y.; Chamorro, L.; Cabrera, Z. Increased Selectivity of Novozym 435 in the Asymmetric Hydrolysis of a Substrate with High Hydrophobicity Through the Use of Deep Eutectic Solvents and High Substrate Concentrations. *Molecules* **2019**, *24*, 792. [CrossRef]
48. Nicolás, P.; Lassalle, V.; Ferreira, M.L. Immobilization of CALB on Lysine-Modified Magnetic Nanoparticles: Influence of the Immobilization Protocol. *Bioprocess. Biosyst. Eng.* **2018**, *41*, 171–184. [CrossRef]
49. Yu, D.; Zhang, X.; Wang, T.; Geng, H.; Wang, L.; Jiang, L.; Elfalleh, W. Immobilized Candida Antarctica Lipase B (CALB) on Functionalized MCM-41: Stability and Catalysis of Transesterification of Soybean Oil and Phytosterol. *Food Biosci.* **2021**, *40*, 100906. [CrossRef]
50. Gkantzou, E.; Govatsi, K.; Chatzikonstantinou, A.V.; Yannopoulos, S.N.; Stamatis, H. Development of a ZnO Nanowire Continuous Flow Microreactor with β-Glucosidase Activity: Characterization and Application for the Glycosylation of Natural Products. *ACS Sustain. Chem. Eng.* **2021**, *9*, 7658–7667. [CrossRef]
51. Gumel, A.M.; Annuar, M.S.M. Thermomyces Lanuginosus Lipase-Catalyzed Synthesis of Natural Flavor Esters in a Continuous Flow Microreactor. *3 Biotech* **2016**, *6*, 24. [CrossRef]
52. Liu, X.; Meng, X.-Y.; Xu, Y.; Dong, T.; Zhang, D.-Y.; Guan, H.-X.; Zhuang, Y.; Wang, J. Enzymatic Synthesis of 1-Caffeoylglycerol with Deep Eutectic Solvent under Continuous Microflow Conditions. *Biochem. Eng. J.* **2019**, *142*, 41–49. [CrossRef]
53. Carvalho, F.; Marques, M.; Fernandes, P. Sucrose Hydrolysis in a Bespoke Capillary Wall-Coated Microreactor. *Catalysts* **2017**, *7*, 42. [CrossRef]
54. Hafeez, S.; Aristodemou, E.; Manos, G.; Al-Salem, S.M.; Constantinou, A. Modelling of Packed Bed and Coated Wall Microreactors for Methanol Steam Reforming for Hydrogen Production. *RSC Adv.* **2020**, *10*, 41680–41692. [CrossRef] [PubMed]
55. Matosevic, S.; Lye, G.J.; Baganz, F. Immobilised Enzyme Microreactor for Screening of Multi-Step Bioconversions: Characterisation of a de Novo Transketolase-ω-Transaminase Pathway to Synthesise Chiral Amino Alcohols. *J. Biotechnol.* **2011**, *155*, 320–329. [CrossRef]
56. Compton, D.L.; Laszlo, J.A.; Evans, K.O. Antioxidant Properties of Feruloyl Glycerol Derivatives. *Ind. Crops Prod.* **2012**, *36*, 217–221. [CrossRef]
57. Yao, N.; Sun, S. Hydrophilic Glyceryl Ferulates Preparation Catalyzed by Free Lipase B from Candida Antartica. *J. Oleo. Sci.* **2020**, *69*, 43–53. [CrossRef]
58. Sun, S.; Chen, X. Kinetics of Enzymatic Synthesis of Monoferuloyl Glycerol and Diferuloyl Glycerol by Transesterification in [BMIM]PF6. *Biochem. Eng. J.* **2015**, *97*, 25–31. [CrossRef]
59. Wang, J.; Gu, S.-S.; Cui, H.-S.; Wu, X.-Y.; Wu, F.-A. A Novel Continuous Flow Biosynthesis of Caffeic Acid Phenethyl Ester from Alkyl Caffeate and Phenethanol in a Packed Bed Microreactor. *Bioresour. Technol.* **2014**, *158*, 39–47. [CrossRef]

Journal of Biotechnology 350 (2022) 75–85

Contents lists available at ScienceDirect

Journal of Biotechnology

journal homepage: www.elsevier.com/locate/jbiotec

3D printed PLA enzyme microreactors: Characterization and application for the modification of bioactive compounds

Elena Gkantzou [a], Anastasia Skonta [a], Aliki Tsakni [b], Angeliki Polydera [a], Dimitrios Moschovas [c], Konstantinos Spyrou [c], Apostolos Avgeropoulos [c], Dimitrios Gournis [c], Dimitra Houhoula [b], Haralambos Stamatis [a,*,1]

[a] Department of Biological Applications and Technologies, University of Ioannina, Laboratory of Biotechnology, Ioannina, Greece
[b] Department of Food Science and Technology, University of West Attica, Athens, Greece
[c] Department of Materials Science and Engineering, University of Ioannina, Ioannina, Greece

ARTICLE INFO

Keywords:
3D printing
Laccase
Continuous flow biocatalysis
Microreactor
Biophenols

ABSTRACT

Process sustainability of biocatalytic processes is significantly empowered with the use of continuous-flow technologies that offer high productivity, minimal wastes and low volumetric consumption. Combining microreactor design with 3D printing technology can broaden the engineering potentials. This work proposes a protocol to modify the surface of 3D-printed PLA scaffolds, based on chitosan deposition. Mimicking the concept of microplates, multi-well plates were designed to facilitate parameter testing. Immobilization of laccase from *Trametes versicolor* was successfully performed, while chitosan and cross-linker concentration and incubation time were optimized. The developed protocol was applied for the continuous flow bioconversion of hydroxyyrosol, yielding a TTN of 438.6 × 10^3 for a total of 10 h continuous use. Also, a peristaltic flow pattern seemed to favor the system performance, reaching 95% bioconversion efficiency in a total of 1 h reaction time. The potential of the developed system was further evaluated for the biotransformation of different biophenols from dietary sources, proving the efficiency of the system as a versatile biotechnological tool.

1. Introduction

Biocatalysis embed technologies that serve as a sustainable alternative for the industrial production of chemicals with high selectivity (Domínguez de María, 2021). In industrial sectors that the foremost requirements are the rising of quality standards, and the time and cost-effectiveness, flow technology has been recognized as key enabling technology for process intensification of chemo- and biocatalytic transformations(Leemans Martin et al., 2020)(Tamborini et al., 2018a). Accordingly, sifting to flow processes can offer desirable benefits such as recycling, parallelization and real-time production control, while minimal wastes and high productivity have also been realized as highly attractive features for sustainable production(Guajardo and Domínguez de María, 2019). Companies elaborating microfluidic systems have already seen the potential to reduce the cost of scale-up and resources deployed to develop safe and stable processes(Rouhi, 2004). So, continuous flow biocatalytic reactions that would also fall within the concept of green chemistry can fulfill the goal for diminishing the environmental impact of industrial processes.

On the other hand, 3D printing technology, a layer-by-layer manufacturing process of three-dimensional objects based on computer-aided design (CAD) program codes, offers almost infinite design possibilities with extremely low costs. Regarding microfluidic applications, there are already published papers with models applied for molecule and protein detection, cell deposition and simulation, bacterial communities, tissue constructs, organ-on-a-chip and microfluidic reactionware(Kong et al., 2016; Zhou, 2017). In the biocatalysis sector, enzymes have already met the hosting of 3D printed carriers for rapid screening of immobilization conditions in customized scaffolds and demonstration of biocatalytic processes(Peris et al., 2017; Spano et al., 2020; Ye et al., 2019).

Continuous flow technologies make use of microreactors, engineered fluidic devices that use microchannels as the reaction space, to manipulate a liquid in the scale of microliters or lower. In the field of

* Corresponding author.
E-mail address: hstamati@uoi.gr (H. Stamatis).
[1] https://doi.org/10.1016/j.cviu.2017.00.000 1077–3142/© 2021 Elsevier Inc. All rights reserved.

https://doi.org/10.1016/j.jbiotec.2022.04.005
Received 23 December 2021; Received in revised form 29 March 2022; Accepted 7 April 2022
Available online 14 April 2022
0168-1656/© 2022 Elsevier B.V. All rights reserved.

biocatalysis, continuous flow microreactors have upgraded the application of enzymes in terms of integrated processing and analytical control (Domínguez et al., 2021; Gkantzou et al., 2018). Internal surface coating of microreactors in their open-tubular form, offers the advantage of catalysts immobilization in a protected environment for multiple uses of one microdevice. The space/time yield in this type of reactor scales reciprocally with the diameter of the channel so high volumetric activities can be reached with high surface-to-volume ratio at the microscale and this way operation in the absence of diffusion limitations is achieved (Bolivar and López-Gallego, 2020). An enzyme may be immobilized in the interior of a microreactor, either directly to the chemically modified surface of the reactor (introduction of surface-active groups e.g. with aminosilanes(Ye et al., 2019)) or on secondary deposited materials like nanomaterials or polymers(Bolivar and López-Gallego, 2020; Gkantzou et al., 2021).

Speaking of potential immobilization matrices that would appear in a 3D printable form, polylactic acid (PLA) is derived from 100% renewable sources, like corn starch and sugarcanes, using bacterial fermentation processes. The PLA macromolecule has aliphatic ester nature and comes from the ring polymerization of lactide, the cyclic dimer of lactic acid (2-hydroxypropanoic acid, HO-CH_3-CH-COOH). The surface modification of 3D printed PLA objects comes from the need for biocompatible and biofunctional objects, when it comes to bio-related applications. The presence of methyl groups renders PLA hydrophobic, so research is headed towards functionalization strategies to introduce -COOH, -NH_2 and -OH groups on the surface. Alkaline hydrolysis is a simple way to impart reactive hydrophilic functional groups, carboxylic acids (-COOH) and hydroxyls (-OH) by cleaving the ester bonds on the PLA main chain. The treatment is performed with a wet chemical method, immersing the polyester in a strong basic solution for a defined amount of time, which depends on the degree of the desired surface functionalization. Sodium hydroxide (NaOH) solution is commonly applied for alkali treatment of PLA, as a cheap and readily available method(Schneider et al., 2020).

As a next step in the functionalization process, biopolymer deposition has been proved to greatly enhance bioactivity of PLA, with cell proliferation and enzyme immobilization studies to be in the center of focus(Jaidev and Chatterjee, 2019; Peris et al., 2017; Wang et al., 2019). The present study focused on chitosan (CS) biopolymer, a polysaccharide made from shells of aquatic animals, as a modification agent for the 3D printed scaffolds. Pahlevanzadeh and his colleagues in their review about 3D printed constructs based on chitosan, have stated several examples of composite materials with chitosan and their enhanced mechanical behavior, while presenting interesting characteristics for bone regeneration, antioxidant and anti-inflammatory activities(Pahlevanzadeh et al., 2020).

On the basis of the above principles, we propose a protocol for surface modification of 3D printed PLA scaffolds, which comprises of four main steps: etching with an alkali solution (NaOH), coating with a bioadhesive polymer (chitosan), modification with a cross-linking agent (glutaraldehyde), and covalent immobilization of an enzyme (laccase). The strategy is simple, cost-effective and makes use of materials from renewable sources. In the first part, we demonstrate the optimization of the proposed protocol using 3D printed PLA well-plates, with the internal surface of each well serving as a platform for enzyme immobilization. It is a concept that mimics the typical microplate concept used for analysis, and it can facilitate the screening of several parameters affecting the immobilization or the biocatalytic behavior of the enzyme. In the second part, we have applied the optimized protocol to immobilize the biocatalyst in the internal surface of a 3D printed PLA microreactor and investigated the performance of the system for continuous flow biocatalytic reactions. The biocatalyst used was laccase from *Trametes versicolor*, a multicopper oxidase that catalyzes polymerization and depolymerization processes which underlie the formation of cuticles in insects and cells walls in plants. Regarding the application of the developed system, we demonstrate the oxidation and subsequent polymerization of phenolic compounds of natural origin. Degradation of phenolics has long concerned researchers, either for treatment of wastewaters, or for textile dyeing, or even cosmetic industry for hair dyeing and personal hygiene products(Martínková et al., 2016; Su et al., 2018). It is also important to note that laccase-catalyzed polymerization of natural phenols yields products of greatly enhanced antioxidant capacity from the mother compounds, while the toxicity of the parent compounds is decreased or diminished after laccase action(Nagarajan et al., 2020).

2. Materials and Methods

2.1. Materials

PLA filament for FDM 3D printers (PrimaValue™) in a natural form was obtained from Prima Creator. Sodium hydroxide with > 98% purity was obtained from Panreac. Reagents obtained from Merck (Sigma-Aldrich) are: chitosan from crab shells 85% deacetylated, acetic acid > 99.8%, laccase from *Trametes versicolor* 0.78 U/mg in lyophilized form, 2,2′-Azino-bis(3-ethylbenzothiazoline-6-sulphonic acid) diammonium salt (ABTS) 98%, rutin hydrate 95%, and caffeic acid 97%. Glutaraldehyde reagent in 25% solution was obtained from Fisher Scientific. Phenolic compounds obtained from Carbosynth are: 3-hydroxytyrosol (3,4-dihydroxyphenyl ethanol- HT), quercetin, dihydromyricetin 98%, catechol, and resveratrol. Gallic acid hydrate 98% was obtained from TCI, p-coumaric acid from Fluka, and ferulic acid 99% from Acros. All solutions used in the present work were prepared in double-distilled (dd) water.

2.2. Methods

2.2.1. 3D design and printing of PLA scaffolds

2.2.1.1. Design. PLA scaffolds were designed using *Fusion 360* CAD program from *Autodesk*. Well-plates were designed with 200 μL volume capacity for each well, while the number of wells of each plate depended on the number of samples for each experiment. Microreactors were designed with 1 mm internal diameter of the channel and volume capacity 200 μL. The channel was designed in a curvilinear pattern in order to achieve higher length in smaller total model surface. An inlet and an outlet were also designed so that intermediate tubing could be connected to the microreactor.

2.2.1.2. Slicing. After completion of the designing process, each model is sent to a 3D print utility that serves as a slicer software. The software used was *Cura* from *Ultimaker*. Print settings for every model were 0.12 mm layer height (resolution), 100% infill density and 80 mm/s print speed. The printing temperature was set at 200 °C and build plate temperature was set at 50 °C, to ensure build plate adhesion. An STL file with the appropriate guidelines for the printing process was saved to be used in a 3D printer (Table S1).

2.2.1.3. Printing. The models were printed using Fused Deposition Modeling (FDM) technology. In this approach 3D objects are fabricated by extruding a molten thermoplastic filament through a heated nozzle onto a platform-bed in a pattern determined from the slicing process. The 3D printer used for this work was *Ender 5* from *Creality*, with filament diameter 1.75 mm and a nozzle diameter of 0.4 mm. Natural PLA filament was used as the feeding material. Printing parameters set at the slicing software are presented in Table S1.

2.2.2. Surface modification and enzyme immobilization on 3D printed PLA scaffolds

2.2.2.1. Modification of well-plates. Step 1: NaOH etching.

200 μL of 1 M sodium hydroxide (NaOH) aqueous solution were added to each well and the plate was incubated at 25 °C for 2 h. After incubation, the NaOH solution was removed and each well was washed by adding 200 μL double distilled (dd) water, twice. The well-plate was dried under vacuum for 30 min

Step 2: Chitosan modification.

200 μL of 0.2% (w/v) chitosan in 1% acetic acid aqueous solution were added to each well and left for 60 s (unless stated otherwise). The solution was removed and 1 M NaOH solution was subsequently added to each well and left for 1 min, so as to neutralize the environment and stabilize the chitosan deposition. The NaOH solution was removed, each well was washed by adding 200 μL dd water, twice, and the plate was dried under vacuum for 30 min

Steps 3&4: Cross-linker modification and enzyme immobilization.

The immobilization of *Trametes versicolor* laccase (TvL) was achieved through covalent linkage using glutaraldehyde (GA) as the cross-linking agent. 200 μL of 2.5% GA solution in 50 mM phosphate buffer pH 7 were added to each well and the plate was incubated at 30 °C for 1 h (unless stated otherwise). After incubation, the GA solution was removed and the wells were washed thrice with the phosphate buffer solution. The well-plate was dried under vacuum for 30 min. An enzymatic solution with a concentration of 0.25 mg/mL was prepared by dissolving the solid enzyme preparation in 50 mM HEPES ((4-(2-hydroxyethyl)− 1-piperazineethanesulfonic acid)) buffer pH 7. 200 μL of the enzymatic solution were added to each well and the plate was incubated at 30 °C for 1 h. After incubation, the enzyme solution was removed and the wells were washed thrice with the HEPES buffer solution. The well-plate was dried under vacuum for 30 min and stored at 4 °C until further use.

2.2.2.2. Modification of microreactors. The modification process for the microreactors was performed by filling the microreactor with the corresponding solution for each step described above for the well-plate modification, using disposable 1 mL syringes. The concentrations and the volumes of the solutions were kept the same as the well-plates, except for the enzyme solution concentration which was 4 mg/mL. The drying process was conducted under N_2 stream in between the modification steps.

2.2.3. Enzymatic activity measurement in the PLA well-plates

The activity of immobilized laccase was determined with a photometric assay using ABTS (2,2′-azino-bis(3-ethylbenzothiazoline-6-sulfonic acid)) as the substrate. Each well was filled with 200 μL of 0.25 mM ABTS solution in sodium acetate buffer pH 5 and the well-plate was incubated at 30 °C for 5 min in order for the reaction to proceed. The reaction solution was then transferred to a microplate and the absorbance of the cationic radical of ABTS that was produced from the enzymatic reaction was measured in an ELISA plate reader at 405 nm. The units of enzymatic activity were calculated using the Beer-Lamberts law with ε coefficient 36.8 mM^{-1} *cm^{-1}.

2.2.4. Estimation of the immobilization yield

To determine the amount of enzyme that was loaded during immobilization process, an activity test was conducted for the enzymatic solution before and after immobilization. A sample from the enzymatic solution before its loading either on a well or on a microreactor was measured with the ABTS protocol described above, and a sample of the enzymatic solution after incubation in the corresponding scaffold was also measured with the same process. Eq. (1) was used for the calculation of the active enzyme amount loaded during immobilization in each scaffold.

$$\text{Immobilization yield } \% = 100 - (\text{activity after immobilization} \times 100) / (\text{activity before immobilization}) \quad (1)$$

2.2.5. Protocol optimization for surface modification of PLA scaffolds

For the biocatalytic assays in the well-plates, the main modification protocol described above was applied and, depending on the assay, a particular step was modified by concentration or incubation time (for chitosan and cross-linker tests) or omitted from the modification process (for blank tests). In detail, for the effect of chitosan modification, chitosan solutions with concentrations 0.1%, 0.2%, 0.5% and 1% were used and each solution was tested for 60, 120, 240, 360 and 600 s. For the effect of cross-linker concentration and time, GA solutions with concentrations 1%, 2.5%, 4% and 10% were used and each solution was tested for incubation times 30 min, 1 h, 2 h and 4 h. The effect of the different conditions was evaluated by measuring the enzymatic activity as described in section 2.3.

2.2.6. Stability studies of immobilized laccase on PLA scaffolds

2.2.6.1. Operational stability. To evaluate the operational stability of the immobilized laccase on PLA scaffolds, 10 successive cycles of use were performed. ABTS oxidative reaction was monitored as described in paragraph 2.3. After completion of each cycle (5 min), the reaction solution was removed and the corresponding well was washed thrice with the reaction buffer. Fresh substrate solution was then filled in each well and the process was repeated for 10 cycles of use. Remaining activity compared to the first cycle was calculated using Eq. (2). The experiment was performed in triplicate.

$$\text{Remaining activity } \% = (\text{activity in each cycle x } 100) / (\text{activity in the first cycle}) \quad (2)$$

2.2.6.2. Thermal stability. The stability of the immobilized system was evaluated for 24 h incubation at 40 °C, 50 °C, and 60 °C. The activity of laccase in each well was measured before incubation, as described in paragraph 2.3. For every temperature tested, three wells were filled with buffer solution and placed in an incubator for 24 h. After this time, the remaining activity of laccase in each well was calculated with the same procedure and the percentage of thermal stability was estimated using Eq. (3).

$$\text{Remaining activity } \% = (\text{activity before incubation x } 100) / (\text{activity after incubation}) \quad (3)$$

2.2.7. Characterization of the 3D printed PLA scaffolds

Scanning Electron Microscopy (SEM) and X-ray Photoelectron Spectroscopy (XPS) for the characterization of the 3D printed scaffolds are described in the Supplementary material.

2.2.8. Assays for PLA microreactors

For the enzymatic assays in the PLA microreactors, the biotransformation of hydroxytyrosol (HYD) was monitored for the different conditions applied. HYD was dissolved in 100 mM citrate phosphate buffer pH 5 and concentration of 1 mg/mL was used for all experiments. The effect of the different parameters in the biotransformation reaction was evaluated with HPLC analysis, as described in the supplementary material. All experiments were performed in triplicate.

2.2.8.1. Effect of enzyme concentration. For the enzyme concentration study, 7 enzyme concentrations of the solution loaded for immobilization in the microreactor, were tested: 0.25 mg/mL, 0.5 mg/mL, 1 mg/mL, 2 mg/mL, 4 mg/mL, 6 mg/mL, and 8 mg/mL. The modification and enzyme immobilization process was followed according to paragraph 3.2, except for the different concentration of the enzymatic solutions. After enzyme immobilization, the effect of the different conditions was evaluated following the biotransformation of HYD for a total residence

time 1 h, using a peristaltic flow pattern with flow rate 10 μL/min. After 3 peristaltic cycles were completed, the reaction solution was collected and analyzed in an HPLC system. The yield of each reaction was estimated based on the consumption of the substrate compound (HYD) and on the production of the main product (HYD trimer), using Eqs. (4) and (5).

HYD consumption % = (area of the substrate peak after enzymatic reaction x 100)/ (area of the substrate peak of the blank measurement) (4)

HYD trimer production % = (area of the product peak x 100)/ (area of the substrate peak after enzymatic reaction + area of the product peak) (5)

2.2.8.2. Effect of flow pattern. For the effect of flow pattern, a syringe pump was used for the single run measurement and a high precision peristaltic pump was used for the measurements performed in multiple runs. A single run was performed by regulating the pump at 200 μL/min flow rate. The effluent was collected and analyzed with HPLC. For the peristaltic pattern tests, flow rate of 10 μL/min was used for 3 runs, 20 min each, 20 μL/min for 6 runs, 10 min each, and 40 μL/min for 12 runs, 5 min each. Each flow pattern was designed in a way that 200 μL reaction solution would flow in the reactor chamber with the minimum dead-space possible, so between the flow periods 5 s or lower passed until the next run entered the reactor space. The effluent was collected after completion of the number of runs and analyzed with HPLC.

2.2.8.3. Operational stability. Operational stability of the immobilized laccase on PLA microreactors was monitored for 10 consecutive hours of use. A syringe pump was used for the continuous reaction, loaded with 2 mL of 1 mg/mL hydroxytyrosol solution in 100 mM citrate phosphate buffer pH 5. After each cycle of use (cycles of 1 h, flow rate 200 μL/h) the effluent was collected and analyzed with HPLC.

2.2.8.4. Process parameters. Reynolds number (Re) was calculated according to Eq. (6) for flow in tubes. The diameter (D_H) was 1 mm, the volumetric flow rate (Q) was 1.66×10^{-10} m^3/sec, and the cross sectional area (A) was 0.7854 m^2. The density (ρ) and dynamic viscosity (μ) refer to the water as the solvent for all the solutions used. Total turnover number (TTN) was calculated according to Eq. (7). The amount of the product refers to the main product (trimer) as it was analyzed with HPLC for 10 consecutive hours of use, with samples measured every 1 h. The amount of biocatalyst was considered 0.6 mg, as the amount that was immobilized in the interior of the microreactor.

$$Re = \frac{\rho Q D_H}{\mu A} \quad (6)$$

$$TTN = \frac{mol\ \ product\ \ (for\ \ a\ \ total\ \ of\ \ 10h\ \ of\ \ use)}{mol\ \ immobilized\ \ biocatalyst} \quad (7)$$

2.2.9. Continuous flow biotransformation of phenolic compounds

The continuous flow biotransformations were performed for a residence time of 1 h under a peristaltic flow pattern (3 runs x 20 min) with a flow rate of 10 μL/min. Temperature was kept constant at 30 °C and the solvent system of the reactions was 90:10 v/v buffer: methanol. Reaction solutions used had a concentration of 5 mM, coming from stock solutions of 50 mM in methanol. 100 mM citrate phosphate buffer pH 5 was used for the compounds quercetin, myricetin, catechol, and resveratrol, while 100 mM sodium acetate buffer pH 5 was used for the compounds caffeic acid, p-coumaric acid, ferulic acid and gallic acid. Rutin was dissolved in dd water. The effluent of each reaction was collected and mixed with equal amount of methanol that was first pumped through each microreactor in order to collect any unreacted amount of substrate. The final reaction products were quantified in terms of conversion efficiency with HPLC and characterized for the identification of the products with MS, as described in the supplamentary material.

2.2.10. Analysis of the reaction products

High Pressure Liquid Chromatography (HPLC) analysis and Mass spectrometry (MS) analysis for the characterization of the reaction products are described in the Supplementary material.

3. Results and Discussion

3.1. 3D design and printing of PLA scaffolds

In the present work, we designed well-plates, with a customized number of wells, which served as scaffolds for easy and fast screening of several factors affecting surface functionalization and enzyme immobilization, with low needs of feeding material and printing capacity. This approach falls within the concept of 3D printed 'reactionware' which allows for fast production of identical scaffolds to facilitate parameter testing, with models of high quality and functionality(Kitson et al., 2014; Peris et al., 2017). Additive manufacturing has also attracted scientific interest in the microreactor technology field because it allows for precise control over the geometry and composition of the designed reactors(Kim et al., 2021). Based on this perspective, we propose here for the first time a microreactor made of polylactic acid (PLA), as a renewable, biocompatible and biodegradable material. The fabrication costs per microreactor model come to 0.1434 € (32 mm × 37 mm) and to 0.3107 € for a 9-well microplate (35 mm × 35 mm). We used FDM printing technology, which produces ready-to-use models (no post-processing needed) and a resolution of 0.12 mm, for the best available quality. Models before and after printing are demonstrated in Fig. 1.

3.2. Protocol optimization for surface modification of PLA scaffolds

The protocol proposed in this work is easy to handle, can be completed in a few hours and utilizes chitosan, a natural-derived polymer, for the introduction of surface functional groups. It comprises four main steps: NaOH etching, chitosan deposition, binding with glutaraldehyde as a cross-linker molecule, and enzyme immobilization. In this section, the optimum concentration and incubation time for the different modification steps are evaluated. Enzyme concentration and incubation time were kept constant in each case. Preliminary blank tests were performed in order to confirm that high and reproducible enzymatic activity is only observed when all the steps of the protocol are followed.

Sodium hydroxide (NaOH) etching or ester backbone hydrolysis of 3D printed PLA was the first step of the modification protocol, intending to promote hydrophilicity of the scaffold. The concentration of alkali solution along with the incubation time with the 3D printed structure has been shown to have an important role in the surface morphology of the material(Durán et al., 2020; Maia-Pinto et al., 2021; Schneider et al., 2020). For the present work, different incubation times of the NaOH solution with the PLA scaffolds (from 30 min to 24 h) did not affect the activity of the immobilized enzymes (data not shown). Chitosan and glutaraldehyde concentrations were kept constant at 2.5% and 0.2%, respectively. X-Ray Photoelectron Spectroscopy was used to confirm the surface enrichment of 3D printed PLA with hydrophilic moieties that would facilitate further surface modification. The results are presented in Fig. 2 and indicate that the C1s photoelectron spectra of the initial PLA scaffold presents the foreseeable C-C/C-H, C-O-C/C-OH and C═O peaks representing 72.8%, 13.3% and 13.9% respectively. After NaOH treatment a significant change in the recorded spectrum is observed. In detail, while the C-OH groups stay unaffected a new peak is observed arriving from the creation of carboxylate groups. These groups represent 14.4% of the whole carbon amount. So, according to the XPS study, high degree of surface enrichment with hydrophilic groups was achieved

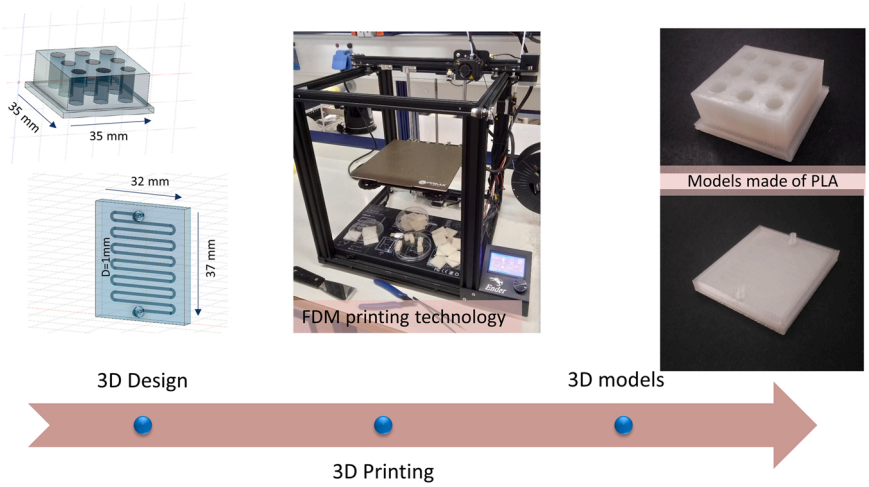


Fig. 1. Well-plates and microreactors made of PLA were produced through 3D design and FDM printing technology.

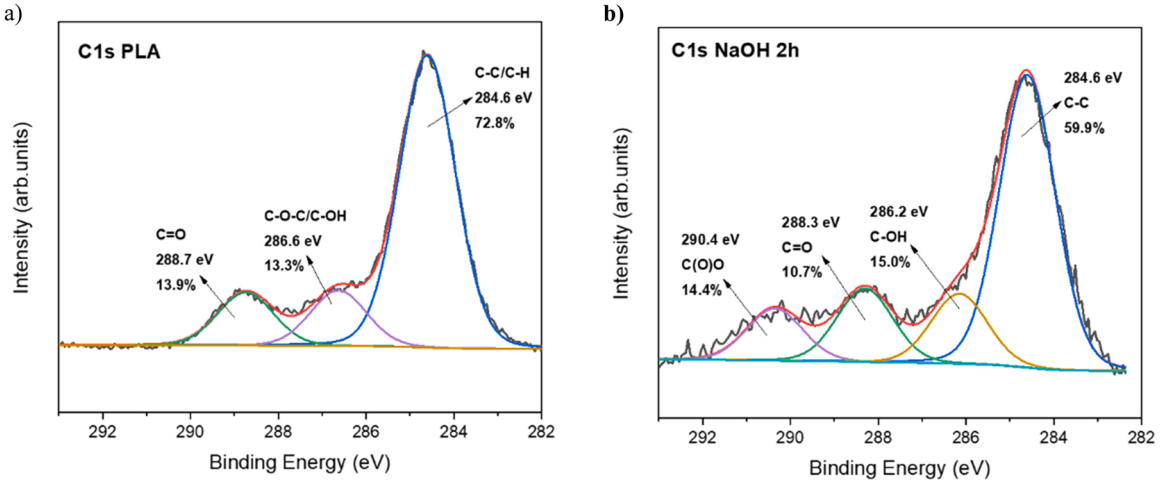


Fig. 2. C1s photoelectron spectra of a) neat PLA and b) PLA after treatment with 1 M NaOH for 2 h at 25 °C.

within 2 h of NaOH treatment of 3D printed PLA. Further incubation did not yield any considerable change in the recorded spectra. As a consequence, these results in combination with literature data, indicated 2 h incubation with 1 M NaOH aqueous solution to be used for the initial treatment of the scaffolds.

3.2.1. Chitosan modification – effect of concentration and incubation time

After surface hydrolysis of PLA, chitosan deposition would be readily achieved. A multi-well plate was used as immobilization support to evaluate the effect of chitosan concentration along with incubation time, on the enzymatic activity of the system. Low concentrations of chitosan give less viscous solutions that could be deposited more homogeneously

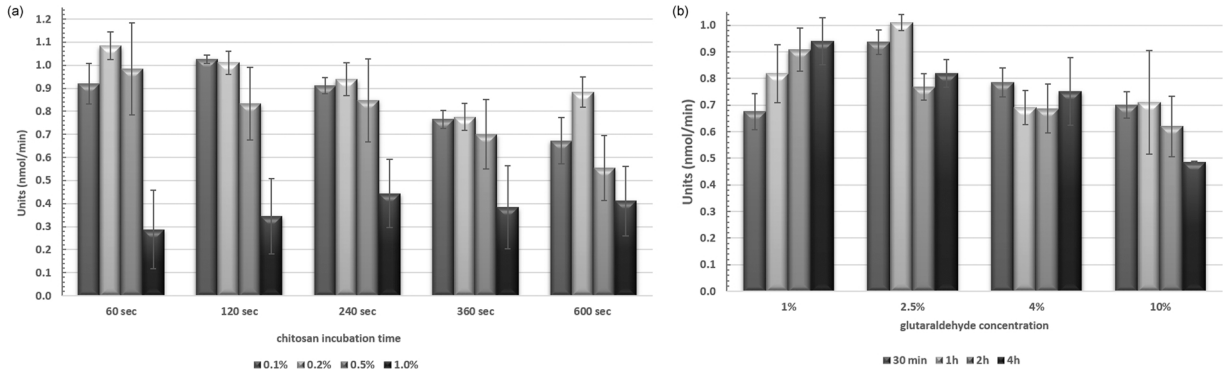


Fig. 3. Protocol optimization for the modification of 3D printed PLA. a) Effect of chitosan concentration and incubation time, b) effect of glutaraldehyde concentration and incubation time. 1 Unit equals to the amount of enzyme that catalyzes the conversion of 1 nanomole of ABTS substrate per minute in 200 μL reaction volume at 30 °C for 5 min.

on macro-scaled surfaces. Literature data for enzyme immobilization on chitosan-coated surfaces also present low concentrations of chitosan solutions used(Wang et al., 2019, 2016). In the present work, a range of 0.1–1% chitosan concentration was used, with each solution subjected to different incubation times on the PLA surface.

The results demonstrated in Fig. 3a), reveal that short incubation times in combination with low chitosan concentrations facilitate the enzymatic performance, although a minimum amount of 0.2% chitosan concentration is necessary to achieve maximum yield. It was observed that while concentration was increasing, activity was decreasing with chitosan concentration of 1% to result in a severe decrease of the enzymatic activity. Samples of 0.2% chitosan concentration and different incubation times (Fig. S1) were also analyzed with Scanning Electron Spectroscopy (SEM). The morphological analysis showed that a low exposure time of the chitosan solution to the PLA surface yields more homogeneously deposited layers of chitosan, while thicker layers are achieved with longer exposure times. Taking these under consideration, 0.2% chitosan concentration for 1 min incubation time were chosen as the conditions producing the optimum results in the study.

3.2.2. *Effect of cross-linker concentration and time*

Coating the PLA surface with chitosan moieties not only created a highly biocompatible environment to the prepared scaffold, but also enriched it with ready-to-react amino groups. As a next step, glutaraldehyde (GA), a bi-functional reagent widely used in the design of biocatalysts, was used to modify the PLA-CS scaffold with the aim to eventually obtain enzyme-support covalent bonds.

Glutaraldehyde may either crosslink the available amino groups of chitosan, leaving no available reactive groups for the enzyme, or it may work as a linker between aldehyde groups formed on the surface of chitosan on the one side and on the enzyme surface on the other side of the bridge, producing stable conformations (Monteiro and Airoldi, 1999) (Barbosa et al., 2013). In the present case, enzyme molecules seem to have been steadily linked to the PLA-chitosan-GA system, as enzymatic activity was high and reproducible, while repeating the protocol in the absence of GA did not yield sufficient enzyme activity. GA-mediated bonding between chitosan and enzymes is commonly reported, and in every case both GA concentration and reaction time need to be investigated(Çelik et al., 2016; Chen et al., 2013; Giannakopoulou et al., 2021; Gür et al., 2017). In the present study, a range from 1% to 10% GA concentration for reaction times from 30 min to 4 h were investigated. It is clearly inferred from Fig. 3b) that high GA concentration (10%) causes about 50% decrease of enzymatic activity compared to the samples where lower GA concentrations were used during immobilization process. Jiang and his group also studied laccase immobilization through GA bonding with chitosan(Jiang et al., 2005) and stated that a rise above 8% of GA concentration leads to extensive interaction of individual enzymes with aldehyde groups that could change the enzyme conformation and cause the drop in enzymatic activity, a conclusion also realized from Çelik et al. in their work on β-glucosidase immobilization on chitosan-coated supports(Çelik et al., 2016). Low GA concentration was also realized to contribute to the operational stability of laccase cross-linked on chitosan supports(Apriceno et al., 2017). Regarding incubation time, a rise above 1 h incubation does not seem to favor the efficiency of the system. So, 2.5% GA concentration for 1 h incubation time with the chitosan-coated support were chosen as the optimal conditions.

3.3. *Stability studies of immobilized laccase on PLA scaffolds*

Following the parameter testing for modification of the immobilization carrier, studying the stabilization of the biocatalyst after exposure to experimental conditions consists a common practice in the designing of biocatalytic systems. More specifically, operational stability is intended as the capability of the biomolecules to maintain as much as possible their activity after repeated catalytic cycles, with intermediate washing and reusing steps. Results for the case of the PLA-TvL biocatalytic system are presented in Fig. 4a). The system showed exceptional stability in the operating conditions, recovering 95% of its initial efficiency after 10 consecutive cycles of use, thus exhibiting a superiority compared with previously published systems with immobilized TvL on chitosan or chitosan-coated carriers(Apriceno et al., 2021, 2018, 2017; Naghdi et al., 2019).

One step further, immobilization through cross-linking agents increase the resistance to harsh experimental conditions, while immobilization via a bifunctional agent like glutaraldehyde, which can also give intramolecular cross-linking, provides rigidity to the immobilized enzymatic structure and results in better resistance towards denaturation agents, like elevated temperatures.(Apriceno et al., 2018). The results from the present study (Fig. 4b) are in accordance with the previous observations for immobilized laccase systems (Apriceno et al., 2021, 2017; Naghdi et al., 2019), with the PLA-TvL system exhibiting high residual activity (82%) even after 24 h of incubation at 50 °C. In all cases tested, the immobilized enzyme appeared significantly more stable than the free enzyme form.

3.4. *3D printed PLA microreactors with immobilized laccase*

Laccase-based microreactor systems have not been widely discussed in the literature. However, the attempts so far have shown remarkable efficiencies, biocatalyst stabilization and process facilitation, outperforming conventional designs(Lin et al., 2010; Lloret et al., 2013; Tišma et al., 2009). It has been also stated that the immobilization of the enzyme in the interior of the microreactors contributes significantly in the process sustainability (Tušek et al., 2017).

In the previous sections, we investigated a protocol to modify the surface of 3D-printed PLA with the aim to make it friendly to host biomolecules. In this section, this protocol was applied to develop PLA microreactors with immobilized laccase to be elaborated in phenolic compounds biotransformation processes. The performance of the developed system was initially evaluated using hydroxytyrosol as a model compound. Hydroxytyrosol (HT), one of the main fractions of olive pomace and olive wastewater, has been widely studied for its antioxidant potential and oligomers coming from HT oxidation reactions, mainly dimers, trimers, and tetramers, expand or enhance the biological activities of the mother compound, playing a significant role in functional food, cosmetic and pharmacy industries(Manzano-Nicolas et al., 2021; Xie et al., 2021a). The oxidative-induced polymerization of HT is given ‘green’ attributes when it is performed with natural catalysts, such as oxidoreductase enzymes. Amongst them, laccases, especially *Trametes versicolor* derived, have been proven the most efficient in terms of bioconversion efficiency(Canfora et al., 2008; Xie et al., 2021a).

The reaction progress monitoring, the conversion of the substrate and the formation of the product from the biotransformation of HT was detected through HPLC and MS analysis. The results refer to the main product peak, assigned to hydroxytyrosol trimer, based on the mass spectrometry analysis (m/z 458.2). The microreactors were loaded with 4 mg/mL enzyme concentration (0.6 mg enzyme preparation immobilized), the substrate (HT) concentration was fixed at 1 mg/mL (6.48 mM) and the reactor was operated for a total of residence time 1 h, performed in 3 consecutive peristaltic runs of 20 min each, unless stated otherwise. The microfluidic apparatus is demonstrated in Figure 8.

3.4.1. *Effect of enzyme concentration*

The main factor affecting the efficiency of an immobilized enzyme system lies in the enzyme loading in accordance with the enzymatic activity. The immobilization yield, i.e. the percentage of biocatalyst immobilized compared to the biocatalyst loaded, was evaluated in terms of active enzyme molecules measuring the activity of the enzyme preparation before and after microreactor loading. The results presented in Table S2, indicate that enzyme loading reaches a critical concentration after which no more active enzyme molecules are present in the

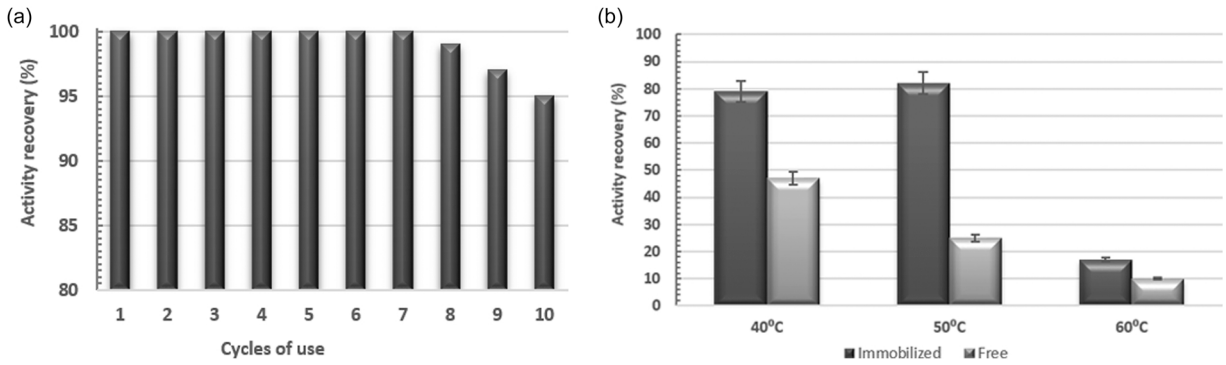


Fig. 4. Stability studies of the PLA-TvL biocatalytic system. a) Operational stability for 10 repeated cycles of use, with intermediated washings, measured for the oxidation reaction of ABTS substrate. 100% activity is considered the one measured after the first use. Standard deviation for all samples was < 0.1. b) Thermal stability for the free and immobilized TvL after 24 h incubation in sodium acetate buffer pH 5 at different temperatures. 100% activity is considered the one exhibited before incubation.

system. This observation is confirmed from the bioconversion study of HT presented in Fig. 5. The bioconversion efficiency (HT consumption) increases with increased enzyme loading, although no sharp increments are observed beyond the value of 1 mg/mL, where 100% immobilization yield is also observed. Regarding the main product yield, HT trimer, maximum efficiency is already reached in low enzyme concentrations. Taking under consideration the reaction mechanism, the main action of the enzyme is primarily devoted to produce free radicals from the substrate(Canfora et al., 2008). The further polymerization of the species produced proceeds in a non-catalytic, spontaneous way. So, although substrate oxidation may continue, polymeric product formation may have reached its maximum yield in a previous time. Considering these, 4 mg/mL (0.6 mg enzyme preparation depending on immobilization yield) was used as an optimum concentration for the subsequent studies.

3.4.2. *Effect of the flow pattern*

Under the scope to optimize the yield capacity of the developed microreactors, an evaluation of the flow pattern was performed. Liquid flow in a microreactor is commonly performed with the use of a syringe or a peristaltic pump. Syringe pumps work in a one-way driving motion, while peristaltic pumps recirculate the fluid with a fixed flow rate. In our case, the one scenario was pumping the substrate solution with a proper flow rate (200 μL/h) in order for the solution to get in contact with the reactor for 1 h, in a one-way working apparatus. The other scenario was to explore the peristaltic runs available for a total of 1 h residence time, by recirculating the substrate solution for 3, 6 or 12 runs, indicative of the times that the substrate would get in touch with the biocatalyst.

The results of the study are presented in Table 1. More peristaltic runs ended up in a higher yield capacity of the system, both in terms of substrate consumption and product yield. A level of 95% of bioconversion efficiency was reached with 12 runs of 5 min each, while the product yield reached 60% of the converted substrate. Accordingly, it is assumed that substrate recirculation enhances the efficiency of the biocatalytic process, as it has been reported in previous studies concerning enzymatic bioreactors(Gambacorta et al., 2021; Xue et al., 2020; Zhang et al., 2013). It is also important to note that this level of efficiency is one of the highest reported so far for HT biotransformation and HT trimer production, at 30 °C, compared not only to immobilized enzyme systems where activity losses are usually observed, but also in comparison with reactions performed with free enzyme forms(Canfora et al., 2008; Xie et al., 2021b, 2021a).

Table 1
Effect of the flow pattern on the bioconversion efficiency (HT consumption) and the product yield (HT trimer). Reactions were performed at 30 °C with substrate concentration 1 mg/mL in 0.1 M citrate phosphate buffer pH 5. Consumption and product yields were recorded with an HPLC system. Standard deviation for all samples was < 0.1.

Runs	Flow rate	Consumption %	Product yield %
1×60min	200 μL/h	40	31
3×20min	10 μL/min	65	32
6×10min	20 μL/min	75	39
12×5min	40 μL/min	95	60

3.4.3. *Operational stability*

Operational stability of microreactor systems consists one of the most important advantages of this technology. When the enzyme is fixed in the interior of the microreactor, substrate solution may be continuously fed to the system so as multiple times of use for a single microreactor can be achieved. Concerning HT conversion, this is the first work

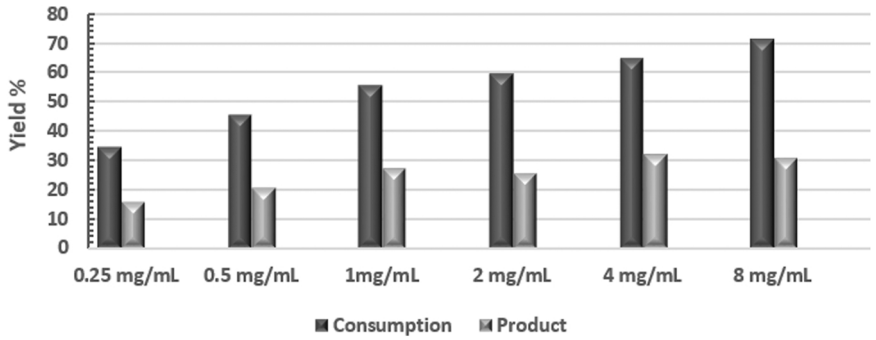


Fig. 5. Effect of enzyme concentration on the system performance. HT consumption and product yield were estimated with HPLC analysis. Enzyme concentrations refer to the concentration of the solution loaded on the PLA microreactor during the immobilization procedure. Reactions were performed for 1 h residence time at 30 °C with substrate concentration 1 mg/mL in 0.1 M citrate phosphate buffer pH 5. Standard deviation for all samples was < 0.1.

demonstrating continuous bioconversion and product acquisition from an immobilized laccase system. Fig. 6 demonstrates a yield of 52% for the trimer product after 10 h of continuous operation and a bioconversion of HT of 31% in the 10th hour of use. The results obtained from this study could contribute to the designing of a sustainable process for the biotransformation of valuable compounds.

3.4.4. Process parameters for PLA-TvL microreactors

Some process parameters indicative of the performance of the microreactor system were also estimated. At first, Reynolds number (Re) describes the viscous forces present in the system. For the PLA-TvL microreactor exhibits Re was calculated equal to 2.1×10^{-7}, so the system works in laminar flow regimes (Re<2000) and is governed by diffusion phenomena. Total turnover number (TTN) indicates the biocatalyst performance and allows for consideration of enzyme degradation over time(Dias Gomes and Woodley, 2019). Here, the PLA-TvL microreactor worked for a total of 10 h and the amount of product was estimated in each cycle, using an immobilized biocatalyst amount of 0.6 mg. TTN number of 438.6×10^3 was obtained for the studied system, indicating the viability of the designed system for repeated use of the immobilized biocatalyst, while reducing operating costs and resources consumption, thus demonstrating a sustainable process design (Rogers and Bommarius, 2010; Tamborini et al., 2018b). Process parameters are presented in Table 2.

3.5. Continuous flow biotransformation of different phenolic compounds

The PLA-TvL microreactor system was further elaborated to investigate its potential for a variety of biotransformation reactions yielding oligomeric products with important biological activities. The tested compounds are biophenols, secondary metabolism molecules and a heterogeneous class of chemical compounds widely defused in plants and found in several dietary sources, like fruits (rutin, myricetin, resveratrol), olive oil and wine (quercetin, catechol, caffeic acid, p-coumaric acid, ferulic acid, gallic acid).

The continuous flow biotransformations were performed for 1 h with a peristaltic flow pattern (3 runs x 20 min) at 30 °C with a solvent system 90:10 v/v 0.1 M (citrate phosphate or sodium acetate) buffer pH 5: methanol. The bioconversion efficiencies are presented in Table 3, as they were recorded from the HPLC analysis. A representation of the operating system is illustrated in Fig. 7. Mass spectrometry analysis of the reactions products (Table 5) identified dimeric, trimer, tetrameric or oligomeric compounds, while high conversion yields were achieved for all the compounds tested. These results highlight the efficiency of the bioprocess and the versatility of the 3D printed microreactor as a biotechnological tool.

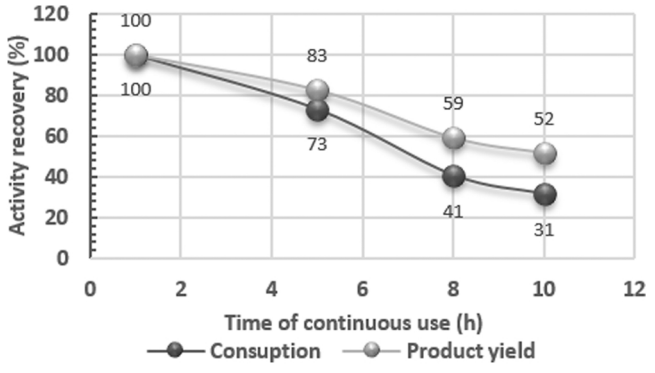


Fig. 6. Activity recovery of the TvL immobilized in the interior of a PLA microreactor working continuously for 10 h. Reactor effluents were analyzed in intermediate times, with 100% considered the activity after the first cycle of use (1 h). Substrate concentration was 1 mg/mLin 0.1 M citrate phosphate buffer pH 5, biocatalyst loading was 0.6 mg and the reaction proceeded at 30 °C. Flow rate was fixed at 200 μL/h. HT consumption and product yield were recorded with HPLC analysis. Standard deviation for all samples was < 0.1.

Table 2
Process parameters calculated for the PLA-TvL microreactor used for the bioconversion of HT. TTN refers to total turnover number calculated for 10 consecutive hours of use. The reaction was performed for a residence time of 1 h at 30 °C in 0.1 M citrate phosphate buffer pH 5.

Substrate concentration	Amount of biocatalyst	Time	Substrate conversion	Re	TTN
1 mg/mL	0.6 mg	1 h	95%	2.1×10^{-7}	438.6×10^3 (mol product/ mol biocatalyst)

Table 3
Continuous flow biotransformation of different phenolic compounds. Bioconversion percentage was recorded with HPLC analysis and product identification was performed with mass spectrometry analysis. The reactions were performed for 1 h residence time with 3 peristaltic runs of 20 min at 30 °C in 90:10 0.1 M (citrate phosphate or sodium acetate) buffer pH 5: methanol solvent system.

Phenolic compound	Bioconversion (%)	Product identification (*m/z*)	Product type	Reference of previously detailed characterization of the products
Rutin	97.5	1219.4	dimer	(Muñiz-Mouro et al., 2018)
Quercetin	75.4	499.0	dimer	(Ghidouche et al., 2007)
		619.0	dimer	
Myricetin	100	635.0	dimer	(Ghidouche et al., 2007)
Catechol	98.8	217.9	dimer	(Koclar Avci and Begum OGEL, 2014)
		325.7	trimer	
		978.8	oligomer	
Resveratrol	94.3	477.0	dimer	(Zhang et al., 2012)
		561.0	trimer	
		801.0	tetramer	
Caffeic acid	100	313.7	dimer	(Koclar Avci and Begum OGEL, 2014)
		715.5	tetramer	
		737.4	tetramer	
Gallic acid	72.1	496.0	trimer	(Gamov et al., 2020)
		674.0	tetramer	
p-Coumaric acid	81.8	326.0	dimer	(Perna et al., 2018)
Ferulic acid	98.6	386.0	dimer	(Perna et al., 2018)

4. Conclusion

In the present work, a method is demonstrated to obtain 3D printed scaffolds for enzyme immobilization, which would be useful for screening different parameters affecting functionalization and immobilization processes, while being effective tools for a variety of continuous flow biotransformation reactions. PLA was utilized as the immobilization matrix, being a material of agricultural origin, biocompatible and biodegradable. In order to render the 3D printed objects biofunctional, a protocol is presented that is easy to handle, can be completed in a few hours and utilizes chitosan, a natural-derived polymer, for the introduction of surface functional groups. It comprises four main steps: NaOH etching, chitosan deposition, binding with glutaraldehyde as a cross-linker molecule, and enzyme immobilization. The scaffolds that were designed fall within two main concepts used in biocatalysis applications, the concept of 'reactionware' and the concept of microreactors. Well-plates, with customized number of wells, served as scaffolds that allow for fast production of identical models of high quality and functionality to facilitate parameter testing. Immobilized laccase (TvL) on the surface of PLA scaffolds showed exceptional stability in the operating

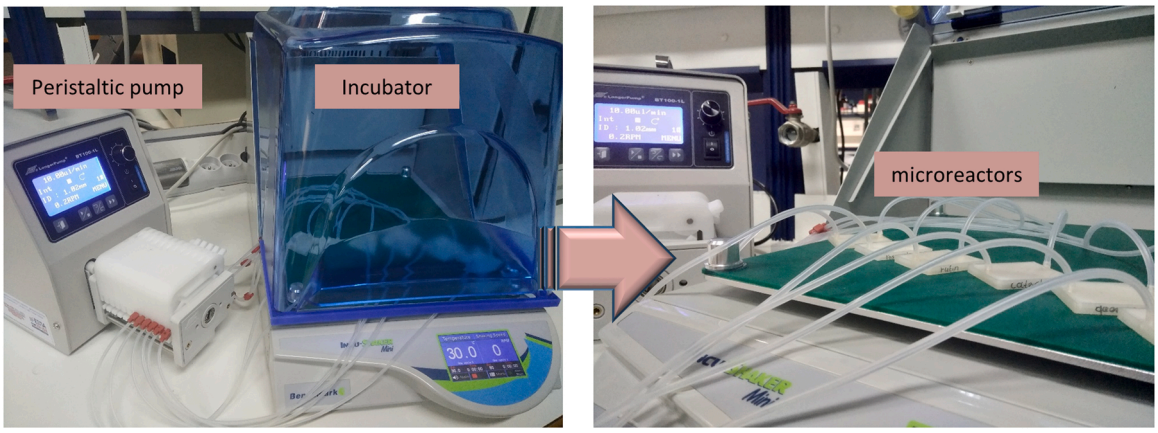


Fig. 7. Arrangement of the microfluidic system used for the biotransformation reactions. A peristaltic pump was regulated at a fixed flow rate and 3D printed microreactors were connected with tygon tubing. The microreactors were then placed in an incubator for the surrounding temperature to be fixed at 30 °C. Reactions were performed for a total of 1 h residence time, with varying peristaltic runs depending on the used flow rate.

conditions, recovering 95% of its initial efficiency after 10 consecutive cycles of use, thus exhibiting a superiority compared with previously published systems with immobilized TvL on chitosan or chitosan-coated carriers. Morphological and optical characterization studies confirmed the successful functionalization of the 3D printed structures and revealed the degree of surface enrichment with functional groups.

The optimized protocol was used for the functionalization of 3D printed PLA microreactors, with surface immobilized laccase, with the aim to investigate the performance of the system for continuous flow biocatalytic reactions. The performance of the developed system was initially evaluated using hydroxytyrosol (HT) as a model compound, since the oxidative-induced polymerization of HT has been proved to give oligomer compounds with superior biological activities than the monomer itself. 95% of bioconversion efficiency was reached with 12 peristaltic runs of 5 min each, while the product yield reached 60% of the converted substrate, with this level of efficiency being one of the highest reported so far for HT biotransformation and HT trimer production. Additionally, a total turnover number (TTN) of 438.6×10^3 was obtained for the studied system, indicating the viability of designed system for repeated use of the immobilized biocatalyst. Thus, the enzymatic microreactor is proposed as a promising alternative to conventional batch reactions for hydroxytyrosol biotransformation described in previous works, since a high conversion efficiency can be achieved in short reaction times, the reactor system can be used multiple times, and reagent consumption is minimized, making the process cost-effective.

The PLA-TvL microreactor system was further elaborated to investigate its potential for the biotransformation of several biophenols from dietary sources. High conversion efficiencies were achieved for all tested compounds and yield of oligomeric products that have been previously proved to have important biological activities. In conclusion, this study presents a promising concept for enzyme immobilization scaffold design, elaborating cost-effective processes with naturally-sourced starting materials. Using additive manufacturing for the construction of simple and low-cost reactor platforms that will facilitate enzyme immobilization may bring biocatalytic reactions one step closer to industrial applications.

CRediT authorship contribution statement

Elena Gkantzou: Conceptualization, Methodology, Software Writing – original draft. **Anastasia Skonta:** Methodology, Software, Validation. **Aliki Tsakni:** Methodology, Software. Angeliki Polydera: Methodology, Software, Data curation. **Dimitrios Moschovas:** Methodology, Software. **Konstantinos Spyrou:** Methodology, Software Validation. **Apostolos Avgeropoulos:** Methodology, Software, Validation. **Dimitrios Gournis:** Writing – review & editing, Validation. **Dimitra Houhoula**: Writing – review & editing. **Haralambos Stamatis**: Supervision,

Declaration of Competing Interest

The authors declare that they have no known competing financial interests or personal relationships that could have appeared to influence the work reported in this paper.

Acknowledgements

This research has been cofinanced by the European Regional Development Fund of the European Union and Greek national funds through the Operational Program Competitiveness, Entrepreneurship, and Innovation, under the call RESEARCH−CREATE-INNOVATE (project code: T2EDK-01410). E.G. is thankful for the financial support to the Operational Program ≪Human Resources Development, Education and Lifelong Learning≫ in the context of the project “Strengthening Human Resources Research Potential via Doctorate Research” (MIS-5000432), implemented by the State Scholarships Foundation (IKϒ), which is co-financed by Greece and the European Union (European Social Fund-ESF).

Statement of informed consent, human/animal rights

No conflicts, informed consent, human or animal rights applicable.

Appendix A. Supporting information

Supplementary data associated with this article can be found in the online version at doi:10.1016/j.jbiotec.2022.04.005.

References

Apriceno, A., Bucci, R., Girelli, A.M., 2017. Immobilization of laccase from trametes versicolor on chitosan macrobeads for anthracene degradation. Anal. Lett. 50, 2308–2322. https://doi.org/10.1080/00032719.2017.1282504.

Apriceno, A., Girelli, A.M., Scuto, F.R., 2018. Design of a heterogeneous enzymatic catalyst on chitosan: investigation of the role of conjugation chemistry in the catalytic activity of a Laccase from Trametes versicolor. J. Chem. Technol. Biotechnol. 93, 1413–1420. https://doi.org/10.1002/jctb.5509.

Apriceno, A., Silvestro, I., Girelli, A., Francolini, I., Pietrelli, L., Piozzi, A., 2021. Preparation and characterization of chitosan-coated manganese-ferrite nanoparticles conjugated with laccase for environmental bioremediation. Polymers 13. https://doi.org/10.3390/polym13091453.

Barbosa, O., Ortiz, C., Berenguer-Murcia, Á., Torres, R., Rodrigues, R.C., Fernandez-Lafuente, R., 2013. Glutaraldehyde in bio-catalysts design: a useful crosslinker and a

versatile tool in enzyme immobilization. RSC Adv. 4, 1583–1600. https://doi.org/10.1039/C3RA45991H.
Bolivar, J.M., López-Gallego, F., 2020. Characterization and evaluation of immobilized enzymes for applications in flow reactors. Curr. Opin. Green Sustain. Chem. 25, 100349 https://doi.org/10.1016/j.cogsc.2020.04.010.
Canfora, L., Iamarino, G., Rao, M.A., Gianfreda, L., 2008. Oxidative transformation of natural and synthetic phenolic mixtures by Trametes versicolor laccase. J. Agric. Food Chem. 56, 1398–1407. https://doi.org/10.1021/jf0728350.
Çelik, A., Dinçer, A., Aydemir, T., 2016. Characterization of β-glucosidase immobilized on chitosan-multiwalled carbon nanotubes (MWCNTS) and their application on tea extracts for aroma enhancement. Int. J. Biol. Macromol. 89, 406–414. https://doi.org/10.1016/J.IJBIOMAC.2016.05.008.
Chen, H., Zhang, Q., Dang, Y., Dang, Y., 2013. The effect of glutaraldehyde cross-linking on the enzyme activity of immobilized &beta-galactosidase on chitosan bead. Adv. J. Food Sci. Technol. 5, 932–935. https://doi.org/10.19026/AJFST.5.3185.
Dias Gomes, M., Woodley, J.M., 2019. Considerations when measuring biocatalyst performance. Molecules 24. https://doi.org/10.3390/molecules24193573.
Domínguez, M.I., Centeno, M.A., Martínez, T., Bobadilla, M., Laguna, L.F., Odriozola, J. A, Ó.H., 2021. Current scenario and prospects in manufacture strategies for glass, quartz, polymers and metallic microreactors: a comprehensive review. Chem. Eng. Res. Des. 171, 13–35. https://doi.org/10.1016/j.cherd.2021.05.001.
Domínguez de María, P., 2021. Biocatalysis, sustainability, and industrial applications: show me the metrics. Curr. Opin. Green Sustain. Chem. 31, 100514 https://doi.org/10.1016/j.cogsc.2021.100514.
Durán, I.R., Vanslambrouck, S., Chevallier, P., Hoesli, C.A., Laroche, G., 2020. Atmospheric pressure cold plasma versus wet-chemical surface treatments for carboxyl functionalization of polylactic acid: a first step toward covalent immobilization of bioactive molecules. Colloids Surf. B Biointerfaces 189, 110847. https://doi.org/10.1016/j.colsurfb.2020.110847.
Gambacorta, G., Sharley, J.S., Baxendale, I.R., 2021. A comprehensive review of flow chemistry techniques tailored to the flavours and fragrances industries. Beilstein J. Org. Chem. 1790 (17), 1181–1312. https://doi.org/10.3762/BJOC.17.90.
Gamov, G.A., Zavalishin, M.N., Khokhlova, A.Y., Gashnikova, A.V., Kiselev, A.N., Zav'yalov, A.V., Aleksandriiskii, V.V., 2020. Kinetics of the oxidation of protocatechuic and gallic acids by atmospheric oxygen in the presence of Laccase from T. versicolor. Russ. J. Phys. Chem. A. https://doi.org/10.1134/S0036024420020119.
Ghidouche, S., Es-Safi, N.E., Ducrot, P.H., 2007. Trtametes versicolor laccase mediated oxidation of flavonoids. Influence of the hydroxylation pattern of ring B of flavonols. Am. J. Food Technol. 2, 630–640. https://doi.org/10.3923/AJFT.2007.630.640.
Giannakopoulou, A., Chatzikonstantinou, A.V., Chalmpes, N., Tsapara, G., Gournis, D., Polydera, A.C., Stamatis, H., 2021. Development of a novel Bi-enzymatic nanobiocatalyst for the efficient bioconversion of oleuropein to hydroxytyrosol, 749 11, 749 Catalysis 11. https://doi.org/10.3390/CATAL11060749.
Gkantzou, E., Patila, M., Stamatis, H., Gkantzou, E., Patila, M., Stamatis, H., 2018. Magnetic microreactors with immobilized enzymes—from assemblage to contemporary applications. Catalysts 8, 282. https://doi.org/10.3390/catal8070282.
Gkantzou, E., Govatsi, K., Chatzikonstantinou, A.V., Yannopoulos, S.N., Stamatis, H., 2021. Development of a ZnO nanowire continuous flow microreactor with β-glucosidase activity: characterization and application for the glycosylation of natural products. ACS Sustain. Chem. Eng. 9, 7658–7667. https://doi.org/10.1021/acssuschemeng.1c02557.
Guajardo, N., Domínguez de María, P., 2019. Continuous biocatalysis in environmentally-friendly media: a triple synergy for future sustainable processes. ChemCatChem 11, 3128–3137. https://doi.org/10.1002/cctc.201900773.
Gür, S.D., İdil, N., Aksöz, N., 2017. Optimization of enzyme co-immobilization with sodium alginate and glutaraldehyde-activated chitosan beads, 2017 1842 184 Appl. Biochem. Biotechnol. 538–552. https://doi.org/10.1007/S12010-017-2566-5.
Jaidev, L.R., Chatterjee, K., 2019. Surface functionalization of 3D printed polymer scaffolds to augment stem cell response. Mater. Des. 161, 44–54. https://doi.org/10.1016/j.matdes.2018.11.018.
Jiang, D.S., Long, S.Y., Huang, J., Xiao, H.Y., Zhou, J.Y., 2005. Immobilization of Pycnoporus sanguineus laccase on magnetic chitosan microspheres. Biochem. Eng. J. 25, 15–23. https://doi.org/10.1016/J.BEJ.2005.03.007.
Kim, S., Kim, D.H., Kim, W., Cho, Y.T., Fang, N.X., 2021. Additive manufacturing of functional microarchitected reactors for energy, environmental, and biological applications. Int. J. Precis. Eng. Manuf. - Green Technol. 8, 303–326. https://doi.org/10.1007/s40684-020-00277-5.
Kitson, P.J., Marshall, R.J., Long, D., Forgan, R.S., Cronin, L., 2014. 3D printed high-throughput hydrothermal reactionware for discovery, optimization, and scale-up. Angew. Chem. Int. Ed. 53, 12723–12728. https://doi.org/10.1002/ANIE.201402654.
Avci, G.K., & Ogel, Z.B. (2014). Oxidation of catechol, (+)-catechin, and caffeic acid by the laccase from Trametes versicolor and tyrosinase from Agaricus bisporus.
Kong, Y.L., Gupta, M.K., Johnson, B.N., McAlpine, M.C., 2016. 3D printed bionic nanodevices. Nano Today 11, 330–350. https://doi.org/10.1016/j.nantod.2016.04.007.
Leemans Martin, L., Peschke, T., Venturoni, F., Mostarda, S., 2020. Pharmaceutical industry perspectives on flow chemocatalysis and biocatalysis. Curr. Opin. Green Sustain. Chem. 25, 100350 https://doi.org/10.1016/J.COGSC.2020.04.011.
Lin, Y., Zhang, Z., Zhao, L., Wang, X., Yu, P., Su, L., Mao, L., 2010. A non-oxidative electrochemical approach to online measurements of dopamine release through laccase-catalyzed oxidation and intramolecular cyclization of dopamine. Biosens. Bioelectron. 25, 1350–1355. https://doi.org/10.1016/j.bios.2009.10.028.
Lloret, L., Eibes, G., Moreira, M.T., Feijoo, G., Lema, J.M., Miyazaki, M., 2013. Improving the catalytic performance of laccase using a novel continuous-flow microreactor. Chem. Eng. J. 223, 497–506. https://doi.org/10.1016/j.cej.2013.03.018.
Maia-Pinto, M.O.C., Brochado, A.C.B., Teixeira, B.N., Sartoretto, S.C., Uzeda, M.J., Alves, A.T.N.N., Alves, G.G., Calasans-Maia, M.D., Thiré, R.M.S.M., 2021. Biomimetic mineralization on 3d printed pla scaffolds: on the response of human primary osteoblasts spheroids and in vivo implantation. Polymers 1–26. https://doi.org/10.3390/polym13010074.
Manzano-Nicolas, J., Taboada-Rodriguez, A., Teruel-Puche, J.A., Marin-Iniesta, F., Garcia-Molina, F., Garcia-Canovas, F., Tudela-Serrano, J., Munoz-Munoz, J., 2021. Enzymatic oxidation of oleuropein and 3-hydroxytyrosol by laccase, peroxidase, and tyrosinase. J. Food Biochem. 45, 1–14. https://doi.org/10.1111/jfbc.13803.
Martínková, L., Kotik, M., Marková, E., Homolka, L., 2016. Biodegradation of phenolic compounds by Basidiomycota and its phenol oxidases: a review. Chemosphere 149, 373–382. https://doi.org/10.1016/j.chemosphere.2016.01.022.
Monteiro, O.A.C., Airoldi, C., 1999. Some studies of crosslinking chitosan–glutaraldehyde interaction in a homogeneous system. Int. J. Biol. Macromol. 26, 119–128. https://doi.org/10.1016/S0141-8130(99)00068-9.
Muñiz-Mouro, A., Gullón, B., Lú-Chau, T.A., Moreira, M.T., Lema, J.M., Eibes, G., 2018. Laccase activity as an essential factor in the oligomerization of rutin, 321 8, 321 Catalysis 8. https://doi.org/10.3390/CATAL8080321.
Nagarajan, S., Nagarajan, R., Kumar, J., Salemme, A., Togna, A.R., Saso, L., Bruno, F., 2020. Antioxidant activity of synthetic polymers of phenolic compounds. Polymers 1–27. https://doi.org/10.3390/POLYM12081646.
Naghdi, M., Taheran, M., Brar, S.K., Kermanshahi-pour, A., Verma, M., Surampalli, R.Y., 2019. Fabrication of nanobiocatalyst using encapsulated laccase onto chitosan-nanobiochar composite. Int. J. Biol. Macromol. 124, 530–536. https://doi.org/10.1016/j.ijbiomac.2018.11.234.
Pahlevanzadeh, F., Emadi, R., Valiani, A., Kharaziha, M., Poursamar, S.A., Bakhsheshi-Rad, H.R., Ismail, A.F., RamaKrishna, S., Berto, F., 2020. Three-dimensional printing constructs based on the chitosan for tissue regeneration: state of the art, developing directions and prospect trends. Materials. https://doi.org/10.3390/ma13112663.
Peris, E., Okafor, O., Kulcinskaja, E., Goodridge, R., Luis, S.V., Garcia-Verdugo, E., O'Reilly, E., Sans, V., 2017. Tuneable 3D printed bioreactors for transaminations under continuous-flow. Green Chem. 19, 5345–5349. https://doi.org/10.1039/c7gc02421e.
Perna, V., Agger, J.W., Holck, J., Meyer, A.S., 2018. Multiple Reaction Monitoring for quantitative laccase kinetics by LC-MS, 2018 81 8 Sci. Rep. 1–9. https://doi.org/10.1038/s41598-018-26523-0.
Rogers, T.A., Bommarius, A.S., 2010. Utilizing simple biochemical measurements to predict lifetime output of biocatalysts in continuous isothermal processes. Chem. Eng. Sci. 65, 2118. https://doi.org/10.1016/J.CES.2009.12.005.
Rouhi, A.M., 2004. Microreactors eyed for industrial use. Chem. Eng. 82, 18–19. https://doi.org/10.1021/CEN-V082N027.P018.
Schneider, M., Fritzsche, N., Puciul-Malinowska, A., Baliś, A., Mostafa, A., Bald, I., Zapotoczny, S., Taubert, A., 2020. Surface etching of 3D printed poly(lactic acid) with NaOH: a systematic approach. Polymers 12. https://doi.org/10.3390/POLYM12081711.
Spano, M.B., Tran, B.H., Majumdar, S., Weiss, G.A., 2020. 3D-printed labware for high-throughput immobilization of enzymes. J. Org. Chem. 85, 8480–8488. https://doi.org/10.1021/acs.joc.0c00789.
Su, J., Fu, J., Wang, Q., Silva, C., Cavaco-Paulo, A., 2018. Laccase: a green catalyst for the biosynthesis of poly-phenols. Crit. Rev. Biotechnol. 38, 294–307. https://doi.org/10.1080/07388551.2017.1354353.
Tamborini, L., Fernandes, P., Paradisi, F., Molinari, F., 2018a. Flow bioreactors as complementary tools for biocatalytic process intensification. Trends Biotechnol. 36, 73–88. https://doi.org/10.1016/j.tibtech.2017.09.005.
Tamborini, L., Fernandes, P., Paradisi, F., Molinari, F., 2018b. Flow bioreactors as complementary tools for biocatalytic process intensification. Trends Biotechnol. 36, 73–88. https://doi.org/10.1016/j.tibtech.2017.09.005.
Tišma, M., Zelić, B., Vasić-Rački, D., Žnidaršič-Plazl, P., Plazl, I., 2009. Modelling of laccase-catalyzed l-DOPA oxidation in a microreactor. Chem. Eng. J. 149, 383–388. https://doi.org/10.1016/j.cej.2009.01.025.
Tušek, A.J., Šalić, A., Zelić, B., 2017. Catechol removal from aqueous media using laccase immobilized in different macro- and microreactor systems. Appl. Biochem. Biotechnol. 182, 1575–1590. https://doi.org/10.1007/s12010-017-2419-2.
Wang, J., Nor Hidayah, Z., Razak, S.I.A., Kadir, M.R.A., Nayan, N.H.M., Li, Y., Amin, K.A. M., 2019. Surface entrapment of chitosan on 3D printed polylactic acid scaffold and its biomimetic growth of hydroxyapatite. Compos. Interfaces 26, 465–478. https://doi.org/10.1080/09276440.2018.1508266.
Wang, Y., Zhang, Y., Hou, C., Liu, M., 2016. Mussel-inspired synthesis of magnetic polydopamine-chitosan nanoparticles as biosorbent for dyes and metals removal. J. Taiwan Inst. Chem. Eng. 61, 292–298. https://doi.org/10.1016/j.jtice.2016.01.008.
Xie, P., Fan, L., Huang, L., Zhang, C., 2021a. Oxidative polymerization process of hydroxytyrosol catalysed by polyphenol oxidases or peroxidase: characterization, kinetics and thermodynamics. Food Chem. 337, 127996 https://doi.org/10.1016/j.foodchem.2020.127996.
Xie, P., Fan, L., Huang, L., Zhang, C., 2021b. Oxidative polymerization of hydroxytyrosol catalyzed by laccase, tyrosinase or horseradish peroxidase: influencing factors and molecular simulations. J. Biomol. Struct. Dyn. 39, 5486–5497. https://doi.org/10.1080/07391102.2020.1801512.
Xue, S., Qiu, L., Guo, X., Yao, Y., 2020. Effect of liquid digestate recirculation on biogas production and enzyme activities for anaerobic digestion of corn straw. Water Sci. Technol. 82, 144–156. https://doi.org/10.2166/WST.2020.338.

Ye, J., Chu, T., Chu, J., Gao, B., He, B., 2019. A versatile approach for enzyme immobilization using chemically modified 3D-printed scaffolds. ACS Sustain. Chem. Eng. 7, 18048–18054. https://doi.org/10.1021/acssuschemeng.9b04980.

Zhang, C., Pang, F., Li, B., Xue, S., Kang, Y., 2013. Recycled aqueous ammonia expansion (RAAE) pretreatment to improve enzymatic digestibility of corn stalks. Bioresour. Technol. 138, 314–320. https://doi.org/10.1016/J.BIORTECH.2013.03.091.

Zhang, H., Xun, E., Wang, J., Chen, G., Cheng, T., Wang, Z., Ji, T., Wang, L., 2012. Immobilization of laccase for oxidative coupling of trans-resveratrol and its derivatives, 13, 5998–6008 Int. J. Mol. Sci. 13, 5998–6008. https://doi.org/10.3390/IJMS13055998.

Zhou, Y., 2017. The recent development and applications of fluidic channels by 3D printing. J. Biomed. Sci. 24, 1–22. https://doi.org/10.1186/s12929-017-0384-2.

3D printed PLA microdevices for evaluation of biological properties and biotransformation reactions

Anastasia Skonta, Myrto G. Bellou, Andreas-Georgios Vasios, Haralambos Stamatis *

Laboratory of Biotechnology, Department of Biological Applications and Technologies, University of Ioannina, Ioannina, Greece
* Corresponding author: hstamati@uoi.gr

Abstract

3D printing is an innovative manufacturing technology that has become ideal for the construction of devices with desirable shapes and sizes, as opposed to other manufacturing techniques. In this technique, layers of the printing material are deposited on top of one another, leading to the formation of the designed model. Polylactic acid (PLA) is a thermoplastic biopolymer extensively used as a printing material, since it possesses eco-friendly characteristics such as biocompatibility, non-toxicity and biodegradability[1].

PLA-based microscaffolds of varying geometries can be designed and printed through 3D printing technology that can be further used for biocatalytic applications[2]. Several enzymes, including lipases, have been immobilized on different PLA scaffolds such as microwell plates and microfluidic reactors for the screening of biological activities of various compounds and for the catalysis of hydrolytic or synthetic reactions, respectively[3,4]. More specifically, the microplate systems can be applied in the time- and cost-effective evaluation of natural extracts, regarding their inhibitory effect on enzymes with pharmaceutical interest. With regard to the microfluidic reactors, they show great potential in the production of bioactive compounds with higher productivities compared to batch systems, due to their larger specific surface. Furthermore, these PLA-based biocatalytic systems have been successfully implemented in biocatalytic transformations that take place in environmentally friendly non-conventional solvents, such as deep eutectic solvents (DES), towards the development of sustainable reaction systems.

References

1. Baran E, Erbil H. Surface Modification of 3D Printed PLA Objects by Fused Deposition Modeling: A Review. *Colloids and Interfaces*. 2019;3(2):43. doi:10.3390/colloids3020043
2. Gkantzou E, Skonta A, Tsakni A, et al. 3D printed PLA enzyme microreactors: Characterization and application for the modification of bioactive compounds. *J Biotechnol*. 2022;350:75-85.
3. Skonta A, Gkantzou E, Spyrou K, et al. 3D Printed Polylactic Acid (PLA) Well Plates for Enzyme Inhibition Studies: The Case of Pancreatic Lipase. *Catal Res*. 2022;2(4):032. doi:10.21926/cr.2203032
4. Bellou MG, Gkantzou E, Skonta A, et al. Development of 3D Printed Enzymatic Microreactors for Lipase-Catalyzed Reactions in Deep Eutectic Solvent-Based Media. *Micromachines*. 2022;13(11):1954. doi:10.3390/mi13111954

Acknowledgements: This research has been co-financed by the European Regional Development Fund of the European Union and Greek national funds through the Operational Program Competitiveness, Entrepreneurship, and Innovation, under the call RESEARCH−CREATE-INNOVATE (project code: T2EDK-01410).

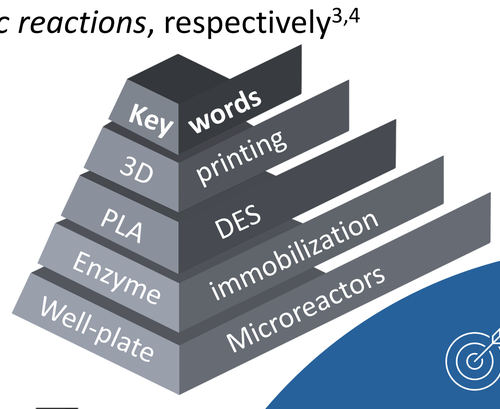
3D printed PLA microdevices for evaluation of biological properties and biotransformation reactions

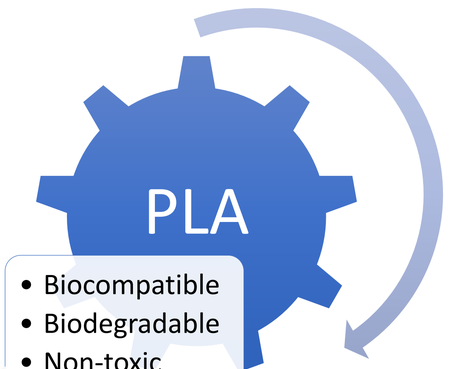
Anastasia Skonta, Myrto G. Bellou, Andreas-Georgios Vasios, Haralambos Stamatis*

Laboratory of Biotechnology, Department of Biological Applications and Technologies, University of Ioannina, Ioannina, Greece
* Corresponding author: hstamati@uoi.gr

1. Introduction

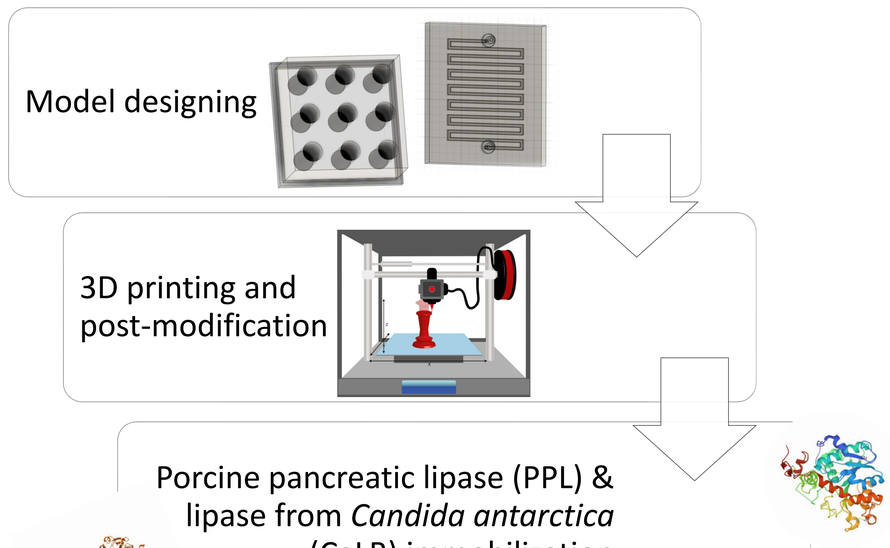
- 3D printing is an innovative manufacturing technology based on the deposition of layers of the printing material, such as polylactic acid (PLA), on top of one another[1]
- PLA-based microscaffolds of varying geometries can be designed and printed through 3D printing technology that can be further used for biocatalytic applications[2]
- Several enzymes, including lipases, have been immobilized on different PLA scaffolds such as **microwell plates** and **microfluidic reactors** for the *screening of biological activities of various compounds* and for the *catalysis of hydrolytic or synthetic reactions*, respectively[3,4]





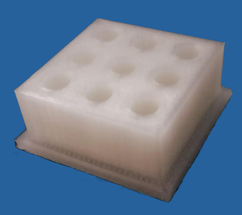


2. Methods



Objectives

PLA well-plate



✓ Time- and cost-effective evaluation of natural extracts regarding their inhibitory effect on enzymes with pharmaceutical interest

Screening of biological activities

PLA microreactor



✓ Production of bioactive compounds
✓ Biocatalytic transformations in environmentally friendly non-conventional solvents, such as deep eutectic solvents (DES)

Catalysis of hydrolytic or synthetic reactions

3. Results

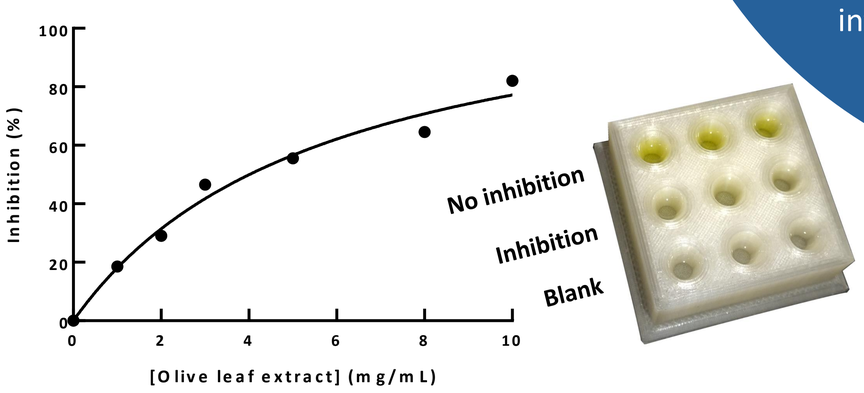


Figure 1. Determination of the values of inhibitory potency (IC_{50}) for olive leaf extract for the immobilized PPL.

Table 1. Inhibitory potency (IC_{50}) of orlistat (model inhibitor) and olive leaf extract on PPL for both its immobilized and free form.

	IC_{50} for the immobilized PPL	IC_{50} for the free PPL
Orlistat	31.73 ± 6.52 nM	8.53 ± 1.68 nM
Olive leaf extract	3.84 ± 0.48 mg/mL	3.46 ± 0.34 mg/mL

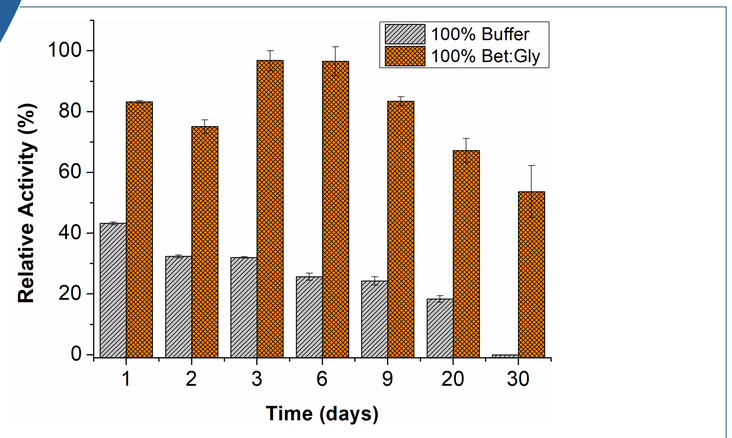
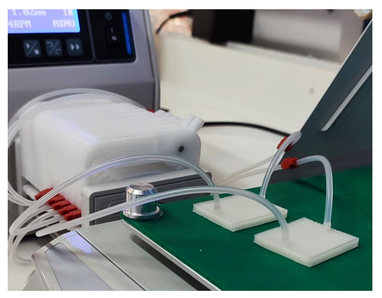
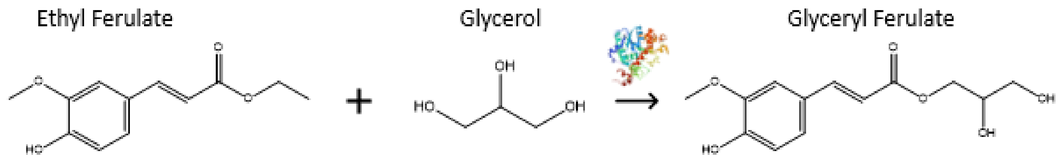


Figure 2. Thermal stability of immobilized CALB in PLA microreactors, after incubation in 100% DES Bet:Gly and 100% buffer, at 60 °C.

Figure 3. Transesterification of ethyl ferulate with glycerol in 100% v/v Bet:Gly. The microreactor system exhibited **23 times higher productivity** (μg product min^{-1} μg $enzyme^{-1}$) than that of a commercial immobilized lipase and **1.2 times higher** than that of the free CALB.





4. Conclusions



- The 3D printed PLA microdevices were successfully employed as immobilization scaffolds
- The immobilized enzyme PLA well-plates could be recruited as an inhibitor screening bioanalytical tool
- The microreactor systems can be used in hydrolytic or synthetic reactions with enhanced productivities

5. References

1. Baran E, Erbil H. Surface Modification of 3D Printed PLA Objects by Fused Deposition Modeling: A Review. *Colloids and Interfaces*. 2019;3(2):43. doi:10.3390/colloids3020043

2. Gkantzou E, Skonta A, Tsakni A, et al. 3D printed PLA enzyme microreactors: Characterization and application for the modification of bioactive compounds. *J Biotechnol*. 2022;350:75-85.

3. Skonta A, Gkantzou E, Spyrou K, et al. 3D Printed Polylactic Acid (PLA) Well Plates for Enzyme Inhibition Studies: The Case of Pancreatic Lipase. *Catal Res*. 2022;2(4):032. doi:10.21926/cr.2203032

4. Bellou MG, Gkantzou E, Skonta A, et al. Development of 3D Printed Enzymatic Microreactors for Lipase-Catalyzed Reactions in Deep Eutectic Solvent-Based Media. *Micromachines*. 2022;13(11):1954. doi:10.3390/mi13111954

Acknowledgements: This research has been co-financed by the European Regional Development Fund of the European Union and Greek national funds through the Operational Program Competitiveness, Entrepreneurship, and Innovation, under the call RESEARCH–CREATE-INNOVATE (project code: T2EDK-01410).


FEMS
10th International Conference
mikrobio
kosmos
All microbes for a
sustainable future
NEW DATES
30 Nov | 02 Dec
2023
Divani
Palace
Larissa
Larissa
Greece
ΜΙΚΡΟ
BIO
ΚΟΣΜΟΣ

Enzymatic treatment of extracts derived from natural sources for the enhancement of their biological activities

Stamatia Spyrou[1], Myrto G. Bellou[1], Alexandra V. Chatzikonstantinou[1], Renia Fotiadou[1], Konstantina Nakou[1], Vasiliki G. Kontogianni[2] and Haralambos Stamatis[1]

[1]*Laboratory of Biotechnology, Department of Biological Applications and Technologies, University of Ioannina, Ioannina, Greece*

[2]*Dairy Research Department, Hellenic Agricultural Organization-DEMETER, Ioannina, Greece*

Tel +302651007116, e-mail: hstamati@uoi.gr

Origanum dictamnus (dittany) is a native herb to the island of Crete which has been employed since antiquity as a remedy for various diseases[1]. Recent evidence has supported the biological activities of extracts derived from dittany, such as antioxidant and antimicrobial, which are mainly attributed to their unique polyphenolic profile[2]. On the other hand, biocatalysis is often used for the targeted modification of extracts of natural origin in a try to enhance their biological activities. Among the enzymes that are often used are oxidoreductases[3]. Alongside, hydrogels employing phenolic compounds are gaining more and more interest for their application in pharmaceutical industry, for example in wound healing, due to their antioxidant and antibacterial activities[4,5]. In the present study, aqueous and methanolic extracts from *Origanum dictamnus*, rich in phenolic compounds, were prepared and studied for their polyphenolic profile, antioxidant and antimicrobial activity against Gram positive and Gram negative bacteria, before and after their enzymatic treatment with oxidoreductases. The main polyphenolic compounds contained in the extracts were further successfully used for the preparation of enzymatically crosslinked biopolymer-based hydrogels in the presence of a deep eutectic solvent (DES), which were studied for their antimicrobial activity.

Keywords: dittany; extract; oxidoreductase; antimicrobial; hydrogel; DES

References

[1] Krigas, N., Lazari, D., Maloupa, E., & Stikoudi, M. (2015). *Inter. J. Gastron. Food Sci.* 2, 112–118.

[2] Chatzopoulou, A., Karioti, A., Gousiadou, C., Lax Vivancos, V., Kyriazopoulos, P., Golegou, S., & Skaltsa, H. (2010). *J. Agric. Food Chem.* 58, 6064–6068.

[3] Antonopoulou, I., Varriale, S., Topakas, E., Rova, U., Christakopoulos, P., & Faraco, V. (2016). *Appl. Microbiol. Biotechnol*. 100, 6519–43.

[4] Yin, Y., Xu, Q., Wei, X., Ma, Q., Li, D., & Zhao, J. (2023). *Molecules* 28, 4034.

[5] Guebitz, G. M., Nyanhongo, G. S. (2018). *Trends Biotechnol*. 36, 1040-1053.

Acknowledgements

This research has been co-financed by the European Regional Development Fund of the European Union and Greek national funds through the Operational Program Competitiveness, Entrepreneurship, and Innovation, under the call RESEARCH−CREATE-INNOVATE (project code: T2EDK-01410).

Enzymatic treatment of extracts derived from natural sources for the enhancement of their biological activities

Stamatia Spyrou[1], Myrto G. Bellou[1], Alexandra V. Chatzikonstantinou[1], Renia Fotiadou[1], Konstantina Nakou[1], Vasiliki G. Kontogianni[2] and Haralambos Stamatis[1*]

[1]*Laboratory of Biotechnology, Department of Biological Applications and Technologies, University of Ioannina, Ioannina, Greece*

[2]*Dairy Research Department, Hellenic Agricultural Organization-DEMETER, Ioannina, Greece*

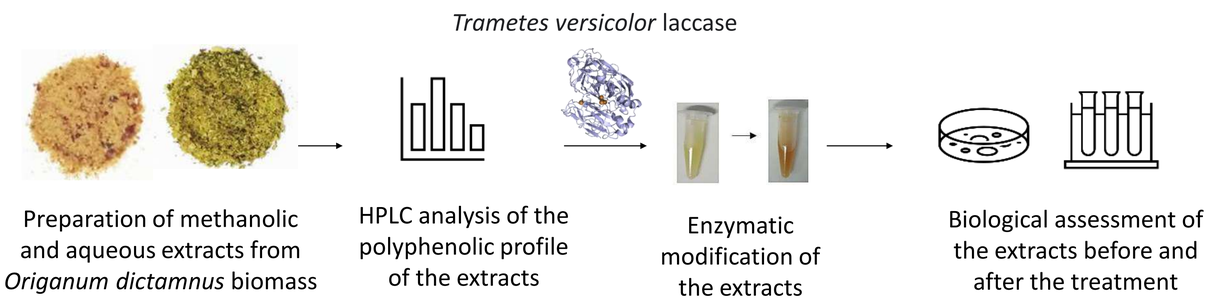
* Corresponding author: hstamati@uoi.gr

Introduction

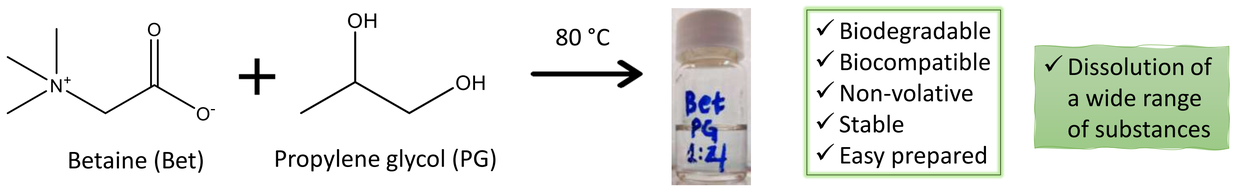
- *Origanum dictamnus* (dittany) is a native herb to the island of Crete which has been employed since antiquity as a remedy for various diseases[1]. Recent evidence has supported the biological activities of extracts derived from dittany, such as antioxidant and antimicrobial, which are mainly attributed to their unique polyphenolic profile[2].
- On the other hand, biocatalysis is often used for the targeted modification of extracts of natural origin in a try to enhance their biological activities. Among the enzymes that are often used are oxidoreductases[3]. Alongside, hydrogels employing phenolic compounds are gaining more and more interest for their application in pharmaceutical industry, for example in wound healing, due to their antioxidant and antibacterial activities[4,5].
- In the present study, aqueous and methanolic extracts from *Origanum dictamnus*, rich in phenolic compounds, were prepared and studied for their polyphenolic profile, antioxidant and antimicrobial activity against Gram negative bacteria, before and after their enzymatic treatment with oxidoreductases. The main polyphenolic compounds contained in the extracts were further successfully used for the preparation of enzymatically crosslinked biopolymer-based hydrogels in the presence of a deep eutectic solvent (DES) and studied for their antimicrobial activity.

Methodology

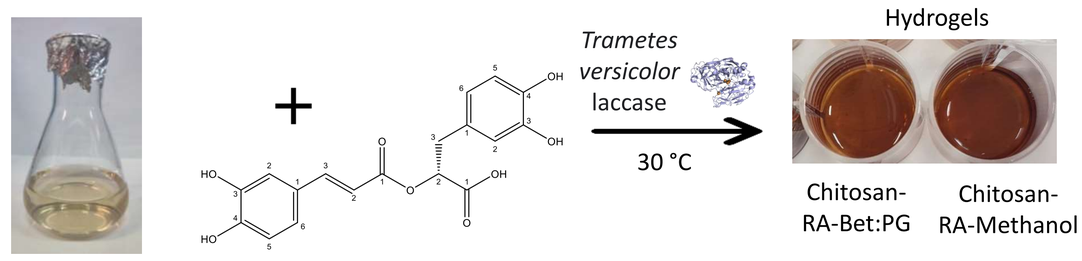
Enzymatic modification of extracts



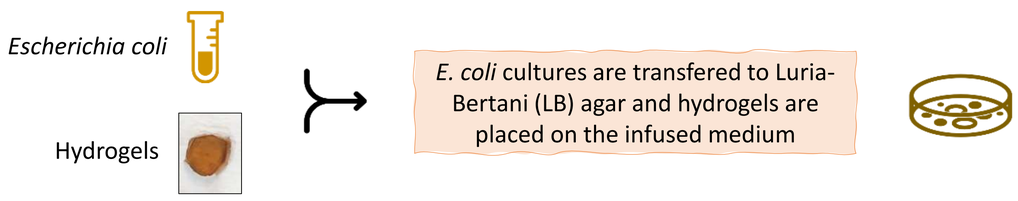
DES preparation



Preparation of rosmarinic acid (RA)-chitosan hydrogels



Antimicrobial study – Inhibition zone



Results

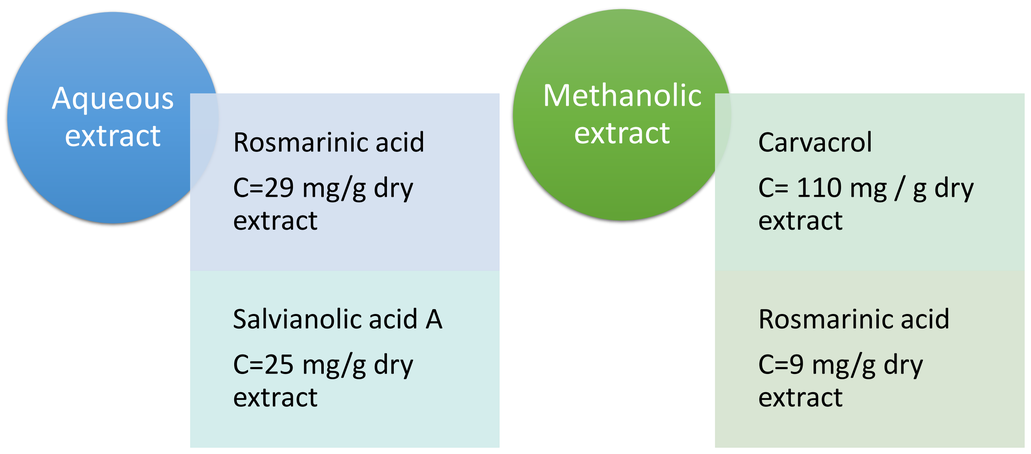


Figure 1. The concentrations of the main polyphenolic compounds in the extracts detected through HPLC analysis.

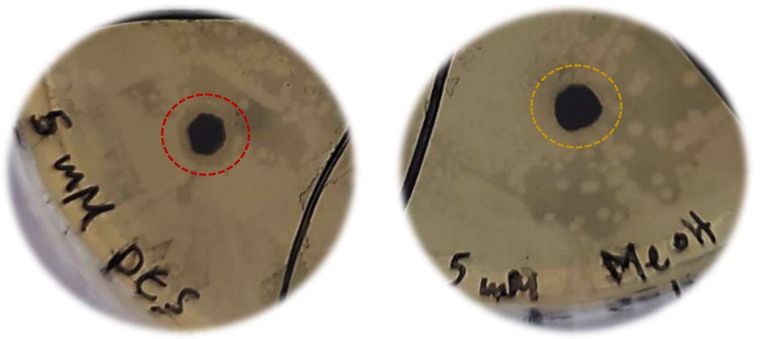
Table 1. Antioxidant activity of the extracts assessed through DPPH assay. The results are expressed as IC50 (μg/mL) (concentration of the inhibitor able to scavenge 50 % of the DPPH initial radical) - Antibacterial activity of the extracts against *Escherichia coli* BL21DE3 assessed through microdilution assay. The results are expressed as MIC (mg/mL) (the lowest concentration of a chemical, which prevents visible in vitro growth of bacteria).

Extracts	Antioxidant activity	Antibacterial activity
Aqueous	15.5 ± 0.9	>5
Modified aqueous	>100	>5
Methanolic	47.2 ± 1	2.5
Modified methanolic	>100	>5

Table 2. Inhibition zones of chitosan hydrogels against *E.coli*.

Hydrogel	Inhibition zone (mm)
Chitosan-RA-Bet:PG	1
Chitosan-RA-Methanol	0

Inhibition zone was detected only in the case of the chitosan hydrogel that contains the DES Bet:PG



Conclusions

- ❖Aqueous and methanolic extracts were prepared from *Origanum dictamnus* biomass and characterized through HPLC analysis in terms of their polyphenolic content. Rosmarinic acid was the main polyphenolic compound in the aqueous extract and carvacrol in the methanolic one
- ❖The extracts were further successfully enzymatically modified with laccase from *Trametes versicolor* to produce phenolic oligomers from the precursor compounds
- ❖The enzymatic modification of the extracts led to lower antioxidant and antimicrobial bioactivities in relation to the non-modified extracts
- ❖Rosmarinic acid was successfully employed in the enzymatic preparation of chitosan hydrogels
- ❖The DES Bet:PG was effectively used for the dissolution of rosmarinic acid as an alternative of methanol and was employed in the preparation of the chitosan hydrogel
- ❖The combination of the biopolymer (chitosan) with the green solvent (DES) and the bioactive polyphenolic compound (RA) led to the production of a hydrogel with antimicrobial activity against gram negative bacteria (*E.coli*) which could be further applied for pharmaceutical purposes.

Acknowledgements

This research has been co-financed by the European Regional Development Fund of the European Union and Greek national funds through the Operational Program Competitiveness, Entrepreneurship, and Innovation, under the call RESEARCH–CREATE-INNOVATE (project code: T2EDK-01410).

References

[1] Krigas, N., Lazari, D., Maloupa, E., & Stikoudi, M. (2015). *Inter. J. Gastron. Food Sci*. 2, 112–118.

[2] Chatzopoulou, A., Karioti, A., Gousiadou, C., Lax Vivancos, V., Kyriazopoulos, P., Golegou, S., & Skaltsa, H. (2010). *J. Agric. Food Chem*. 58, 6064–6068.

[3] Antonopoulou, I., Varriale, S., Topakas, E., Rova, U., Christakopoulos, P., & Faraco, V. (2016). *Appl. Microbiol. Biotechnol*. 100, 6519–43.

[4] Yin, Y., Xu, Q., Wei, X., Ma, Q., Li, D., & Zhao, J. (2023). *Molecules* 28, 4034.

[5] Guebitz, G. M., Nyanhongo, G. S. (2018). *Trends Biotechnol*. 36, 1040-1053.